DESIGN, SYNTHESIS, AND IMMUNOLOGICAL STUDIES TOWARD THE DEVELOPMENT OF CARBOHYDRATE BASED CANCER VACCINES

By

Philip Allen Bentley

A THESIS

Submitted to
Michigan State University
in partial fulfillment of the requirements
for the degree of

MASTER OF SCIENCE

Chemistry

2011

ABSTRACT

DESIGN, SYNTHESIS, AND IMMUNOLOGICAL STUDIES TOWARD
THE DEVELOPMENT OF CARBOHYDRATE BASED CANCER VACCINES

By

Philip Allen Bentley

Cancer is a disease that affects nearly everyone, either directly and/ or indirectly. In 2008 alone, there were nearly 12.7 million new cancer cases reported and close to 7.6 million people lost their battle with this disease worldwide. In the past several years, unique carbohydrate antigens known as tumor-associated carbohydrate antigens (TACAs) were found to be expressed at abnormal levels on cancer cell surfaces differentiating them from normal cells. This makes them viable targets for vaccine design.

One such TACA is the Tn antigen. The immunological responses of this B-cell epitope conjugated to T-cell epitopes such as Tobacco Mosaic Virus (TMV), a mutant of TMV, and the Qβ capsid were evaluated. Additionally, several control vaccines were synthesized and immunologically evaluated to determine the affect of the linkers during an immune response.

Analysis of the vaccine constructs by enzyme-linked immunosorbent assay (ELISA) revealed discrepancies between the antibody titers measured for the control and experimental populations. This led to the investigation into the measured background absorbance using each vaccine construct. Changing from an ELISA plate coated with NeutrAvidin to one coated with bovine serum albumin (BSA) resulted in a much lower background.

Finally, three glyco-polymers conjugated to the surface of a protein carrier, expressing the Tn antigen in varying degrees, were synthesized in hopes of further enhancing the immune response elicited.

ACKNOWLEDGEMENTS

I would like to start by thanking my advisor, Professor Xuefei Huang for his patience and guidance during the past three years of my graduate studies. He was instrumental in my growth as a researcher and person and will pave the foundation of my future studies. I also give special thanks to my guidance committee members, Professors William Wulff and Kevin Walker for their critical insight into my research and their valuable time spent serving on my committee.

Dr. Daniel Holmes and Mr. Kermit Johnson played vital roles in my NMR training and molecular analysis, Dr. Daniel Jones and Lijun Chen were very helpful in training me how to use the mass spectrometer, and Dr. Jeannie Gaymer shared her expertise in the handling and well-being of the mice used during the course of my studies.

I also thank those present and past members of the Huang group: Bo, Dino, Gilbert, Gopinath, Herbert, Hongguang, Hovig, Keisuke, Medha, Moe, Qian, Steve, Xiaowei (Vivian), and Zhaojun who, on several occasions, were more than willing to assist me in my day-to-day research. In addition to these group members, undergraduate researchers Sarah McKee and Claire Baniel and high school student David Huynh gave me the opportunity and pleasure to teach and learn from them. Special thanks to Dr. Medha Kamat and her husband Dr. Bala Ramanathan for all the hours they excluded from their own research to help teach me techniques and concepts that will be invaluable in my future research endeavors. Many thanks to Dr. Zhaojun Yin for his dedication and contributions to the vaccine project, specifically the work he contributed to the understanding of the ELISA results, and Dr. Adeline Miermont, whose work in the laboratory prior to my arrival set the foundation for my research project.

I thank all the friends I came to know during the course of my graduate studies who helped keep me positive when it seemed as though nothing in the laboratory worked as I hoped.

All of the soccer games, bowling nights, and just plain hanging out watching Michigan State sports or cheering for our respective countries in the World Cup gave me a much better appreciation for the different cultures; I hope that I too have reciprocated this.

I must thank my parents, sister, and grandparents who were always there to support me over the past many years of my education. And last, but certainly not least, I express my deepest thanks to my new wife, Ashley, who was always emotionally in my corner each night I came home either disappointed or perhaps even when I was a bit difficult to be around.

TABLE OF CONTENTS

LIST OF TABLES

LIST OF FIGURES

LIST OF SCHEMES

LIST OF ABBREVIATIONS

AcOH	Acetic acid
Ac_2O	Acetic anhydride
AD	Alzheimer's Disease
AgCl	Silver chloride
ATRP	Atom Transfer Radical Polymerization
Bn	Benzyl
BnBr	Benzyl bromide
Boc	*tert*-Butyloxycarbonyl
BOP	Benzotriazole-1-yl-oxy-tris-(dimethylamino)-phosphonium hexafluorophosphate
BSA	Bovine serum albumin
cat.	Catalytic
Cl_3CCN	Trichloroacetonitrile
$Ce(NH_4)_2(NO_3)_6$	Ammonium cerium (IV) nitrate
$(NH_4)_6Mo_7O_{24} * 4H_2O$	Ammonium molybdate tetrahydrate
CFA	Complete Freund's Adjuvant
conc.	Concentrated
COSY	Correlation Spectroscopy
CPMV	Cowpea mosaic virus
$CuSO_4*5H_2O$	Copper (II) Sulfate pentahydrate
CuI	Copper (I) Iodide

d	Day
DCM	Dichloromethane
DBU	1,8-Diazabicyclo[5.4.0]undec-7-ene
DIPEA	Diisopropylethylamine
DMAP	4-Dimethylaminopyridine
DMF	Dimethylformamide
DMSO	Dimethyl sulfoxide
dOSM	Desialylated ovine submaxillary mucin
EDC. HCl	1-Ethyl-3-(3-dimethylaminopropyl) carbodiimide Hydrochloride
ELISA	Enzyme-linked immunosorbent assay
EtOAc	Ethyl acetate
FACS	Fluorescence-assisted cell sorting
FITC	Fluorescein isothiocyanate
Fmoc	9-Fluorenylmethoxycarbonyl
Gal	Galactose
GalNAc	N-Acetyl galactosamine
Glc	Glucose
h	Hour
H_2	Hydrogen gas
H_2O	Water
H_2SO_4	Sulfuric acid
HBF_4	Fluoroboric acid

HCl	Hydrochloric acid
HMBC	Heteronuclear multiple bond correlation
HMQC	Heteronuclear multiple quantum coherence
HOBt	Hydroxybenzotriazole
HRMS	High Resolution Mass Spectrometry
HRP	Horseradish peroxidase
IFA	Incomplete Freund's Adjuvant
Ig	Immunoglobulin
K_2CO_3	Potassium carbonate
$KHCO_3$	Potassium bicarbonate
KDa	Kilo-Dalton
KLH	Keyhole limpet haemocyanin
NHS	N-Hydroxysuccinimide ester
NH_3	Ammonia
MeOH	Methanol
NaOCN	Sodium cyanate
$NaHSO_3$	Sodium bisulfite
NaN_3	Sodium azide
$NaNO_2$	Sodium nitrite
NMP	N-Methylpyrrolidone
NMR	Nuclear Magnetic Resonance
OAc	Acetate

OVA	Ovalbumin
PBS	Phosphate Buffered Saline
PBST	Tween 20 surfactant in Phosphate Buffered Saline
py	Pyridine
RAFT	Regioselectivity Addressable Functionalized Template
RNA	Ribonucleic acid
RPM	Revolutions per minute
rt	Room temperature
SBA	Soybean agglutinin
S-CPMV	Mutant form of the CPMVcapsid bearing cysteine residues
sec	Second
Ser	Serine
TACA	Tumor-associated carbohydrate antigen
TBAI	Tetrabutylammonium iodide
TEA	Triethylamine
THF `	Tetrahydrofuran
Thr	Threonine
TLC	Thin layer chromatography
TMB	3,3',5,5'-Tetramethylbenzidine
TMSOTf	Trimethylsilyl trifluoromethanesulfonate
TMV	Tobacco mosaic virus
TMV-Tn-N_3	Native TMV Tn conjugate linked to **20**

TMV-Tn-PEG-N_3	Native TMV- Tn conjugate w/ PEG linker
TMV-1Cys	Mutant TMV w/ inserted cysteine residue
TMV-1Cys-Tn-N_3	Mutant TMV- Tn conjugate linked to **20**
TMV-1Cys-Tn-bromo	Mutant TMV- Tn conjugate linked w/ bromoacetamide linker (**48**)
Tn (C)	Tn clustered
Tos- Cl	4-methylbenzenesulfonyl chloride
TTX	Tetanus toxin
YAF	YAFKYARHANVGRNAFELFL peptide
Zn	Zinc

Chapter 1 – Design and Synthesis of a Glycopolymer Based Vaccine

1.1 Introduction

Cancer is a disease that impacts nearly all of the World's population, either directly and/ or indirectly. According to a report published by the American Cancer Society,[1] cancer is the second leading cause of death in economically developed countries behind only heart disease, and the third leading cause of death in developing countries (following heart diseases and diarrheal diseases). Based on data collected in 2008, the International Agency for Research on Cancer reported nearly 12.7 million new cancer cases and close to 7.6 million people lost their battle with this disease worldwide.[2] This is equal to around 13% of all deaths globally. These numbers are predicted to grow drastically as the world's population continues to grow and age. It is predicted that by 2050, there could be as many as 27 million new cases and 17.5 million deaths caused by cancer.[1]

The current treatment of the various forms of cancer employs such methods as chemotherapy, radiation, and surgery. One major drawback of these current methods, however, is they often do not completely eradicate the tumor cells. Additionally, by the time the cancer is diagnosed, it may be too far progressed to be treatable. As the statistics prove, more effective therapeutic interventions are necessary.

One such alternative is immunotherapy because it harnesses the body's natural defense mechanisms; however, immunotherapy also comes with challenges. For instance, the immune system has developed mechanisms to protect itself from attacking the cells and tissues of the host, which is known as self-tolerance.[3, 4] A few of these examples include negative selection of

B cells and T cells in the bone marrow and thymus respectively, expression of tissue-specific proteins in the thymus, suppression of autoimmune responses by regulatory T cells, and the induction of anergy in autoreactive B and T cells.[4] This self tolerance causes tumor associated antigens to be only weakly immunogenic.

To develop a vaccine that can avoid self-tolerance, it becomes crucial to fully understand the complexity of the immune system. In brief, when a pathogen, or antigen (in the case of immunotherapy), enters the body, there is an immediate response known as innate immunity. Once the foreign pathogen or microbe has invaded the body, there will be a secondary response, known as adaptive immunity. Both the innate and the adaptive branches of the immune system are mutually important toward the prevention of the disease state. However, the adaptive branch is of most interest toward developing a successful vaccine. Once inside the body, the foreign pathogen will be recognized, up-taken, and digested by circulating cells, know as antigen presenting cells, more specifically macrophages and dendritic cells. These cells will present fragments of these digested antigens on their cell surface known as epitopes. Then, these antigen presenting cells will display the epitopes to naïve B cells (a mature B cell that has not yet been exposed to its specific antigen). Once exposed for the first time, these naïve B cells will become activated B cells that can begin secreting low affinity antibodies of the IgM subtype. This initial response is an important step because it indicates to the researcher that the antigen is being recognized by the host as non-self. This response transient, lasting only a few weeks; therefore, a successful vaccine for application in cancer therapy requires a long-term immunogenic response. For this to occur there must be a class switch from low-affinity IgM isotypes to high-affinity IgG isotypes. This can occur when both a naïve B-cell and naïve T cell recognize the same pathogen or antigen and differentiate into an activated B cell and an effector T cell,

respectively. Effector T cells are divided into two classes known as CD4 and CD8 T cells corresponding to the surface protein they present. CD8 T cells, otherwise known as Tc cells or cytotoxic T cells, will circulate and monitor the surface of the host cells for the antigen that they were first activated from. If recognized, the CD8 T cell will bind to the infected cell and cause it to undergo apoptosis, otherwise known as programmed cell death. CD4 T cells, otherwise known as Th cells or T helper cells are designed to help further activate antigen presenting cells. Activated B cells, in addition to secreting low-affinity IgM antibodies, also become antigen presenting cells and can display antigens to these effector CD4 T cells by means of an MHC class II complex. When this happens, the CD4 T cells will bind, and begin releasing small molecule cytokines into the microenvironment, which will cause the B cells to undergo an isotype class switch and begin secreting higher affinity antibodies of the IgG subtype. The complexity of this pathway contributes to the challenges of designing a synthetic strategy toward a successful vaccine. For example, in the study described herein, the desired immune response is developed utilizing a carbohydrate epitope, which are not recognized by T cell receptors; therefore, the activated B cells cannot display antigens to the CD4 T cells along the pathway to IgG isotypes. Because these carbohydrates can only be recognized by B cells, they are considered B cell epitopes. Considering that T cell epitopes can only recognize protein peptides (T cell epitopes), it is believed that a carbohydrate antigen capable of being recognized by a naïve B cell conjugated to a protein, which contains these Th peptide epitopes. should induce activation of B cells and their subsequent interaction with CD4 T cells. When the B cell/ CD4-complex is formed, the effector T cell secrete cytokines that induce isotype switching which in turn cause the generation of memory B cells. These memory B cells are desired for long-term immunity, whereby a stronger and faster immune response is induced each time the body is

exposed to the same antigen. Knowledge of the mechanism of this complicated communication within the immune system is absolutely necessary when developing an effective immunotherapy.

Despite the complexities and difficulties of overcoming intrinsic immunological tolerance in cancer therapy, great interest remains toward treating the disease by targeting Tumor-Associated Carbohydrate Antigens (TACAs). It is known that tumor cells express specific antigens on their cell surface that are be recognized by the immune system, including antigenic carbohydrates. Tumor cells can be distinguished from normal cells by the over-expression of unique oligosaccharides on their cell surfaces. Additionally, different TACAs are shared amongst a variety of different cancer cell lines (**Table 1.1**). This makes them an intriguing target for cancer immunotherapy. Thus, targeting TACAs on the surfaces of small metastatic cells (cells that have spread from the primary tumor site to other tissues) can potentially improve the efficiency of treatment by eliciting humoral immune responses (one involving B cells) hopefully generating immuno-surveillance. This immuno-surveillance can allow the immune system to recognize cancer cells at an early stage and eliminate them before the cause of disease. This could allow for the treatment of cancer, but more importantly, even preventing it all together.

Table 1.1: Major TACAs Identified in Cancer Tissues

Cancer Type	Tumor Antigens
Melanoma	GM2, GM3, GD2
Neuroblastoma	GM2,GD2,polysialic acid
Sarcoma	GM2, GD2,GD3
B cell lymphoma	GM2, GD2
Small-cell lung	GM2, fucosyl-GM1, polysialic acid, Globo-H
Breast	GM2, Globo-H, TF(c), Tn(c), LeY
Prostate	GM2, Globo-H, Tn(c), TF(c), sTn(c), LeY
Lung	GM2, Globo-H, LeY
Colon	GM2,Tn, sTn(c), TF(c), LeY
Ovary	GM2, Globo-H, sTn(c), TF(c), LeY
Stomach	GM2, LeY, LeA, sialyl-LeA

However, a challenge of using TACAs in immunotherapy is, that alone, they only weakly activate the antibody secreting B cells. As mentioned above, this weak activation and lack of T cell help prevents isotype switching; thus, only low titers of low affinity IgM antibodies can be generated. To strengthen the antigenicity of TACAs, it therefore is important to link them to an immunogenic carrier that contains epitopes recognizable by CD4 T cells. Once activated, these effector T cells then recognize matched antigens presented by activated B cells and bind to them. This T cell/ B cell complex induces cytokine production by the T cells into the surrounding microenvironment. These cytokines allow additional activation of B cells which undergo isotype class switching from low affinity IgM to high affinity IgG type antibodies. Several studies continue to try and elucidate the complex mechanisms of cancer so an immunotherapy approach can be further honed and optimized.

1.2 An Account of On-going Research with TACAs

Two protein carriers extensively examined and found to contain helper T-cell epitopes are bovine serum albumin (BSA,) and Keyhole Limpet Haemocyanin (KLH). These macromolecular carriers provide the opportunity for isotype switching and generation of immunological memory which allows the immune system to make a quicker, stronger adaptive immune response to each successive encounter to an antigen. Danishefsky and coworkers attached several different TACA epitopes, including Globo-H (**1**), Lewis^y (**2**), Fucosyl GM1 (**3**), TF (**4**), and Tn (**5**) antigens, to BSA and KLH (**Figure 1.1**).[5]

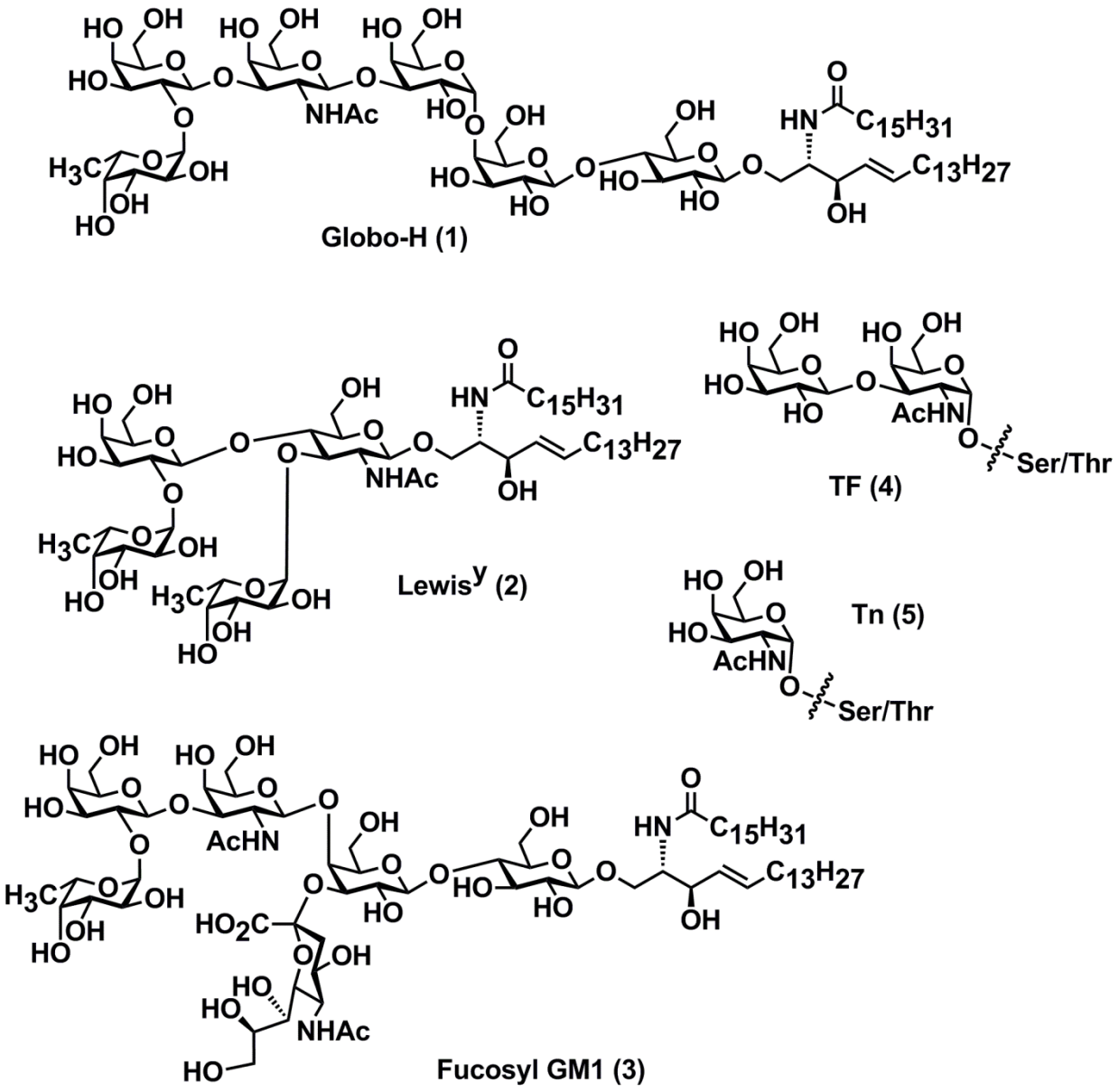

Figure 1.1: Tumor-Associated Carbohydrate Antigens

Deprotected precursors of the epitopes (**Figure 1.1**) were designed to be bioconjugated with a protein carrier. These precursors were synthesized to display an aldehyde linker at the reducing end of the sugar moiety which by means of reductive amination[6, 7] were conjugated to the desired protein carrier. Despite the difficulty of controlling the number of antigens attached

to the surface of these large protein carriers, encouraging results were observed from *in vivo* mouse studies. One study by Danishefsky and coworkers[8] involved synthesizing **6** as a control containing three copies of the Tn antigen (Tn-cluster, designated Tn (c)) and vaccines **7** as the experimental vaccine linked to both BSA and KLH (**7-BSA** and **7-KLH**) to demonstrate the advantage of using a protein carrier (**Figure 1.2**). Both IgG and IgM antibodies, isolated from mouse serum, made against Tn (c) at pre-vaccination isolated for all three of the *in vivo* vaccines were not detectable by ELISA method, as expected. Ten days following Danishefsky's two week injection into mice, the ELISA analysis of antibody titers against Tn (c) induced by compound **6** indicated IgM titers of 1,350 (antibody titers is considered a unit-less number) and IgG titers of 150, the **7-BSA** complex of 1,350 and 150, and the **7-KLH** complex of 12,150 and 450, respectively. These data suggested that KLH functions as a better carrier than BSA. Interestingly, 317 copies of their Tn cluster attached to the surface of KLH as opposed to only 7 copies attached to BSA. Antibody detection by Fluoresence-Activated Cell Sorting (FACS) analysis gave comparable data to the ELISA, except the effects of the two protein carriers were essentially the same. These findings demonstrate that a successful vaccine would require a protein carrier containing a T-cell epitope, to elicit a stronger immune response.

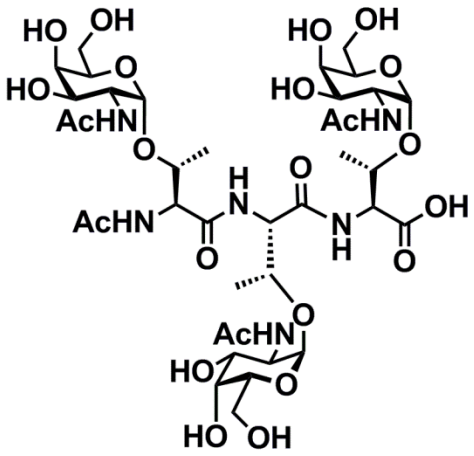

Tn clustered control (6)

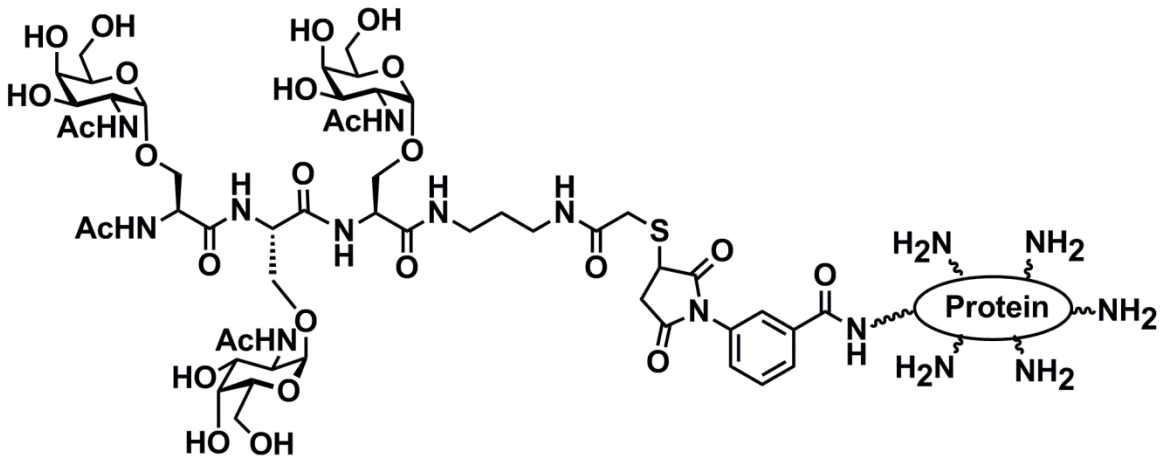

Tn clustered vaccine (7)

Figure 1.2: Clustered Tn antigen and conjugated to protein carrier using MBS linker

Considering a protein carrier induced an immune response as a T-cell epitope, Danishefsky and coworkers explored multivalent vaccines, compounds containing more than one antigen, to generate an even stronger immune response. One major shortcoming of previous studies was the lack of significant immune responses mediated by the T-cells likely resulting from the monovalency of the vaccine. They compared immune responses of vaccines, monomer **5** (Tn) to trivalent **7** (Tn (c)) (**Figure 1.1** and **Figure 1.2**),[9] in mouse hosts and analysis of the

serum by ELISA showed IgG tiers of 30 and 320, respectively, measured against desialylated ovine submaxillary mucin (dOSM; a natural source of Tn), and IgM ELISA titers of 40 and 1,280 for **5** and **7**, respectively. It was concluded based on these findings that multivalency has a crucial role in the immune response generated. They also reconfirmed in this study that KLH, elicited a better immune response than BSA. As mentioned above, it remained unknown whether these results were caused by less antigen conjugation to BSA compared to that of KLH; however, based on two different batches of Tn (c)- KLH tested, the authors state, that the "…method and intensity of conjugation plays a major role in increasing the immunogenicity of the antigen."

Danishefsky and coworkers continued the multivalency concept by designing and synthesizing the first multi-antigenic glyco-conjugates **8** and **9** (**Figure 1.3**).[10] These multi-antigenic constructs were conjugated to KLH, using the same linker as mentioned above, generating the desired vaccines which were then injected into mice. Overall the antibody titers generated in this study were quite low, however, it is interesting to note that antibodies were generated not only against the trivalent constructs but also against each individual antigen portion.[10] They also injected only the trivalent constructs as a control and found that only IgM type antibodies are induced further supporting that a protein carrier is required for the induction of a T-cell response. These findings suggested that combining different antigens, into a multi-component vaccine, which might be over-expressed on the surface of a certain cancer cell type, could help produce a stronger more efficient immune response than that of a monovalent antigenic vaccine. This earlier work describes multi-antigenic constructs as better mimics of the natural organization of the TACA environment on the surface of cancer cells. They predicted that the organization of the various over-expressed carbohydrate motifs on the cancer cell

surfaces is very heterogeneous much like a vaccine presenting multiple antigens. Furthermore, it was also mentioned that vaccine **9** generated a lesser immune response than that of vaccine **8**. Danishefsky's group also found that multiple α-O-linked GalNAc based glycans in the same construct results in an increase in structural rigidity.[11] These findings suggested that vaccine **9**, which contained these α-O-GalNAc linkages, should be more rigid than that of **8**, causing **9** to more closely match mucin glycoproteins. They suggested that this close similarity between the host mucin glycoproteins and the structural core of vaccine **9**, can prevent an immune response from being generated due to the immunological tolerance within the hosts, discussed above.

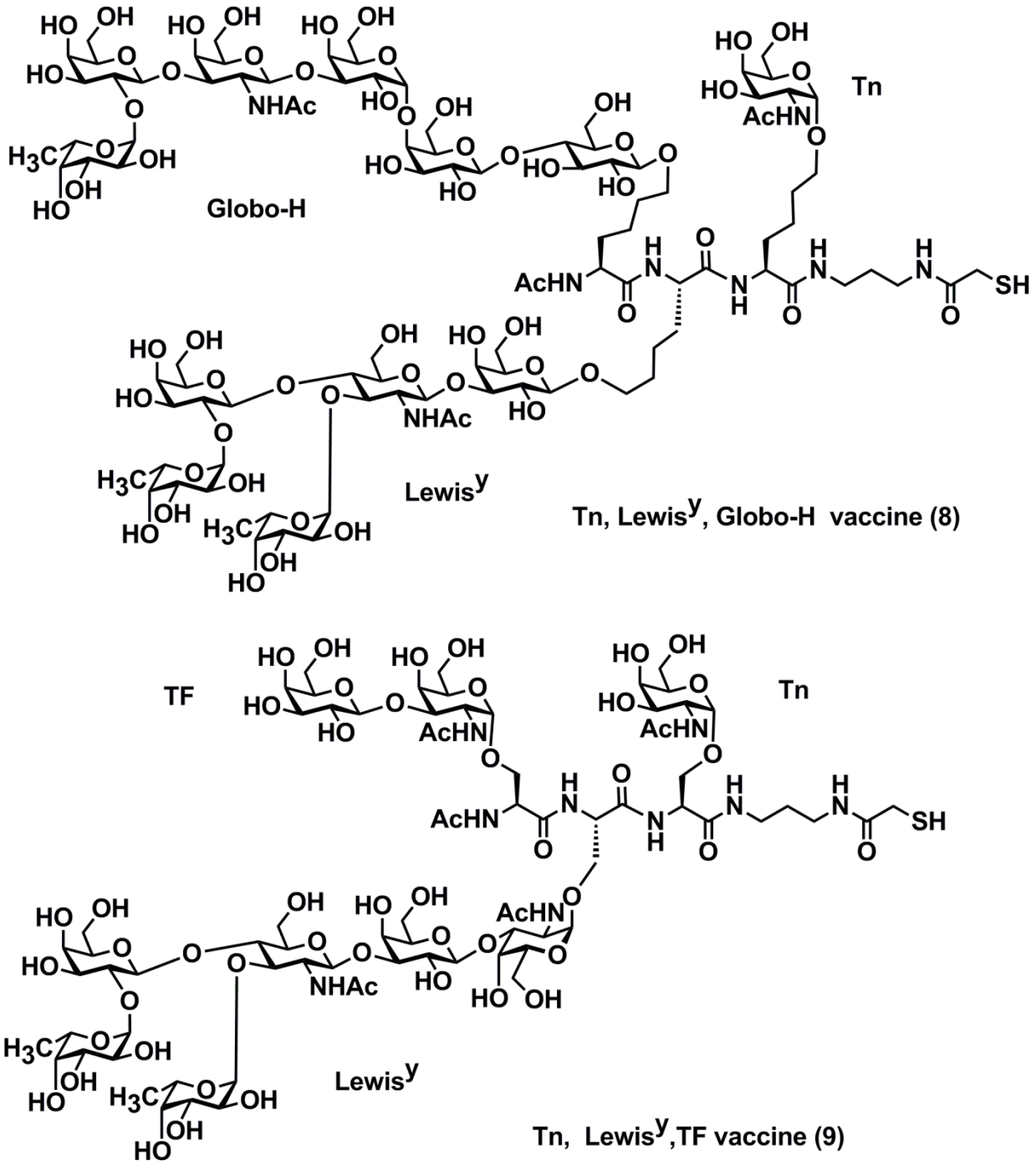

Figure 1.3: Unimolecular trivalent antigen constructs

The results from the proof-of-principle study encouraged Danishefsky et a. to synthesize a first generation unimolecular pentavalent construct displaying the Tn, TF, STn, Lewis^y, and

Globo-H antigens and unimolecular hexavalent construct containing the Tn, TF, STn, GM2, Lewis^{y}, and Globo-H antigens.[12] Modeling the assays used to test the immunogenicity of the trivalent constructs, antibodies were generated against each unimolecular multivalent vaccine, unfortunately the titers analyzed by ELISA were much lower than they had predicted. More recently, the same group synthesized a second generation unimolecular pentavalent construct displaying the Tn, TF, STn, GM2, and Globo-H antigens which is expected to enter phase 1 of clinical trials.[13] The synthetic effort accomplished in the foregoing studies to access a viable cancer vaccine is an amazing step forward in this field. As mentioned above, the IgG antibody titers expressed by the immune response were relatively modest; thus, additional research is needed to further increase the production of the desired IgG antibodies and, more importantly, the generation of long-term immunological memory.

Intrigued by the positive results of multi-antigenic vaccinations, Boons and co-workers tested whether the antibodies generated were against the entire construct, each individual antigen, or both. They synthesized the dimeric Lewis^{y}Lewis^{x} heptasaccharide construct (**10**) (**Figure 1.4**) and then conjugated it to the protein carrier KLH.[14]

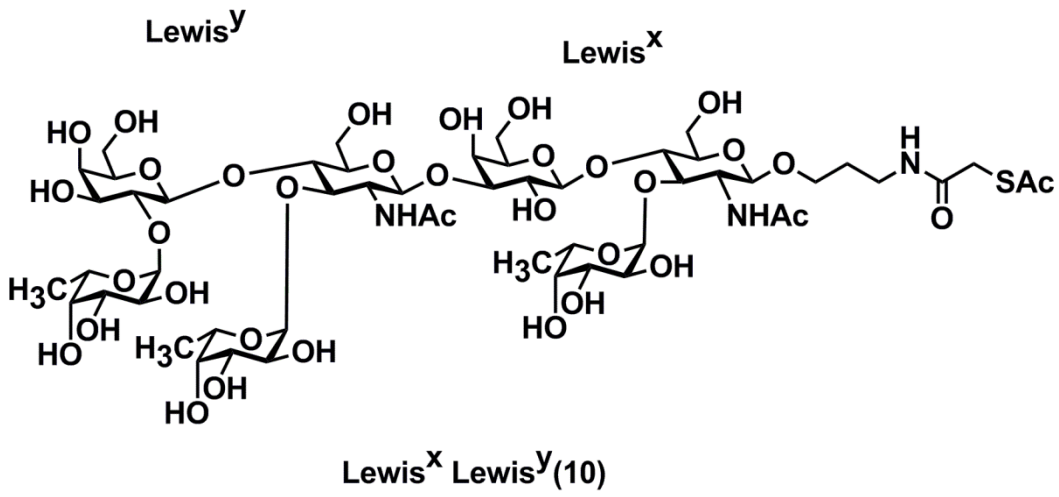

Figure 1.4: Dimeric Lewis^{x}Lewis^y antigen construct

Mice were immunized three times with compound **10** conjugated to KLH (KLH-**10**) and then, after ~28 days, sera were collected and ELISA was used to measure the antibody titers made against Lewis^{x}Lewis^y conjugated to BSA protein. ELISA plates were coated with BSA-Lewis^{x}Lewis^y instead of KLH-Lewis^{x}Lewis^y as to not potentially skew the data by measuring antibodies generated against the protein carrier. They measured titers of IgG (31,645) that were ~30 times higher than those of the IgM subtype (1,060). Next, they evaluated the cross-reactivity of antibodies from their sera samples isolated earlier against BSA-linked separately to either Lewis^x or Lewis^y antigens. Boon et al. hypothesized that titers against the individual antigens would be similar to those measured for the dimeric compound KLH-**10,** suggesting that the sera antibodies made against KLH-**10** also recognize the monomeric antigens with the same affinity. By contrast, however, IgG antibodies titers measured by ELISA against the BSA-linked Lewis^y antigen (3,115) were ~10-fold lower than that for the dimeric form (31,645): IgM titers were less than 120. By comparison, the titers of IgM for the BSA-linked Lewis^x antigen were

undetectable and those for IgG were at 500. These findings imply that it may be possible to design a specific vaccine to target a certain form of tumor. However, a major limitation to this approach is that to develop an efficient preventative vaccine would be daunting because several different forms of that exist. Even targeted treatment would have its major disadvantages; the design, synthesis, and manufacturing of the several specific compounds needed to address the specific cancer type would be overwhelming.

Another important contribution to the field by Boons and coworkers was their work on understanding how different linkers played a role in immunological responses. They wanted to determine how different linkers between protein carrier and TACA affected immune response.[15] They decided to use two different linkers, conjugating KLH to the Lewis^y tetrasaccharide. The first linker precursor they employed was 4-(maleimidomethyl)cyclohexane-1-carboxylate (**11**) because of its widespread use, and when incorporated into the final structure, it looks similar to the MBS linker used by Danishefsky's group (**Figure 1.2**). The second linker precursor choice was the smaller and more flexible 3-(bromoacetamido)propionate (**12**) (**Figure 1.5**).

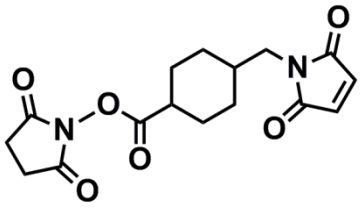

sulfo-SMCC (11)

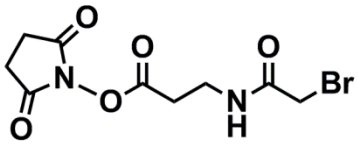

SBAP (12)

Figure 1.5: Maleimide and bromoacetamido linkers

In their first study, they injected the KLH-**11**-Lewis^{y} construct into mice, and sera were collected and analyzed by ELISA to determine antibody titers made against KLH-**11** alone the linker alone or the KLH-**11**-Lewis^{y} conjugate. They coated their ELISA plates with BSA-Lewis^{y} antigen conjugate, linked separately with each of the two linkers. BSA was used to avoid detection of anti-KLH antibodies. Although high IgG titers (358,928) against BSA-**11**-Lewis^{y} were induced, they later deduced through control experiments that only a titer of 120 was against the Lewis^{y} antigen.[15] During the conjugation, KLH was derivatized with linker **11** first, and then Lewis^{y} was added to the terminal end of **11**. This last reaction step is significant because any unbound linker would likely undergo hydrolysis to form maleamic acid (**Scheme 1.1**). Boons and coworkers had predicted the principally observed anti-linker immune response was caused by only the terminal hydrolyzed maleimides. To avoid this, they changed the order of steps in their synthesis by first coupling the linker to Lewis^{y} antigen followed by conjugation to KLH. This would ensure that there would be no hydrolyzed linker present. After inoculating this compound in mice and measuring titers by ELISA, they found that the IgG titers against the Lewis^{y} epitope were much better going from 120 to 10,066. Even with improvement in the immune response against the antigen epitope, titers against the linker were still ten times higher (106,894).

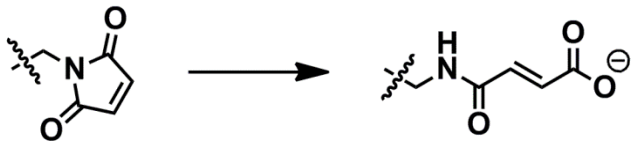

Scheme 1.1: Hydrolysis of the Maleimide linker

Linker **12** was used to construct KLH-**12**-Lewis^y, and this inoculum was injected into mice. The titers of IgG antibodies against BSA-**12**-Lewis^y were much lower (3,957) than when linker **11** was used, however, it is interesting to note that only about 17% (663) of these titers were generated against the linker. These results clearly showed the impact of the linker-type when trying to generate an immune response. If a linker induces a strong immune response, thus producing antibodies against it, then there is a good chance that a desirable immune response may not be generated against the lesser immunogenic TACA.

Others, like Kunz and coworkers, took a slightly more synthetically challenging approach to design and synthesize a vaccine that displays the STn antigen on a MUC1 (cell surface associated mucin type) B-cell epitope linked to a T-cell peptide epitope from tetanus toxin (ttx)[16] (**13**) (**Figure 1.6**) or ovalbumin (OVA)[17] (**14**) (**Figure 1.7**). Based on their findings after inoculating three mice with vaccine (**14**) (**Figure 1.7**), one mouse generated a significant immune response as measured by ELISA binding of the serum antibodies to MUC1-BSA coating the plates. More interestingly, the serum antibodies measured, after the third immunization, were significantly higher than those measured after the first and second, indicating that immunological memory was developing. To further verify the specificity of the antibodies generated, they tested the cross- reactivity of the serum samples to that of the tumor associated sialyl-Tn glycopeptide antigen (MUC1), an un-glycosylated MUC1 peptide antigen, sialyl-Tn

glycopeptides antigen variant (MUC4), and an un-glycosylated MUC4 peptide antigen. Based on their findings, it was determined that the antibodies were highly specific to the entire vaccine construct containing both carbohydrate and peptide sequence contained in vaccine **14** and not to the individual peptide or carbohydrate motifs.

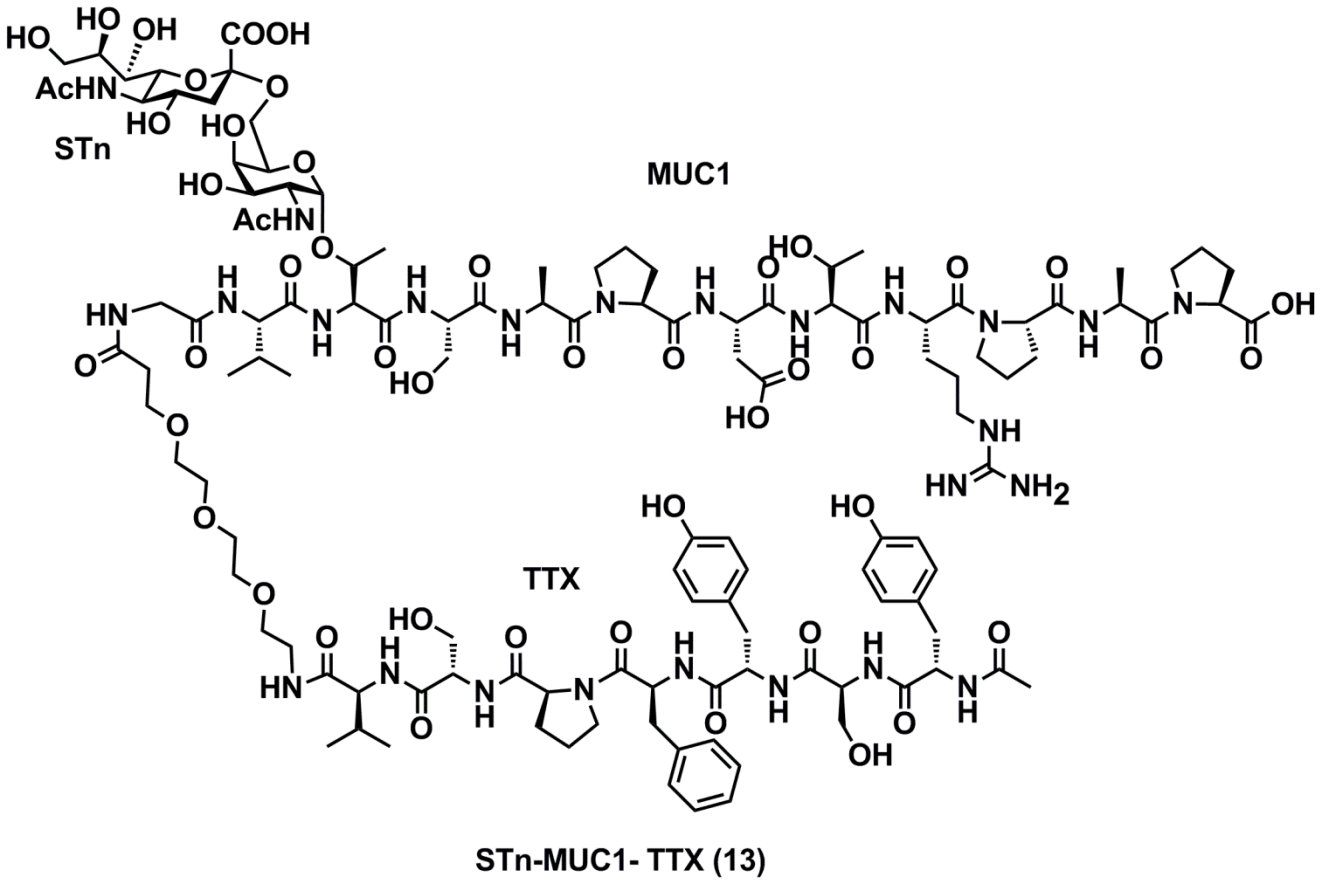

Figure 1.6: MUC1-STn construct **13**

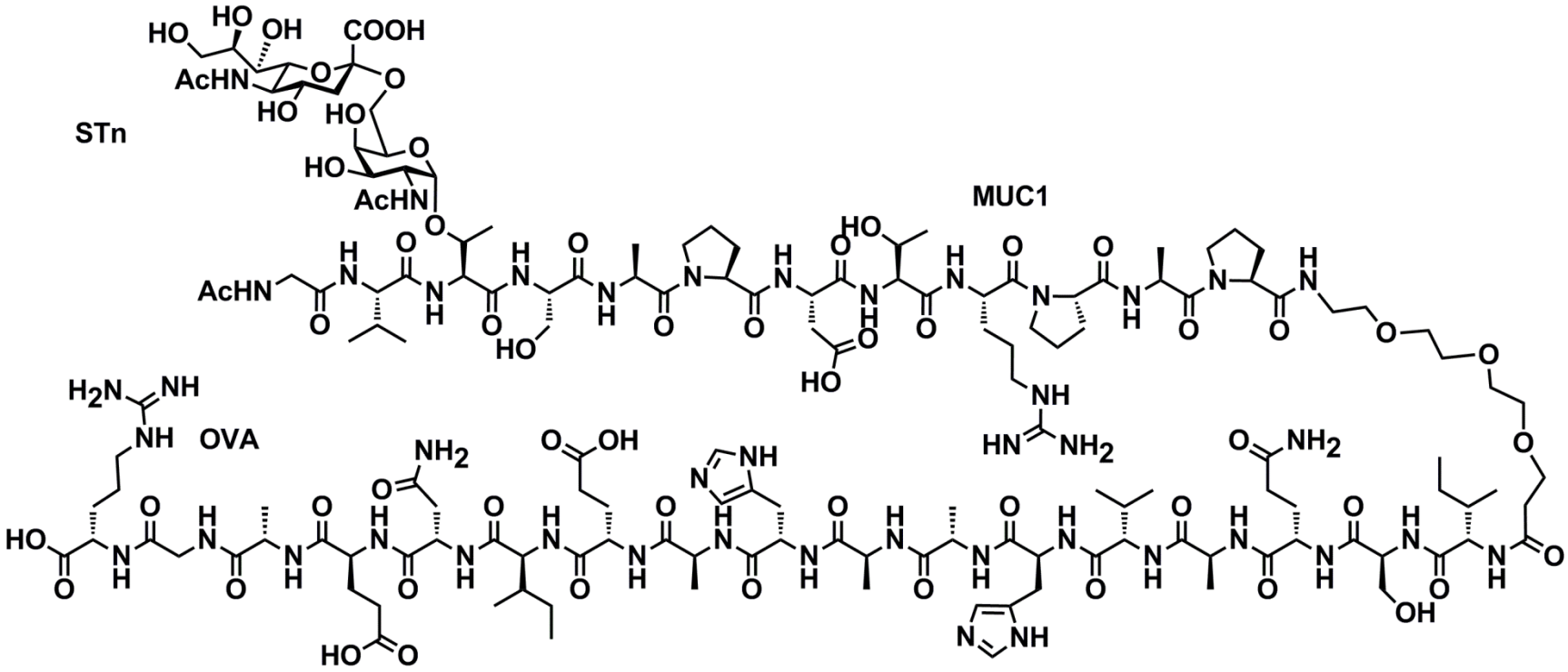

Figure 1.7: MUC1-STn construct **14**

Although not previously discussed, an adjuvant was used as a third component with each vaccine discussed above. Adjuvants are "substances used in experimental immunology and in vaccines to enhance the adaptive immune response to an antigen."[4] This prevents a vaccine from being cleared from the host prior to the immunological response. Boons and coworkers[18] designed and synthesized a vaccine that combined all three of these important parts into one complete construct, represented in construct **15**. Included were the Tn antigen as their B-cell epitope, the peptide YAFKYARHANVGRNAFELFL (YAF) as the T-cell epitope, and the lipopeptide Pam_3Cys which acts as an immuno-adjuvant (**Figure 1.8**).

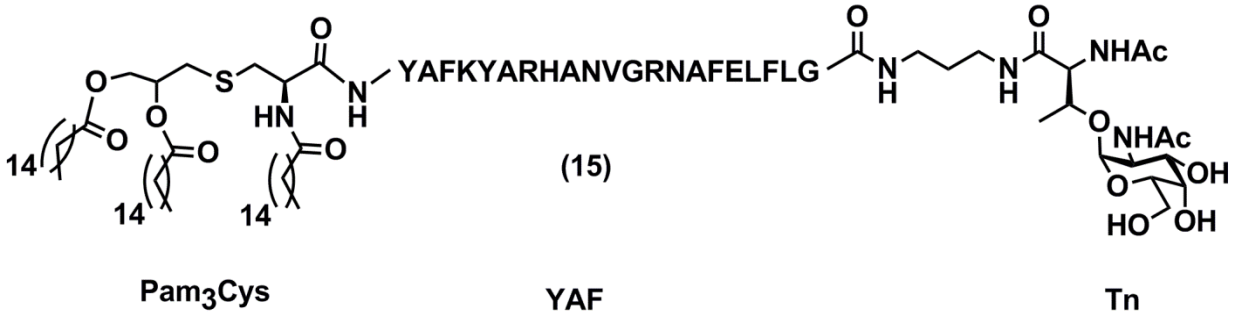

Figure 1.8: Structure of Boons' first generation three component vaccine (**15**)

Due to the low solubility of this compound, it was incorporated into phospholipid based liposomes and then used to inoculate mice. Interestingly, once the antibody titers from the sera were measured by ELISA against BSA conjugated to Tn bound to a 96- well plate, IgM and IgG titers were low, but produced nevertheless. More importantly, however, the IgG titer was higher than the IgM titer indicting that isotype class switch had taken place. With this encouraging proof-of-concept, Boons et al. synthesized a second-generation, three-component vaccine.[19] This vaccine construct was conceived from the first generation construct discussed above, and

varied only slightly. First, the YAF T-cell epitope, derived from the outer-membrane protein of *Neisseria mengitides*, was exchanged with a T-cell epitope with one derived from the polio virus (103-KLFAVWKITYKDT-115). Second, the Tn antigen used as the B-cell epitope was changed to a tumor associated glycopeptide derived from MUC1. And finally, the Pam_3Cys T-cell epitope was replaced with either Pam_2CysSK_4 (**16**) or Pam_3CysSK_4 (**17**) (**Figure 1.9**).

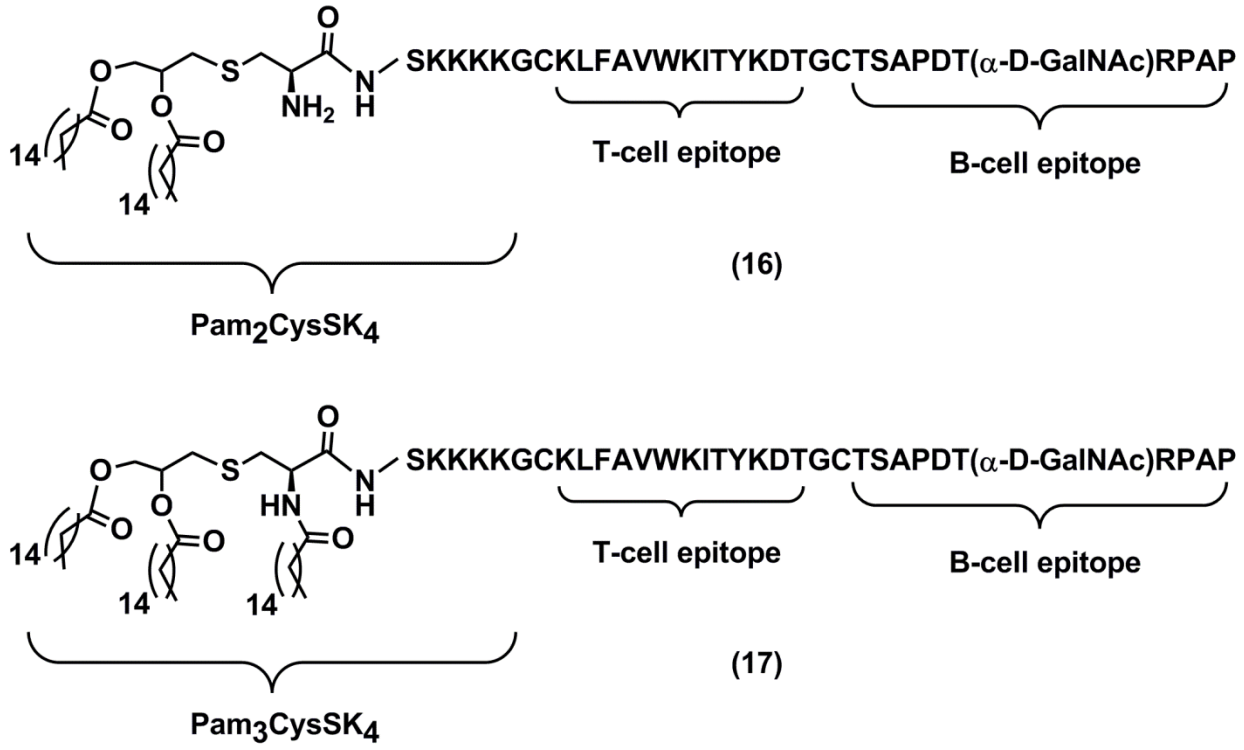

Figure 1.9: Boons' second generation three-component vaccine constructs **16** and **17**

After inoculating the vaccine constructs into mice with and without an additional adjuvant (QS-21), antibody titers were measured using ELISA plates coated with BSA-BrAc-MUC1. After four immunizations, the IgG titers (without adjuvant added) ranged from 20,900 for vaccine **16** to 169,600 for vaccine **17** (**Table 1.2**). In addition, it appeared that adding the

adjuvant helped to stimulate the generation of IgG titers, thereby indicating isotype switching of the B-cells

Table 1.2: IgM and IgG ELISA titers after vaccination with vaccines **16** and **17**

Immunization	IgM	IgG
Vaccine **16**	1,400	20,900
Vaccine **16** & QS-21	1,100	30,200
Vaccine **17**	7,200	169,600
Vaccine **17** & QS-21	5,000	322,800

Encouraged by these findings, Boons et al. tested the specificity of the IgG antibodies to the native MUC1 antigen present on cancer cells using flow cytometry. They found that the antisera elicited against vaccines **16** and **17** reacted very strongly to MCF7 human breast cancer cells which are known to express MUC1,[9] whereas they found no binding to SK-MEL-28 cell which do not contain MUC1. These results indicated that their vaccine construct was capable of not only generating high quantities of IgG antibodies but also that they were highly specific.

Lo-Man and coworkers have investigated an alternative approach that avoids the requirement of a protein carrier and thus takes advantage regioselectively addressable functionalized templates (RAFTS) (**18**) as display platforms for the Tn antigen (**Figure 1.10**).[20] This construct has the advantage over other protein carriers in that it is easier to control of the number of antigen copies being expressed, consequently allowing for better vaccine reproducibility during synthesis.

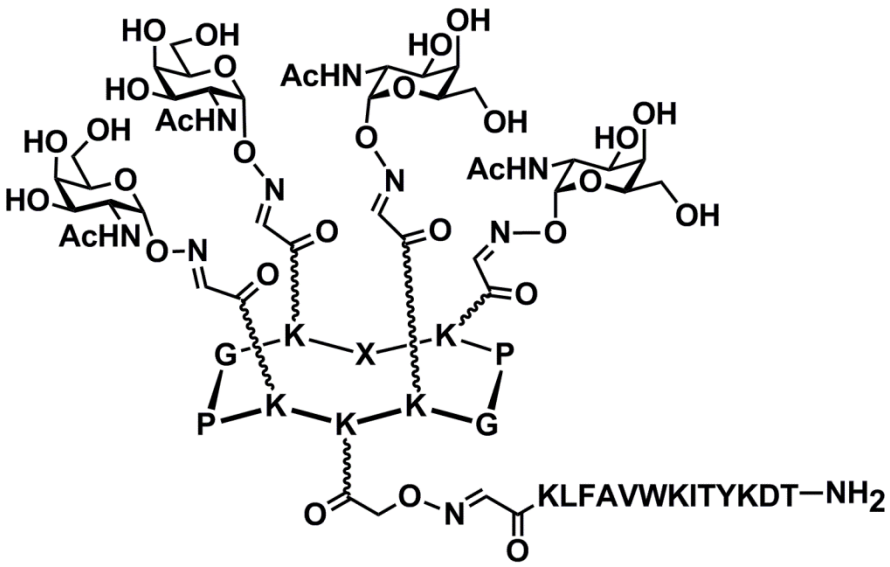

18a: X=A

18b: X=K($COCH_2ON=CHCO$-peptide-NH_2)

(18)

Figure 1.10: Structure of RAFT construct

1.3 The Tn Antigen

The Tn antigen was first reported in 1957 by Moreau, Dausset, and co-workers[21, 22] at a time when it was associated with an extremely rare disease "Tn syndrome," which can be characterized by the tendency of certain red blood cells to be agglutinated by all human sera, regardless of the ABO blood group involved.[23] In a study carried out by Dr. Hustings of the Swiss Red Cross in 1994, of 150,000 donated blood samples screened, all came back negative for the disease.[24] It was not until about 20 years after Moreau identified the Tn antigen that Springer and co-workers associated it to carcinoma and determined its structure.[25, 26] The native Tn antigen is characterized as GalNAc-α-O-serine/ threonine (**Figure 1.11**).

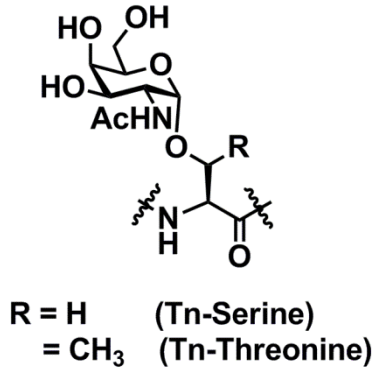

Figure 1.11: Native Tn antigen

1.4 Synthesis of Tn Analogs

The Tn antigen (**Figure 1.1** and **Figure 1.11**) is expressed on a number of different cancer cell types, primarily breast, colon, and prostate.[27] Notably, the Tn antigen, when administered alone, is not immunogenic. Therefore, to generate a desirable immune response, it is paramount to conjugate the Tn antigen to a protein carrier to elicit a T-cell mediated immune response. The protein carriers principally used in the studies described in this thesis were the tobacco mosaic virus (TMV), enterobacteria phage Qβ, and Keyhole Limpet Hemocyanin (KLH).

With this knowledge and understanding of the ongoing work within the field of immunotherapy, as well as the complexities behind the immune system, our lab developed several carbohydrate based vaccines. Each potential vaccine contained this Tn antigen conjugated to various protein carriers, in the presence of an adjuvant, in hopes of eliciting a strong humoral immune response. In the proceeding sections, these vaccines will be discussed in further detail, including their synthesis and analysis by *in vivo* immunological methods.

To conjugate the Tn antigen to TMV-1Cys, Qβ, BSA, and my desired glycopolymer, discussed later in **Section 1.5**, as well as to immobilize Tn on a 96-well plate for ELISA assays, Tn analogs **19 (**containing a biotin moiety), **20** (containing a terminal azide for crosslinking), and **21** (containing a terminal acryamide polymerization) were synthesized (**Figure 1.12**) from a common amine intermediate (**34**).

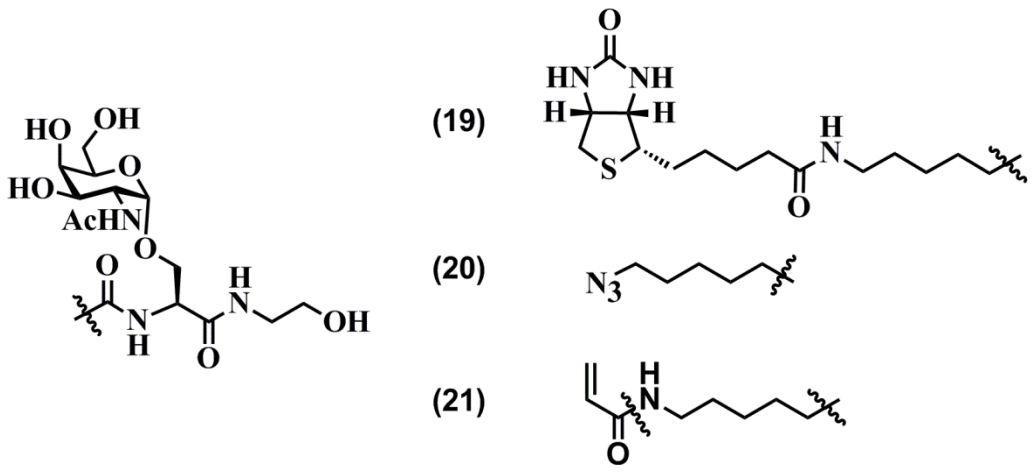

Figure 1.12: Tn analogs **19**, **20**, and **21**

Amine (**34**) was synthesized starting from the commercially available D-galactosamine hydrochloride **23**. Shelf-stable imidazole-1-sulfonyl azide hydrochloride **22** was used for diazo transfer[28] to make compound **24** (65% yield) (**Scheme 1.2**). Application of trifluoromethanesulfonyl azide more commonly used in the diazo transfer method was avoided since trifluoromethanesulfonyl azide can react explosively and needs to be freshly made each time. The white crystalline imidazole sulfonyl azide reagent **22** is advantageous since it is suitable for long-term storage and the risk of explosion is drastically reduced. Compound **24** was globally acetylated to afford **25** 85% yield. This step was generally quite slow and usually required addition of excess Ac_2O throughout the reaction.

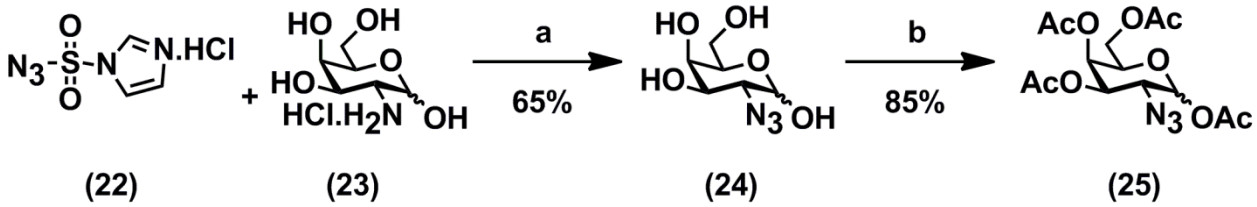

(22) (23) (24) (25)

Reagents and conditions : a) K_2CO_3, $CuSO_4$ * $5H_2O$, MeOH, r.t., 12 h
b) Ac_2O, py, cat. DMAP, r.t., 3-5 days

Scheme 1.2: Synthesis of globally protected **25**

Next, selective deacylation of **25** to liberate the anomeric hydroxyl group was accomplished using hydrazine acetate in DMF to yield **26**. Then, **26** was reacted under basic conditions with trichloroacetonitrile[29] to afford **27** in 79% yield over two steps (**Scheme 1.3**).

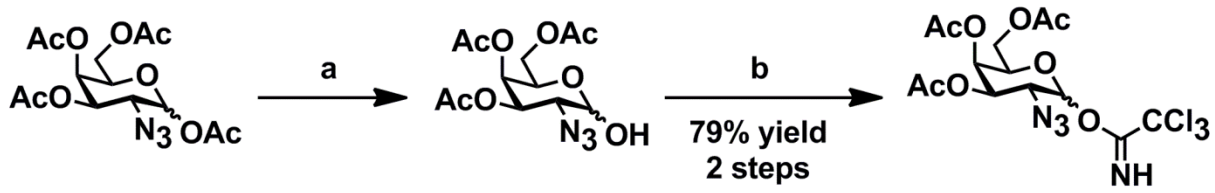

(25) (26) (27)

Reagents and conditions : a) Hydrazine acetate; DMF, r.t., 2 h
b) Cl_3CCN, K_2CO_3, DCM, r.t., ~15 h

Scheme 1.3: Synthesis of donor **27**

With donor **27** in hand, acceptor **29** was synthesized (94% yield) from the commercially available Fmoc-serine **28** by means of selective benzylation of the carboxylic acid residue using potassium bicarbonate, tetrabutylammonium iodide and benzyl bromine in DMSO (**Scheme 1.4**).[30]

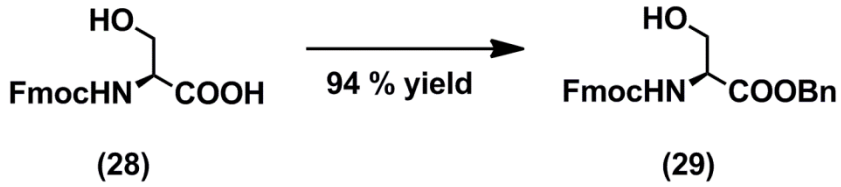

(28) **(29)**

Reagents and conditions : $KHCO_3$, TBAI, DMSO, then add BnBr, r.t., 20 h

Scheme 1.4: Synthesis of acceptor **29**

The native Tn antigen contains only the α-linkage at the anomeric carbon; therefore, the Schmidt's glycosylimidate synthetic strategy[31] was used to favor the formation of the α-anomer over the unnatural β-anomer in high yield.[29] Both donor **27** and acceptor **29** were desiccated under vacuum overnight and then added to a mixture of dichloromethane to ether (1:1, v/v) previously stirred over freshly activated AW-300 molecular sieves for 2 h to remove residual water which affects glycosylation (**Scheme 1.5**). The reaction was cooled to -30 ^{o}C (dry ice in acetonitrile) and then trimethylsilyl trifluoromethanesulfonate was added dropwise. The reaction was stirred for 30 minutes at -30 ^{o}C and then quenched with pyridine. The desired α-glycoside **30** was isolated in 71% yield. The Karplus equation[32, 33] was used to predict the 3-bond coupling constants of the proton at the anomeric carbon of the α-isomer (^{3}J predicted to be

larger) and β-isomer by NMR. The α- and β-isomers were identified using this estimation, and the ^{1}H NMR signals for the anomeric protons were integrated to calculate the ratio of α- to β-anomer at 4:1, regardless of the scale of the reaction (tested ≤2.5 g scale). Based on precedents within the Huang group,[34] a one pot reaction containing zinc dust, acetic anhydride, and acetic acid was employed to reduce and acetylate azide **30** to the fully protected Tn building block **31,** obtained in 93% yield after ~15 h.

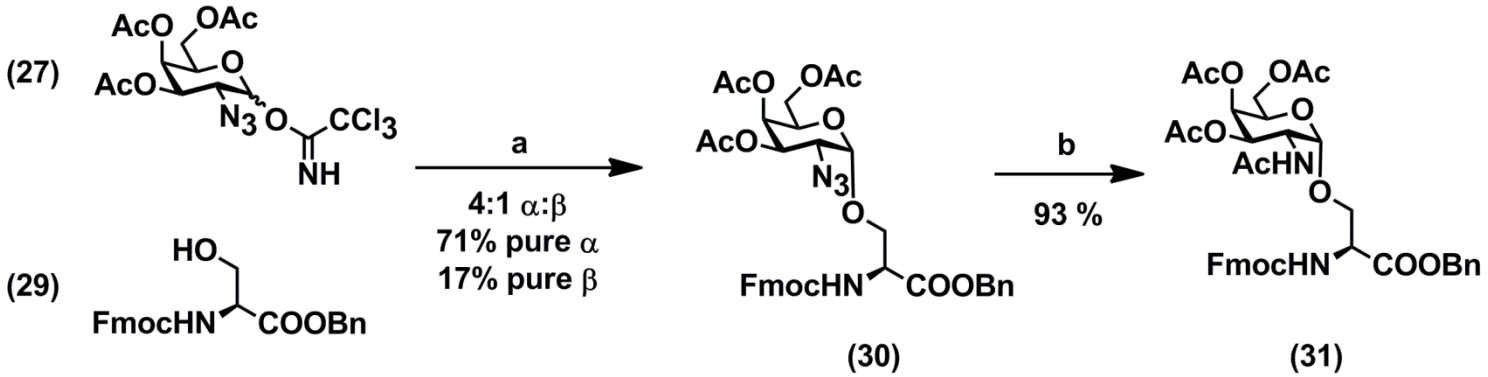

Scheme 1.5: Synthesis of fully protected Tn building block **31**

The next step in this reaction required cleavage of the benzyl ester by catalytic hydrogenolysis: a step which was closely monitored to avoid concomitant removal of the Fmoc protecting group. Initial attempts at hydrogenolysis without acetic acid, used generally to speed up hydrogenation reactions, unfortunately, resulted in significant benzyl and Fmoc removal within 15-20 mins as assessed by TLC analysis. This was surprising since Fmoc is cleaved under basic conditions and the reaction pH was near neutral. Therefore, the pH of the reaction was decreased to 3-4 with acetic acid to prevent Fmoc cleavage. It appeared that acetic acid may have increased the reaction rate only slightly, but, more significantly, prohibited the deprotection of the Fmoc group. Under these conditions and monitoring the reaction progress by TLC, the benzyl ester was removed after 15-30 min to produce the free acid **32**. This free acid was purified by silica gel flash column chromatography using a DCM:MeOH:AcOH (94.5:5:0.5, v/v/v) to yield **32** in 92% yield (**Scheme 1.6**).

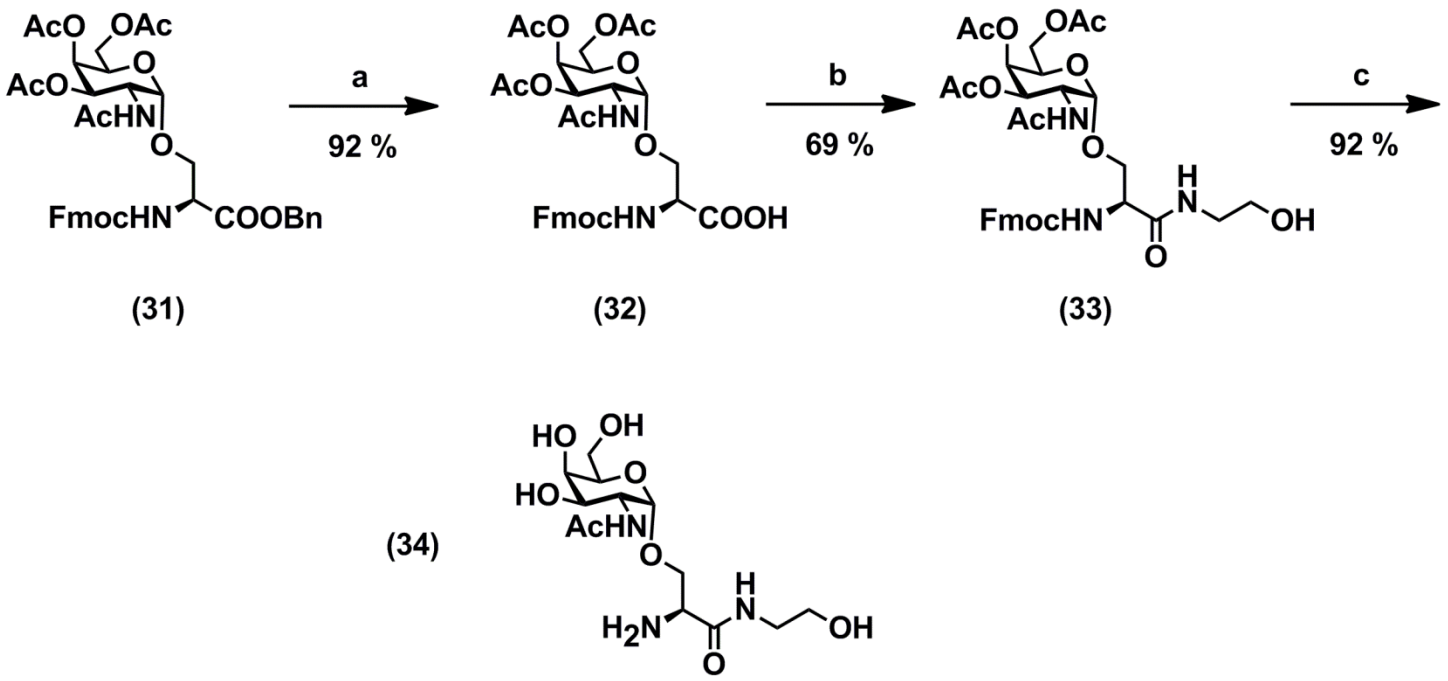

Scheme 1.6: Synthesis of deprotected common intermediate **34**

Ethanolamide **33** was made by reacting **32** with ethanolamine. This cap was chosen to help increase the product solubility in the hydrophilic *in vivo* environment; moreover, it was deemed non-antigenic, and thus the immune response could be localized on the carbohydrate moiety. The acid was pre-activated for 1 h with benzotriazole-1-yl-oxy-tris-(dimethylamino)-phosphonium hexafluorophosphate (BOP) in the presence of dichloromethane: THF (1:1, v/v) and DIPEA. Once activated, ethanolamine was added, and the reaction was stirred 2-5 h until completion, as monitored by TLC. This target **33** was purified by silica gel flash column chromatography using either DCM:MeOH (19:1, v/v) or acetone: toluene (3:2, v/v) leading to 69% yield of **33**. Although the final global deprotection was rather straight forward, it was essential to use concentrated ammonia in methanol. Early attempts using dilute 2M ammonia in methanol resulted in very low yields, even after 24-48 h. By contrast, the reaction proceeded smoothly when 7N ammonia in methanol solution was used, resulting in **34**. Compound **34** needed to be >99% pure prior to its use to make the final Tn analogs so that purification of the latter were simplified. Compound **34** was purified by silica gel column chromatography using a DCM:MeOH:NH_4OH (5:3:1, v/v/v), resulting in 92% yield. The overall yield of the 9-step synthesis of **34** starting from the commercially available D-galactosamine hydrochloride was ~17%.

With the desired building block in hand, compounds **19** and **20** were synthesized. The biotinated analog **19** was prepared by adding commercially available biotinated amino caproic acid N-hydroxysuccinimide ester (**35**) to **34** in NMP (**Scheme 1.7**) and stirred for 15 h. The crude mixture was purified by precipitation using ether followed by silica gel column chromatography using a DCM:MeOH:H_2O (60:34:6, v/v/v), and compound **19** was obtained at 57% yield. The relatively low yield was likely caused by a minor impurity ($\leq$ 5%), undetectable

by ^{1}H NMR, with the similar R_f as the starting material (**34**) on TLC. This impurity was later discovered by TLC analysis of the starting amine (thought to be pure) when 6% (by volume) water was added to the eluent. Compound **19** was used to coat the 96-well plates to quantify antibody titers by ELISA, as discussed later in this chapter.

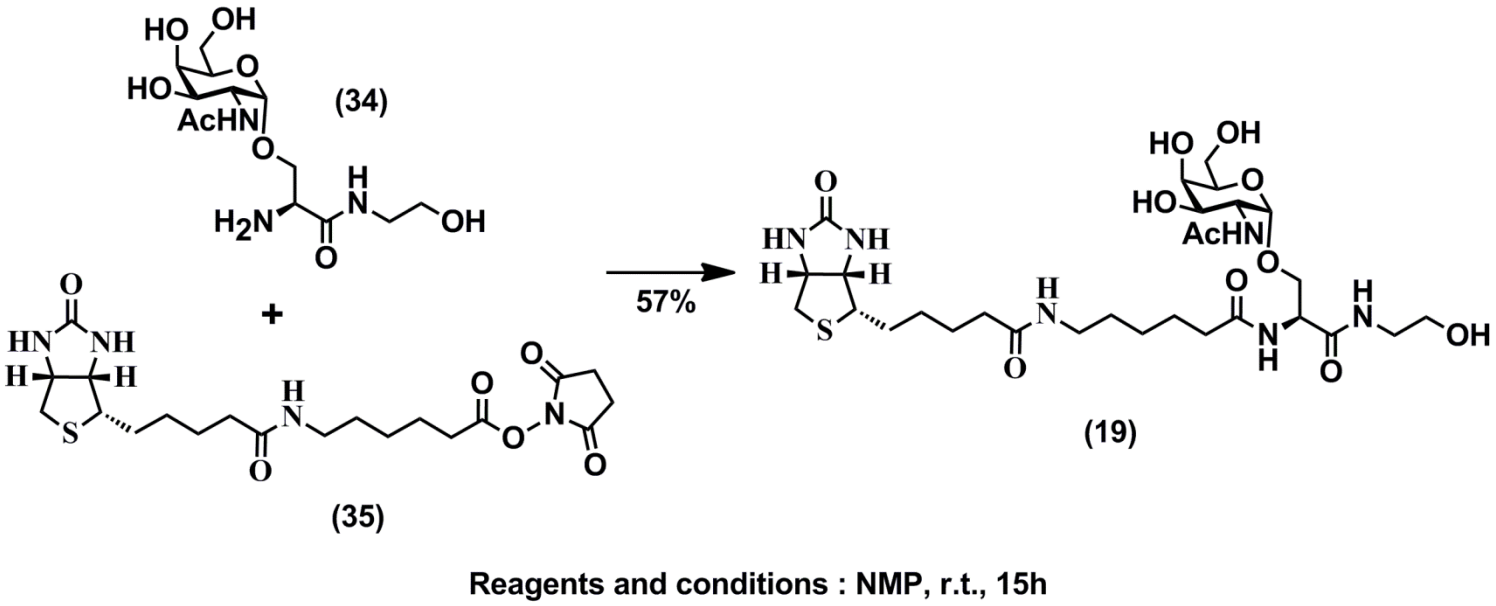

Scheme 1.7: Synthesis of Tn analog **19**

The next target Tn analog synthesized was **20**. This compound required the synthesis of the 6-azido caproic acid linker (**37**) (**Scheme 1.8**) from the commercially available 6-amino caproic acid (**36**). This was accomplished in 66% yield using the imidazole-1-sulfonyl azide hydrochloride (**22**) method.[28]

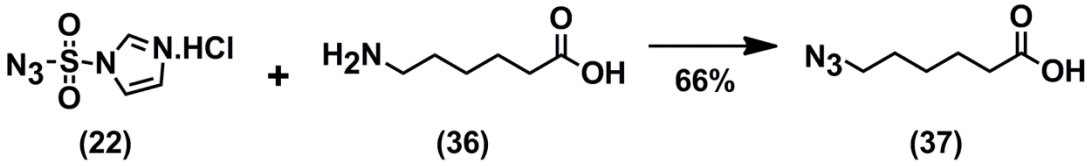

(22) **(36)** **(37)**

Reagents and conditions : K_2CO_3, $CuSO_4$ * $5H_2O$, MeOH, r.t., 36 h

Scheme 1.8: Synthesis of azido linker **37**

Linker **37** was synthesized and coupled to free amine **34** by the classic amidation reaction conditions using BOP, HOBt, and DIPEA in NMP and stirred at room temperature (**Scheme 1.9**). The desired azido compound (**20**) was synthesized in 94% yield after reaction overnight. Some of this compound was sent to our collaborators at the Scripps Research Institute, M.G. Finn and coworkers. They conjugated this compound to a mutant strain of the tobacco mosaic virus (TMV) which will be discussed in more detail in a later section of this chapter.

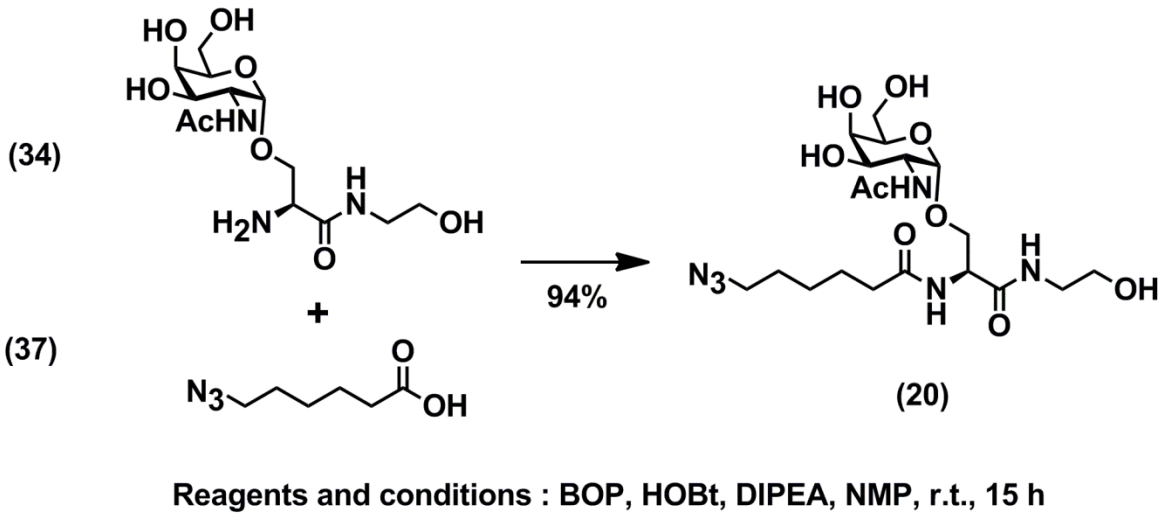

Scheme 1.9: Synthesis of Tn analog **20.**

Our group also wanted to expand on the previous research and knowledge on the multivalency effect, discussed in the introduction. Although an immunological response may be produced when monovalent Tn subunits are attached to the surface of a protein carrier, a multivalent glycopolymer construct might generate and even greater response. This synthesized construct (see target vaccine **38** in **Figure 1.13**) could then be attached to a carrier protein increasing the number of carbohydrate motifs presented to the immune system. Thus, the multivalent glycopolymer could potentially cause more isotype switching and induce immunological memory than the monovalent cognate.

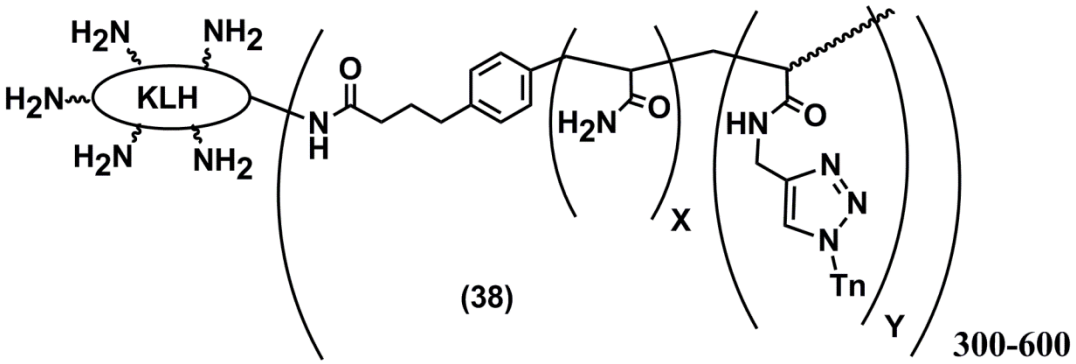

Figure 1.13: KLH conjugated to glycopolymer based vaccine **38**

1.5 Synthesis of the Glycopolymer

Several polymerization methods exist such as the well known atom transfer radical polymerization[35] (ATRP), reversible addition-fragmentation chain transfer,[36, 37] and nitroxide-mediated polymerization.[38] Because of the harsh reaction conditions and the challenging synthetic nature of these previous methods, we used a cyanoxyl-mediated free radical polymerization method established by Dr. Elliot Chaikof.[39-42] This method called for milder reaction conditions at reduced temperatures and water as the solvent. The latter was worthwhile since fully deprotected sugars could be dissolved in the reaction medium to facilitate their coupling to the polymer. By contrast, several other techniques needed to employ the protected sugars due to compatibility in organic media. In addition, Chaikof's research group found that these cyanoxyl persistent radicals react with controlled polymerization, making it an attractive method.

Construction of the polymerizable subunit **21**. We imagined that compound **21** (**Scheme 1.10**) could be generated by a simple amidation reaction between glycomonomer **34** and linker **39,** which contained a terminal end primed for polymerization. Compound **39** could, in turn, be generated by reaction of 6-amino caproic acid (**36**) with acrylic acid, acrylic anhydride, or acryloyl chloride. After trying many different conditions and routes, it became clear that the synthetic route to linker **39** was not feasible, due to, primarily, self polymerization of the reagents and product. It was evident that this problem was occurring during the reaction, the work up, and the brief storage periods. A concern was that self-polymerization of **39** would cause low yields from the reaction coupling of Tn compound **34** with **39** in the next step.

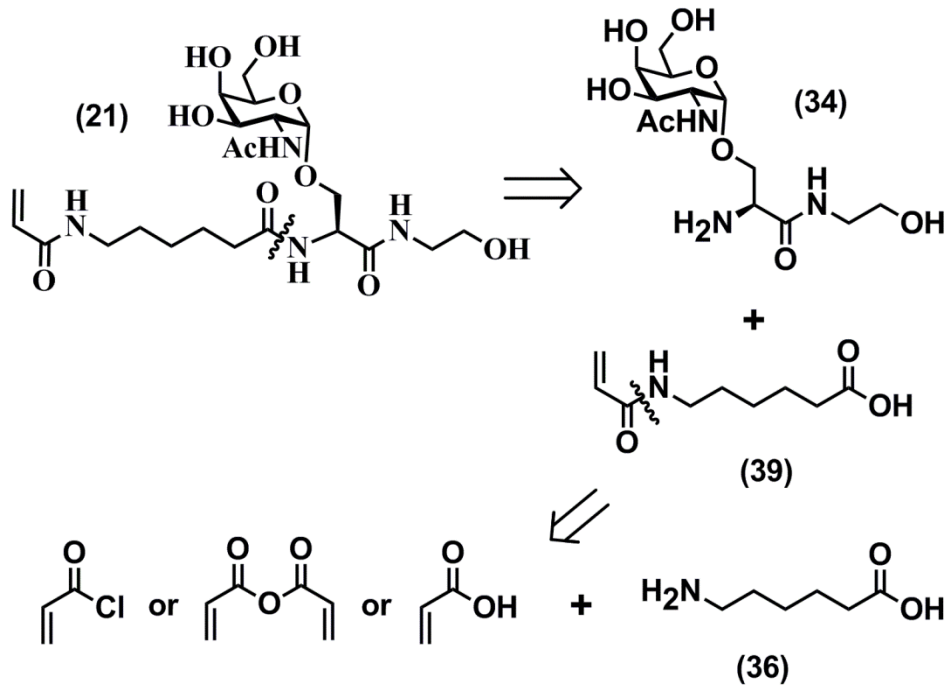

Scheme 1.10: Retrosynthetic analysis of polymerizable design of **21**

Alternative polymerizable design. Thus, an alternative synthetic approach was designed so polymerization occurred prior to addition of the Tn analog. (Trimethylsilyl)propargyl acrylamide (**42**) (**Scheme 1.11**) was selected as our polymer precursor, since it could be copolymerized first, after which, click chemistry could be used to conjugate the glyco-monomer to the alkyne moiety. Using procedures previously established by Professor Craig Hawker and coworkers,[43] the synthesis of **42** started by adding to a solution of propargyl amine (**40)** (commercially available) in dichloromethane was added DIPEA (at 0^{o}C), and then acryloyl chloride was added (**Scheme 1.11**). After work up and purification, propargyl acrylamide (**41**) was obtained in 84% yield. To prevent the terminal alkyne of **41** from participating in the polymerization process, a solution of **41** in dichloromethane was treated with DBU, silver chloride (to activate the alkyne), followed by slow addition of TMS-Cl; the reaction was heated

at 45 ^{o}C for ~1 day. Although the yield of this protection (**Scheme 1.11**) was only 57%, it was ~25% higher than that reported in the literature (32.9%).[43] Based on the TLC analysis it appeared as though a large amount of starting material (**41**) remained in the product mixture. I believe that this step may be reversible due to the reaction conditions, because even when more TMS-Cl was added, the reaction did not proceed further. It is likely that the silver in the reaction is driving this reversibility.[44]

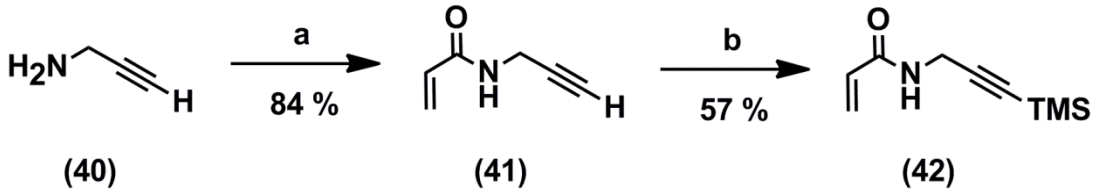

Reagents and conditions : a) DIPEA, DCM cool to 0 ^{o}C; then add acryloyl chloride, r.t., 20 h

b) DBU, AgCl, DCM, r.t., 30 min; then TMSCl, 45 ^{o}C, 22 h

Scheme 1.11: Generation of TMS protected propargyl acrylamide

With (trimethylsilyl)propargyl acrylamide (**42**) in hand, the next step was to copolymerize it with acrylamide using the cyanoxyl-mediated free radical polymerization technique. Carboxylic acid **43** was selected since it would ultimately conjugate the polymer to the protein carrier KLH, which contains free amines, and the aryl amine functional group was used to generate the arenediazonium salt **44** to initiate polymerization. The radical based reaction was carried out under an argon atmosphere, since it was sensitive to oxygen. Commercially available 4-(4-aminophenyl) butyric acid (**43**), sodium nitrite, and a 50% flouroboric acid solution were added to a 1:1 mixture of H_2O and THF (THF helps with the solubility of the (TMS) propargyl acrylamide (**42**)) and cooled to 0 ^{o}C for 30 min (**Scheme 1.12**). The reaction flask was opened briefly to add the sodium cyanate, (TMS) propargyl acrylamide (**42**), and the acrylamide to reduce their exposure to air. The reaction flask was resealed, evacuated, and filled with argon. The reaction was heated at 50 ^{o}C for ~16 h. This generated the cyanoxyl radical intermediate **45** *in situ*, which allowed the polymerization to occur.

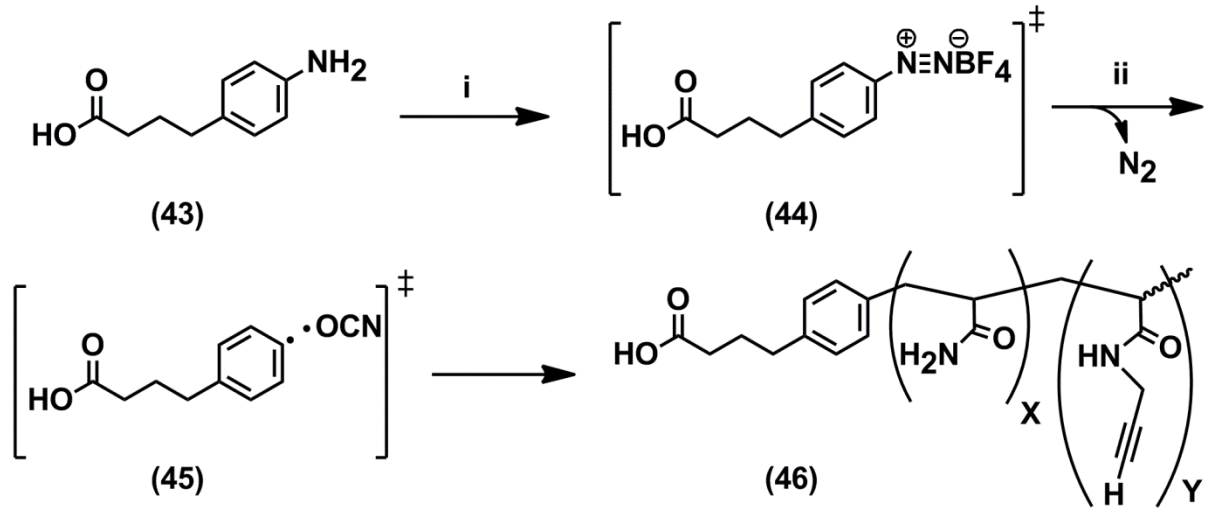

Reagents and conditions : i) $NaNO_2$, 50% HBF_4, THF/ H_2O (1:1), 0 ^{O}C, 30 min
ii) cat. NaOCN, (TMS) propargyl acrylamide (42) [10 eq],
acrylamide [40 eq] 50 ^{O}C, 16 h

Scheme 1.12: Synthesis of copolymer **46**

To calculate the approximate yield of this reaction, complete incorporation of compound **43**, (TMS) propargyl acrylamide (**42**), and acrylamide, and complete deprotection of the TMS protecting group were assumed. This was an interesting and exciting observation based on NMR analysis of the final polymer **46**. Apparently, during extended reaction times, majority of the TMS was deprotected. With those assumptions, yields were generally very low (ranging from 15-25%). One source of the low yield could be atmospheric oxygen dissolved in the reaction solvents. Removal of this residual oxygen by degassing might improve the polymerization yield. Recently, after discussing this issue with a member of Professor Xue-Long Sun's group at Cleveland State University, the low yields were considered a consequence of the purification method and not from reactive oxygen. Professor Sun's group informed me that they too had similar low yields following this technique. They were able to drastically enhance their isolated

yields by evaporating all THF from the reaction and then dialyzing in pure water. Thus, dialysis over 3-4 days was used to separate the un-polymerized components of the reaction. Sun's group informed that THF does not appear to affect the integrity of the membrane, based on visualizing by sight, but low recovery from the dialysis step indicated that larger polymers escaped the dialysis tubing. Regardless of the low yields, polymers **46A** (50 mg), **46B** (24 mg), and **46C** (134 mg) (**Figure 1.14**) were obtained via coupling of the alkyne substituents, added at various ratios. These ratios were determined by integrating the area under the broad peak at ~1.75 ppm (corresponding to CH_2 of polymer backbone), the broad peak at ~2.25 ppm (corresponding to CH of polymer backbone), the peak at ~2.75 ppm (corresponding to CH of alkyne), and the peak at ~4.0 ppm (corresponding to CH_2 of propargyl amide substituent). [See **Figure 1.42** in the Appendix for a visual representation of this.] These chemical shifts values corresponded nicely with analogous polymers synthesized by Chaikof et al.[39-42] The number of propargyl amide substituents were determined based on the integration of the peaks coming around δ 2.5 and 3.8. By subtracting the number of CH's from the integration of the broad peak ~2 ppm, the number of acrylamide substituents incorporated into our polymer was determined. We normalized our peak integration to the small aromatic peaks at ~7.25 ppm (4 protons).

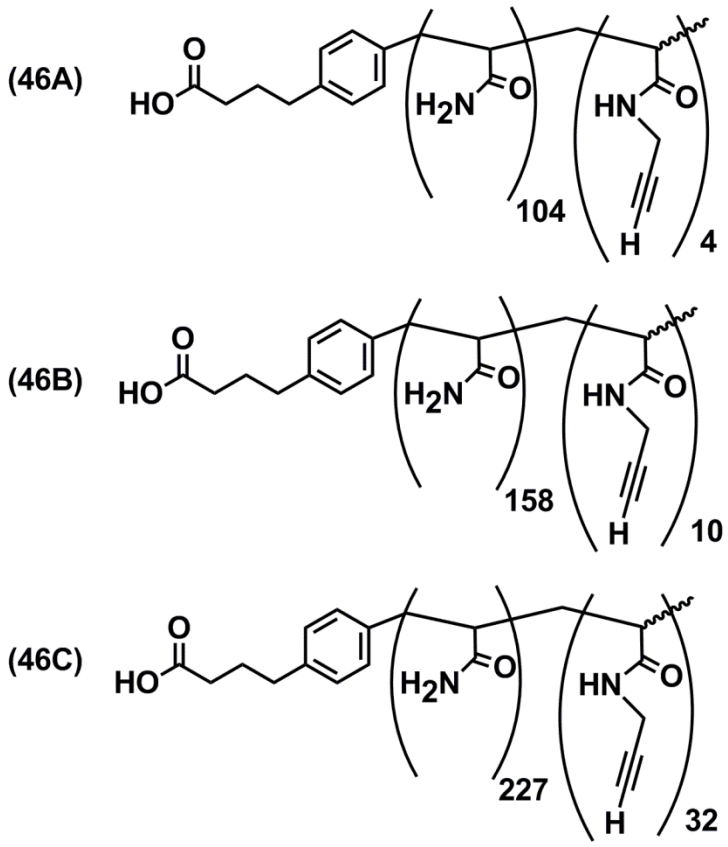

Figure 1.14: Structures of polymers **46A**, **46B**, and **46C**

*Addition of Tn antigen **20** to polymer 46A, B, and C.* A classic click condition optimized by Professor Morten Meldal and coworkers was used for this polymer coupling reaction with an analog of the Tn antigen (**20**) (**Figure 1.12**).[45] To a mixture of the alkyne polymer (**46A** or **46B**) and the azido Tn analog (**20**) in DMF were added CuI and diisopropylamine, and the reaction was stirred for ~4 days. After dialysis and purification, glycopolymer **47B** (12 mg, 79% yield) was obtained (**Scheme 1.13**); glycopolymer **47A** (14 mg) was obtained in similar yields (**Figure 1.15**). The extent of this click coupling was determined by comparing the integration of the carbohydrate protons to those protons corresponding to the polymer backbone and propargyl amine linker discussed above. A proof of an immunogenic response by **47A** and **47B** in mice

will be evaluated prior to constructing glycopolymer **47C** to conserve azido analog **20** because of the amount required for polymer cycloaddition.

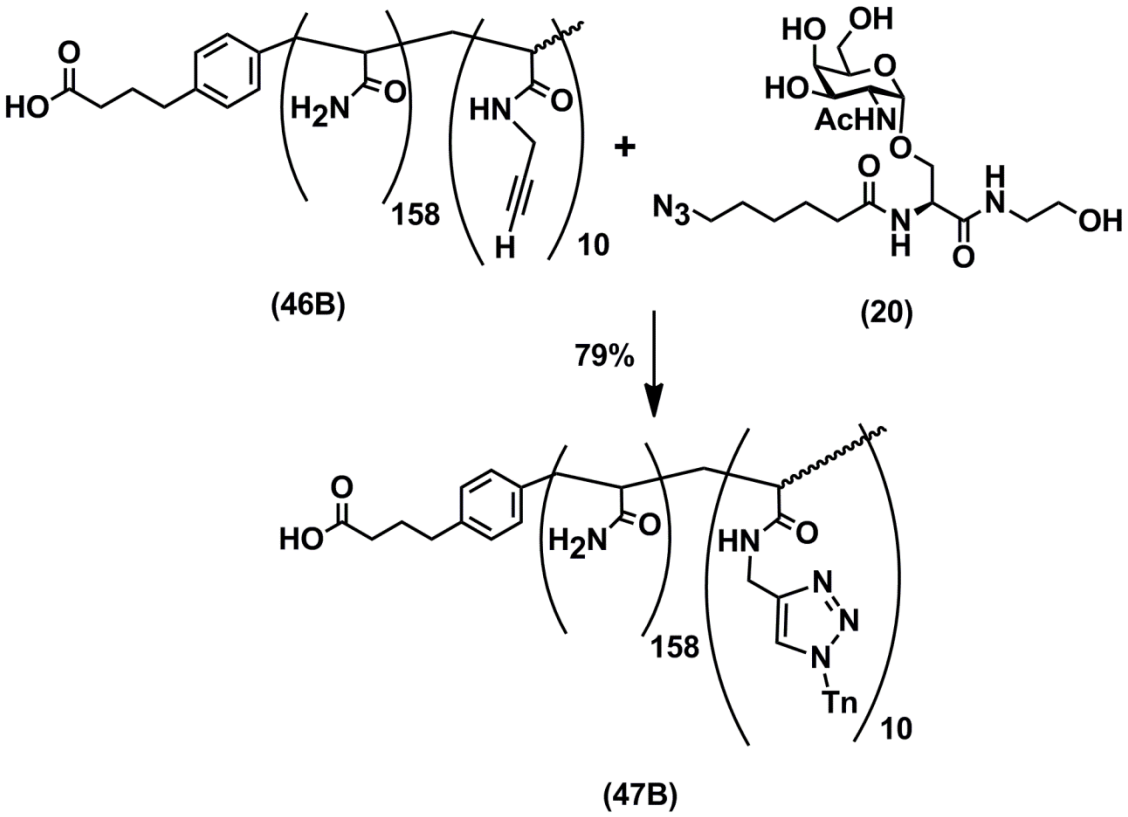

Scheme 1.13: Synthesis of glycopolymer **47B**

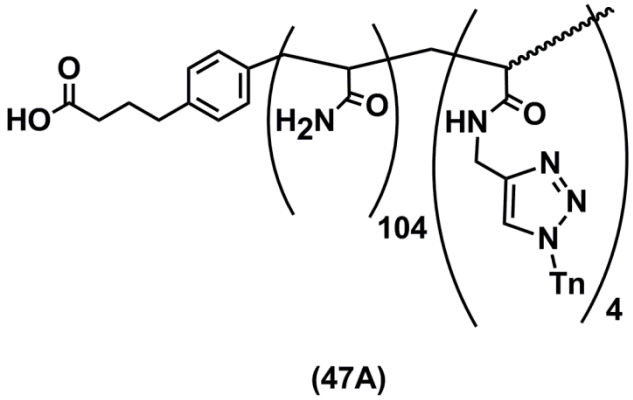

Figure 1.15: Structures of glycopolymer **47A**

1.6 Conjugation to KLH

The desired glycopolymers **47** were synthetically coupled to KLH protein by standard 1-ethyl-3-(3-dimethylaminopropyl) carbodiimide (EDC) coupling conditions.[46] A glycopolymer **47** was first activated with EDC under acidic conditions, which generated a highly reactive o-acylisourea intermediate. The KLH protein expresses over 2,000 free amines from lysine residues on its surface.[46] Many of these lysine groups are not accessible for reaction with the activated carboxylate due to the sterics of the protein conformation. It was predicted then, that only about 300 to 600 residues are actually exposed for reaction. Assuming complete conjugation to all accessible residues (300-600) of KLH (8,000-9,000 kDa) by the glycopolymer (~13 kDa) results in a massive and intricate glycopolymer complex (**38**) (**Scheme 1.14** for an example). Thus, characterization by standard NMR or mass spectrometry determination techniques is precluded.

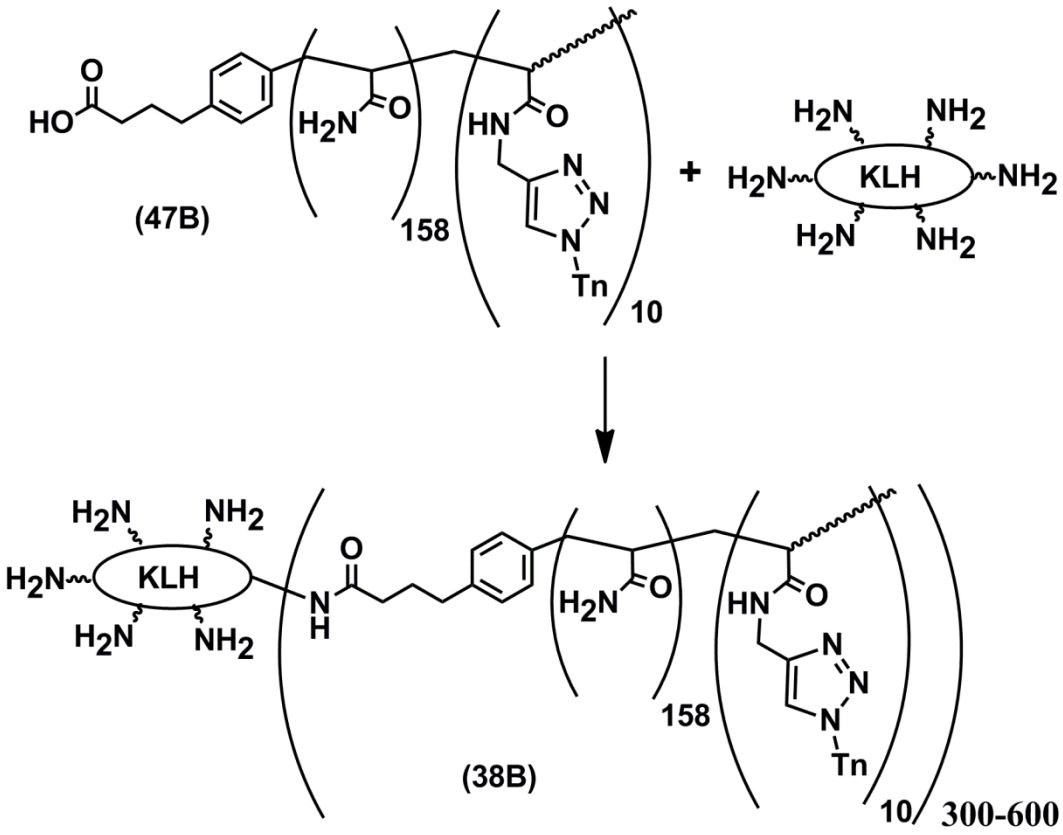

Scheme 1.14: Synthesis of KLH conjugated glycopolymer vaccine **38B**

Also since the exact molecular weight of the glycopolymer vaccine is unknown, size separation of the unbound KLH and bound KLH is not practical. However, dialysis was effective to remove any unbound glycopolymer, but it must be noted that during this process, a 1M sodium chloride solution was used. Dialysis in pure water caused the KLH protein and/or KLH conjugated glycopolymer to precipitate; these precipitates were impossible to re-dissolve into solution. A colorimetric assay based on the phenyl sulfuric acid method[47] was employed to quantify KLH-associated complexes in the current study. The same protocol could be used to hydrolyze the sugar groups from the KLH conjugated vaccine, and the quantity of liberated sugar

could be calculated by the colorimetric assay by comparison to a standard curve correlating sugar concentration and absorbance. A standard curve for galactose concentration against absorbance (A_{490}) constructed by the Dubois method in our lab were comparable (**Figure 1.16**) to those previously reported.[47] The limitations of this method quickly became evident when very low concentrations (<30 μg/ mL) of KLH gave very high absorbance measurements in comparison to the individual sugars. This was not surprising since KLH is a glycoprotein containing a very large diversity of sugars, including GalNAc, on its surface that can be hydrolyzed off. Different sugar types have been found independently by our group, and earlier by Dubois, to produce significantly different absorbance maxima (e.g., GalNAc and galactose shown in **Figure 1.16**), even when the same concentrations of carbohydrate were used. This may suggest that the carbohydrates on the surface of KLH produce a higher absorbance response than that of GalNAc. The other possibility is that the KLH protein produces a significant amount of color. The issue these findings present is that even if our Tn antigen was successfully conjugated to KLH, it is extremely likely that the absorbance of KLH would mask that of GalNAc contained within the Tn antigen.

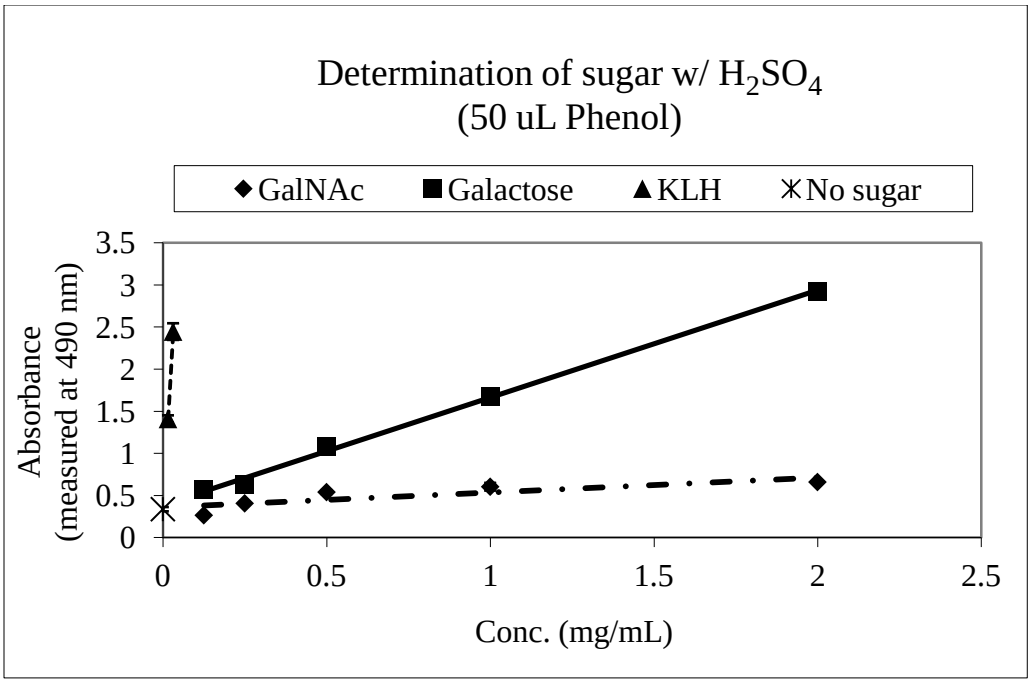

Figure 1.16: Standard curves for KLH and respective sugars

An alternative colorimetric method was tried that employed 1,3-dihydroxynaphthalene to selectively increase the absorbance of GalNAc over background signal. However, this method resulted in an even less distinguishable response than the phenol sulfuric acid method discussed above. The results prompted a survey of an extremely sensitive method, reported by Jahnel and coworkers, in which high performance anion exchange chromatography with pulsed amperometric detection (HPAE-PAD) of the effluent was used to quantitate carbohydrates.[48] Full analysis of the KLH-conjugates has yet to be determined, but, based on preliminary data, this technique does allow for detection of GalNAc and separation of the different carbohydrates derived from KLH after hydrolysis, even at extremely low concentrations. Once the identities of **38A** and **38B** are characterized, demonstrating successful conjugation, the two KLH-conjugated glycopolymer vaccines (**38A** and **38B**) and the third KLH conjugated glycopolymer (**38C**), yet to be synthesized, will be dissolved in PBS buffer mixed with an adjuvant and used to inoculate

mice. It is hypothesized that these multivalent glycopolymer constructs can elicit strong immune responses.

1.7 Conjugation to TMV and Immunological Studies

Based on previous work carried out within our group,[49] it was determined that the tobacco mosaic virus (TMV) could be a promising protein carrier. All past work done within the group, used the native form of TMV (**Figure 1.17**).

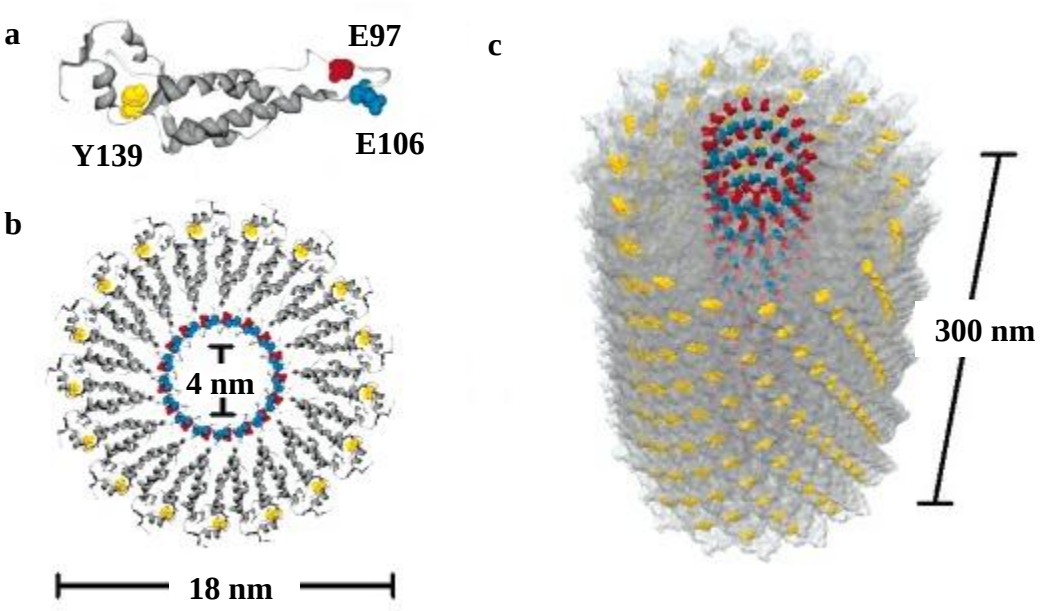

Figure 1.17: Native TMV protein
a) reactive sites (tyrosine 139, glutamate 97, glutamate 106) within a monomeric unit of the protein coat
b) planar disk aggregate
c) fully assembled capsid
"For interpretation of the references to color in this and all other figures, the reader is referred to the electronic version of the thesis."

This conjugation to TMV was carried out in Professor Qian Wang's laboratory at The University of South Carolina. The key step in this reaction used click chemistry to couple the terminal azide of the Tn antigen linker (**20**) to an alkyne moiety pre-installed on the native TMV platform (**Scheme 1.15**). This alkyne was attached to residue Tyrosine 139, one of three

identified reactive sites on the native TMV protein scaffold. A first generation **TMV-Tn-N_3** glyco-conjugate (**Scheme 1.15**), similar to the **TMV-1Cys-Tn-N_3** constructs (**Scheme 1.16**) within the current work, was evaluated previously within the Huang group. After immunological analysis of the **TMV-Tn-N_3**, ELISA of the antibodies titers contained in sera had the following subtypes: total IgG + IgM titers were 2,500, IgG titers of 3,200, and IgM titers of 7,000. It was worth noticing that although IgG titers were produced indicating class switching had occurred, the titers of IgM were still much higher.

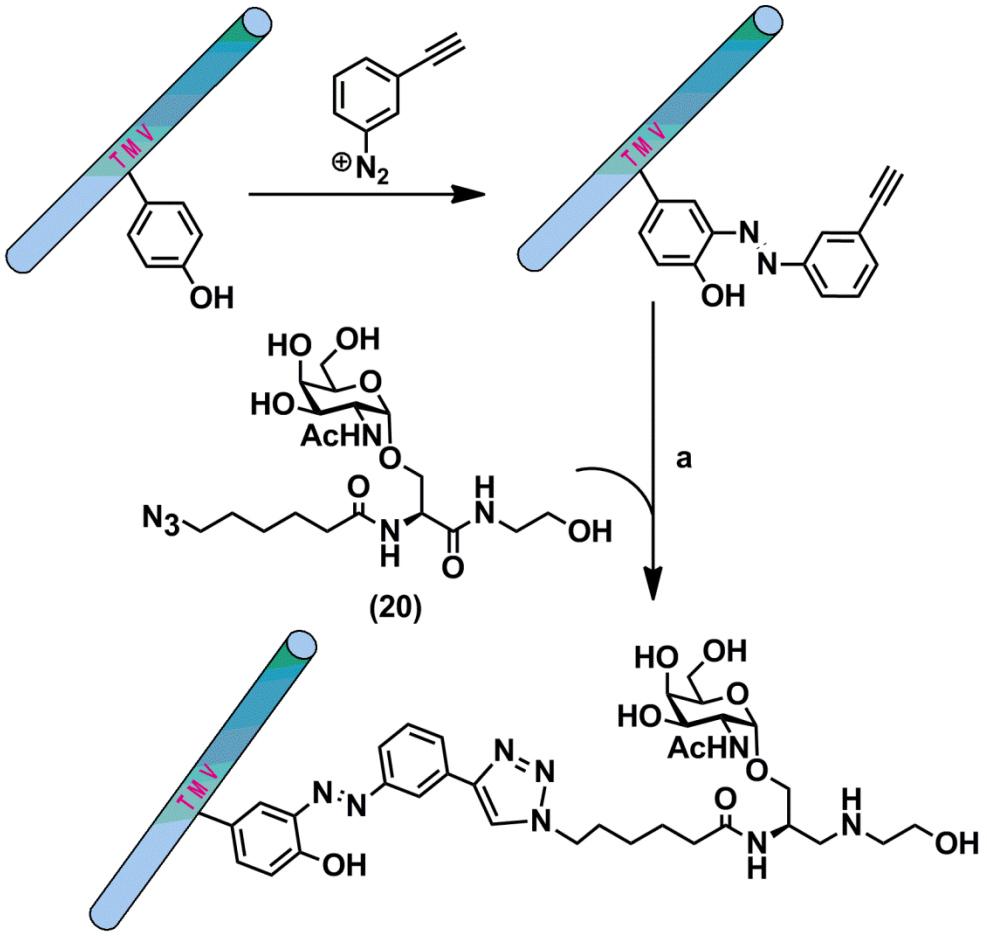

Reagents and conditions : a) i. 1 mM $CuSO_4$, 2 mM NaAsc

ii. 10% DMSO, 10 mM Tris buffer, pH 8.0, 0 ^{o}C 2h

iii. Dialysis against 1x PBS

Scheme 1.15: Synthesis of **TMV-Tn-N_3** conjugate using the native TMV

Based on these findings and by other examples presented in the literature,[15] it was predicted that this could be caused by the relatively short length and rigidity of the linker used in the conjugation between protein carrier and Tn antigen construct. To test this theory, a second

generation construct **TMV-Tn-PEG-N_3** was developed which took advantage of a longer PEG linker (**Figure 1.18**).

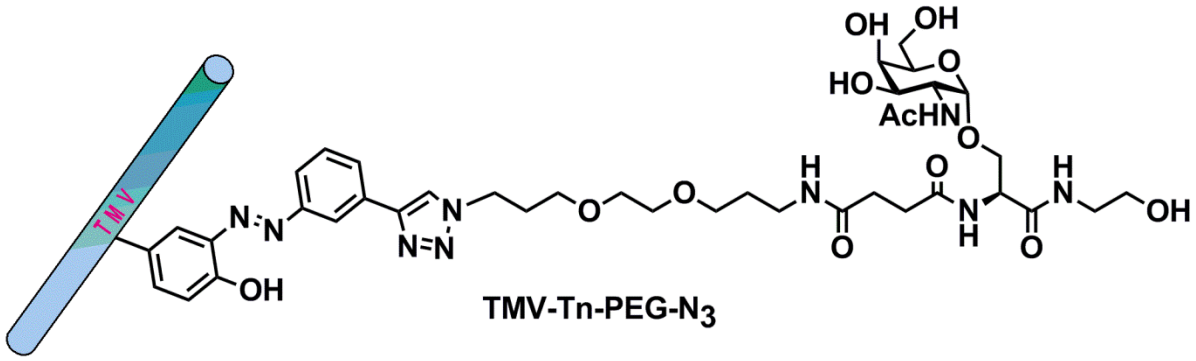

Figure 1.18: Structure of **TMV-Tn-PEG-N_3** conjugate using the native TMV

Three different **TMV-Tn-PEG-N_3** constructs were synthesized and immunologically tested, having 1 μg, 4 μg, and 20 μg of Tn loading respectively. After immunological studies using these constructs, it was found that even when a longer linker was used, the responses generated were comparable to those generated against the first generation **TMV-TN-N_3** construct mentioned above. There were two left over serum samples from the 4 μg, and 20 μg PEG constructs, referred to from this point forward as **AM-4** and **AM-20**, respectively (AM refers to Dr. Adeline Miermont who carried out these previous studies and the number refers to the amount of Tn antigen used). It would have been more desirable to directly compare serum samples generated against the current constructs to a serum sample of the first generation construct due to the closer similarities between the two. However, serum samples from that study were exhausted. Even so, with knowledge that the second generation constructs gave similar ELISA results to those of the first generation construct, comparisons could still be made.

It was thought that if the length of linker alone was not enough to improve immune function than perhaps the location of the carbohydrate presented on the protein coat of TMV could be essential.

Professor Kenneth Palmer's laboratory produced a genetically modified version of the protein coating the TMV RNA in which they inserted a surface reactive lysine at the N-terminus.[50] Modeling this approach, our collaborators Professor Qian Wang, inserted a cysteine residue between residues Serine 2 and Tyrosine 3 in the monomeric subunit of the native TMV protein (designated **TMV-1Cys**) (**Figure 1.19**). This modified TMV offered an alternative site to couple with our Tn antigen. This might allow better presentation to the host immune response, thus improving immune function.

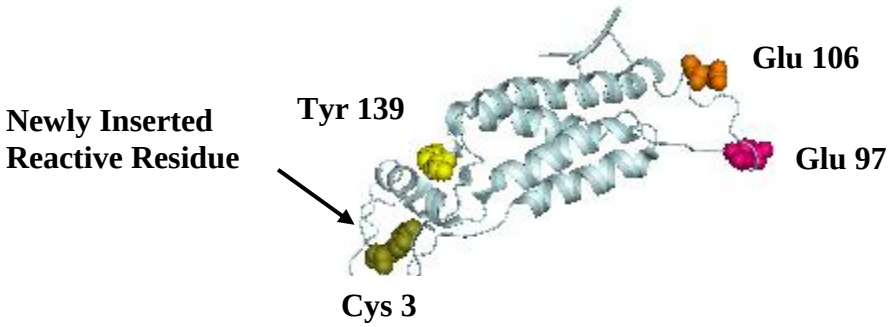

Figure 1.19: TMV Mutant

TMV-1Cys-Tn-N_3, like the native **TMV-Tn-N_3**, contains a triazole linker; however, its linker is slightly smaller and less rigid compared to the linker used in the native construct (**Scheme 1.16** and **Scheme 1.15**, respectively). This could play a major role on the immune response generated as Boons and coworkers found with the two linkers they tested (**Figure 1.5**).[15] Again, our collaborator Professor Qian Wang performed the glyco-conjugation. **TMV-1Cys** was reacted directly with a bromoacetamide functional group (**48**) resulting in **TMV-1Cys-**

Tn-bromoacetamide vaccine construct (**Scheme 1.16**). Alternately, **TMV-1Cys** was first reacted with N-propargylmaleimide, generating an alkyne functionalized TMV particle. This particle can then be subjected to click conditions with the desired azide compound yielding the desired **TMV-1Cys-N_3** vaccine construct.

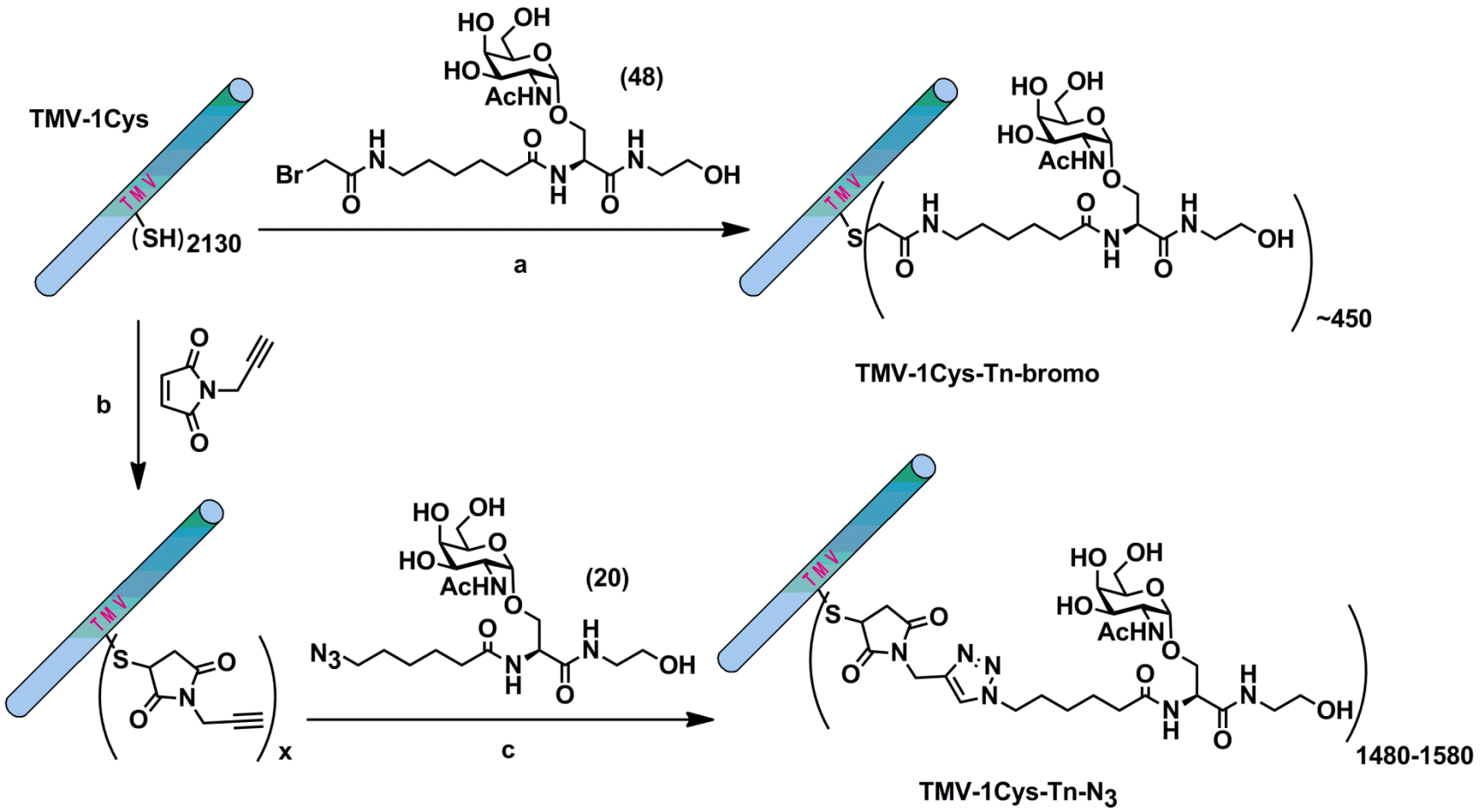

Scheme 1.16: Synthesis of Tn conjugates using mutant TMV

With both **TMV-1Cys-Tn-bromo** and **TMV-1Cys-Tn-N_3** in hand, two immunological studies were carried out using C57BL/6 female mice to evaluate the immunogenicity of these conjugates *in vivo*. In the first study, the mice were divided into four experimental groups. Group 1 (negative control group) included five mice inoculated subcutaneously on day 0 with **TMV-1Cys** (240 μg) (without the Tn antigen tether) as a 1:1 emulsion in Complete Freund's Adjuvant (CFA). The first experimental group included five mice, each inoculated on day 0 with **TMV-1Cys-Tn-N_3** (60 μg equivalent to 522 ng GalNAc) as a 1:1 emulsion in CFA. The second experimental population of five mice was injected on day 0 with a ~4x concentration of **TMV-1Cys-Tn-N_3** (240 μg equivalent to 2.1 μg GalNAc) as a 1:1 emulsion in CFA. And the final experimental population, having only three mice, was each inoculated on day 0 with **TMV-1Cys-Tn-bromo** (52 μg equivalent to 137 ng GalNAc) as a 1:1 emulsion in CFA. Booster injection were given subcutaneously on days 14 and 21 (Note: day 21 injection was given a week early by mistake should have been day 28) in the same doses as listed for day 0. The only difference was that Incomplete Freund's Adjuvant (IFA) was used to generate the emulsions instead of CFA. Blood samples were collected from all groups on days 0, 7, 28 and, 35, and serum was isolated and antibody titers were analyzed by Enzyme- Linked Immunosorbent Assay (ELISA). To avoid measuring antibodies against the TMV protein, biotinated **19** (containing a Tn moiety, **Figure 1.12**) was immobilized on a microtiter plate coated with NeutrAvidin. The serum was then added to each well and the total antibody titers (IgG + IgM) and titers of the IgG and IgM subtypes were measured photometrically using secondary IgG + IgM, IgG, and IgM antibodies conjugated to horseradish peroxidase (HRP).

The first few ELISA studies that were undertaken were designed to determine which mice had elicited the best immune responses. This was accomplished by measuring each mouse on day 0, 7, 28, and 35 at one chosen sera dilution (1/1600) point. In addition, all three secondary HRP-coated antibodies were used. Although not pictured, antibody titers at day 0 and 7 and titers measured at days 28 and 35, did not show significant differences. As can be seen in **Figure 1.20**, there was an obvious increase in antibody titers for all mouse groups over the 35 day time course of the study. Of more importance was that in nearly all mice, the observed IgG titers were higher than those of the IgM subtype at day 35, which was encouraging. However, one puzzling observation was that the control **TMV-1Cys** group displayed similar trends. The fact that titers were measured against the biotinated Tn antigen, likely indicated that there was a significant amount of non-specific binding of the antibodies produced against the proteins of the TMV coat.

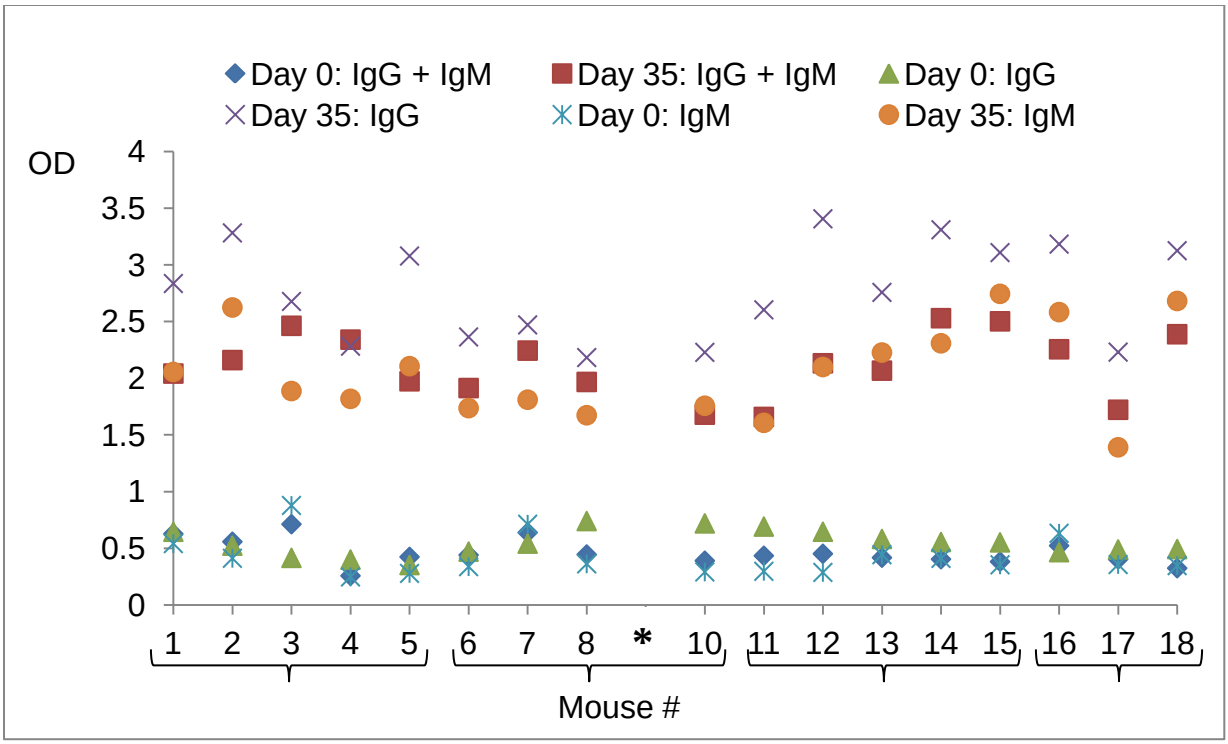

Figure 1.20: Antibody Titers for Study 1: all mice
Based on these findings, it can be seen that there is a significant change in both IgG and IgM titers when comparing Day 0 to Day 35. Study groups are as follows: Mice 1-5: TMV-1Cys Control; Mice 6-10: TMV-1Cys-N_3 (137 ng GalNAc); Mice 11-15: TMV-1Cys-N_3 (2.1 μg GalNAc); Mice 16-18: TMV-1Cys-bromo (137 ng GalNAc). *Note: mouse 9 died on Day 0 prior to first immunization

Based on the above information, the mouse that elicited the best immune response from each group, toward each respective vaccine, was chosen. Each serum sample, including the two older native TMV serum samples, AM- 4 and AM- 20, were subjected to full analysis by ELISA. It appeared that the native TMV vaccine constructs generated significantly more IgG antibodies than those by the **TMV-1Cys** carrier (**Figure 1.21**). However, it must be speculated that perhaps the amount of vaccine administered could be playing a role. Based on past findings within the lab, **TMV-Tn-PEG-N_3** vaccine (1 μg) generated very low levels of IgG compared to the 4 μg or 20 μg groups. Based on the discrepancies in the present and past findings between the two

constructs, the significantly high **TMV-1Cys** control titer responses, and the fact that the second booster administration had been given a week early out of error, it was decided that it might be worth evaluating the reproducibility of the vaccination process.

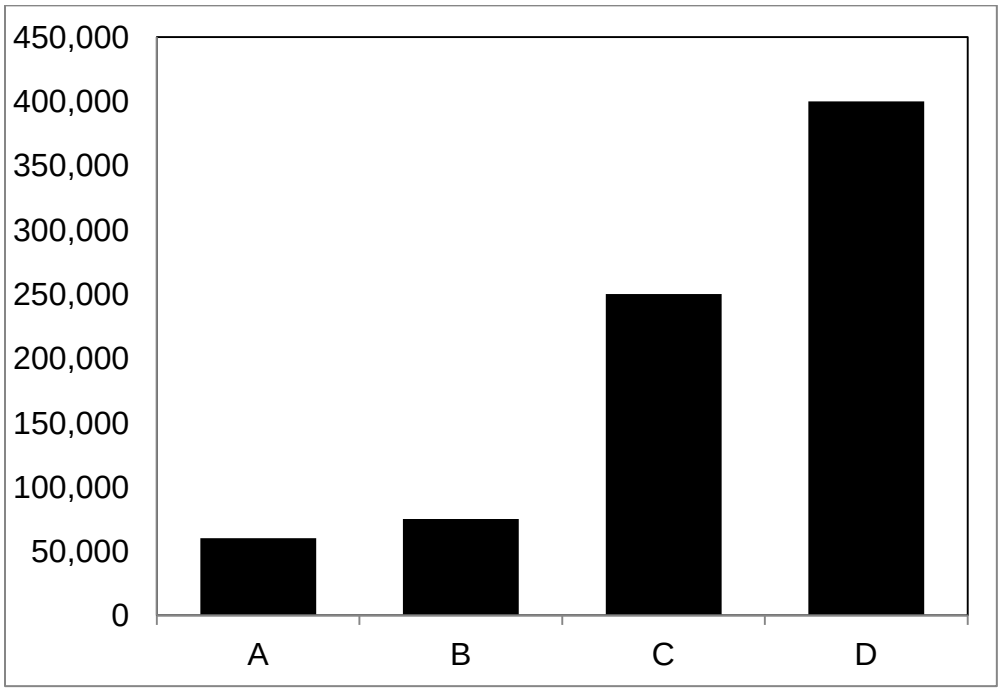

Figure 1.21: IgG titers after 35 days using native and mutant TMV constructs
Titers generated against the native construct are significantly higher than those against the mutant construct. Each bar represents the best mouse chosen from each experimental group using both native and mutant constructs A) Mouse 7: TMV-1Cys-Tn-N_3 (137 ng GalNAc); B) Mouse 12: TMV-1Cys- Tn- N_3 (2.1 μg GalNAc) C) AM-4 D) AM-20

In the second study, the mice were split into three groups. The first group included four mice inoculated subcutaneously on day 0, with TMV-1Cys (240 μg) as a 1:1 emulsion in (CFA). The second group included four mice each inoculated on day 0 with **TMV-1Cys-Tn-N_3** (240 μg equivalent to 2.1 μg GalNAc) as a 1:1 emulsion in CFA. Booster injections were given subcutaneously on days 14 and 28 in the same doses as listed for day 0. Again the only

difference being that IFA was used to generate the emulsions instead of CFA. The third group was simply a no injection control group of two mice. We wanted to ensure that the mice were not generating non-specific antibodies due to environmental or age-related sources which could skew our results. Blood samples were collected from all groups on days 0, 7, and 35, and serum was isolated and antibody titers were analyzed by ELISA as before.

As in the first study, to save time and resources, ELISA was run on all mice at 1/1600 dilution (**Figure 1.22**). This allowed for the mice with the most favorable immune responses to be analyzed further.

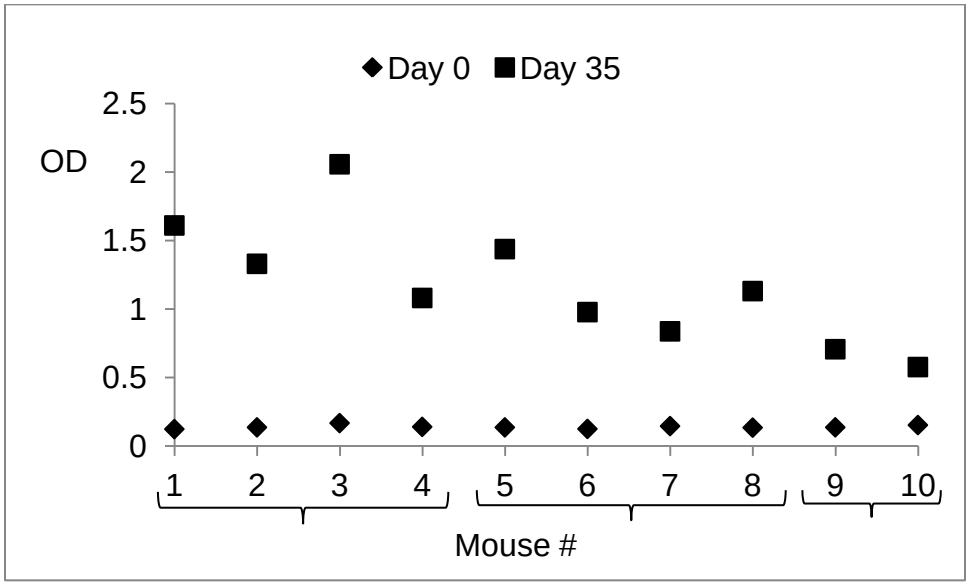

Figure 1.22: IgG Antibody Titers for Study 2: all mice
Like in Study 2, it can be seen that significant IgG titers have been generated after the 35 day experiment. Study groups are as follows: Mice 1-4: TMV-1Cys-N_3 (2.1 μg GalNAc); Mice 5-8; TMV-1Cys Control; Mice 9-10: No Injection Control

Just like in study 1, we observed a noticeable difference in the antibody titers between day 0 and Day 35. In addition, we, again, observed unexpectedly high titers in the control groups. Since one of the main reasons for this second study was to determine the reproducibility

of the immunological study, it was important to measure antibody titers from both studies at the same time, so as to eliminate the potential for slight differences between experimental analyses. The similar magnitudes of bar A to bar B (**Figure 1.23**) show that the antibody titers generated in the first study and second study were reproducible. Bar C again suggests that **TMV-1Cys** control sample must be generating non-specific antibodies. To our surprise, the group of mice that were not injected with anything, bar D, had significant antibodies generated against the Tn antigen. This observation, along with the high titer counts observed for previous control groups, as well as one other experiment, will be discussed below.

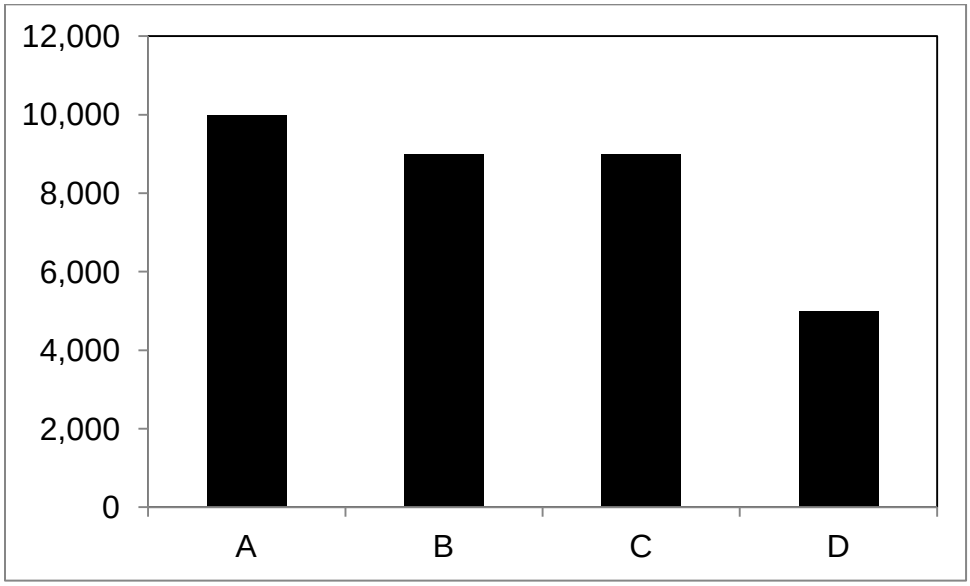

Figure 1.23: IgG titers at Day 35: Study 1 vs. Study 2
Based on these results it can be concluded that there is reproducibility between Study 1 and Study 2. In addition, it also shows that the control groups have significant amounts of non specific antibodies A) Study 1, Mouse 15: TMV-1Cys-N_3 (2.1 μg GalNAc); B) Study 2, Mouse 3: TMV-1Cys-N_3 (2.1 μg GalNAc) C) Study 2, Mouse 7: TMV-1Cys- Control D) Study 2, Mouse 9: No Injection

Having measured noticeable IgG titers in all groups, the next direction was to determine the specificity of these antibodies toward the Tn antigen. The results of a competition ELISA

(100 μL of GalNAc were added to each well at the same time as the diluted serum samples) were compared to that of a normal ELISA (**Figure 1.24**). The idea was that if the antibodies are specific to Tn, then they should bind to GalNAc in a competition assay, thus not binding to the antibody stacking complex in the plate, resulting in low optical densities. Bar A shows the results of Mouse 12 that yielded the highest number of IgG antibodies from Study 1. This sample was run alongside the two native TMV serum samples (B: **AD-4** and C: **AD-20**) (**Figure 1.24**), all three samples, have only slight competitive binding with GalNAc indicating that the antibodies present were not produced in response to the Tn antigen.

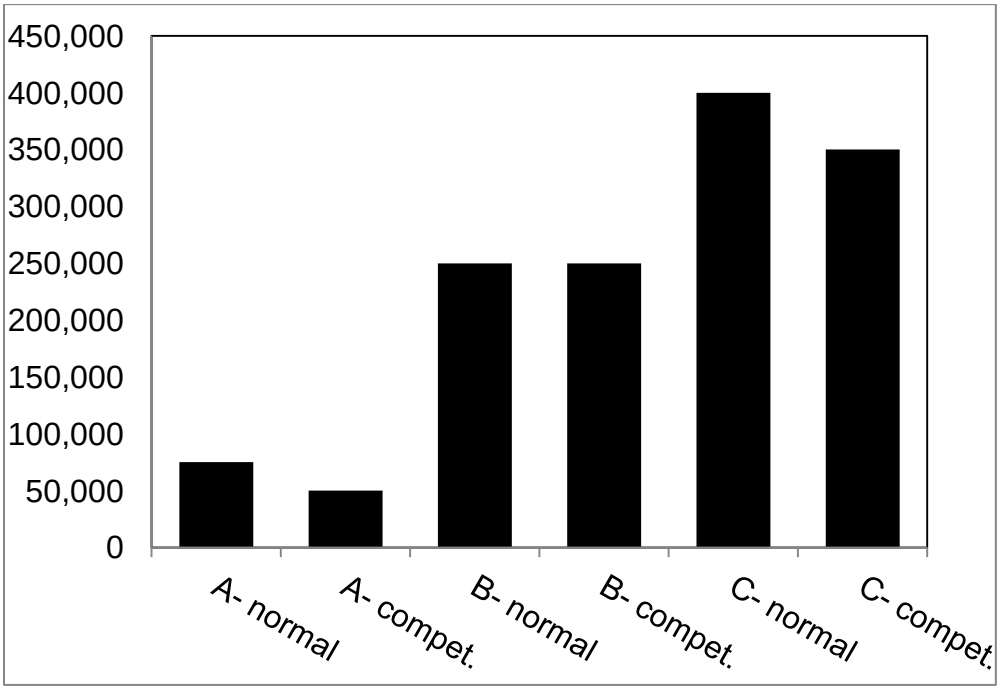

Figure 1.24: Competitive ELISA vs. Normal ELISA: IgG Antibodies specific for GalNAc
Based on these results, it can be deduced that the native TMV constructs elicited a stronger immune response then the mutant. Additionally, it can be determined that none of the samples have generated Tn specific antibodies. If selective antibodies were present, a significant drop in the titer for the competitive cases should have been observed. A) Study 1, Mouse 12: TMV-1 Cys-N_3 (2.1 μg GalNAc) B) Study 2, Mouse 4: TMV- 1 Cys-N_3 (2.1 μg GalNAc) C) AM-4 D) AM-20

It can be concluded that the native TMV vaccine produced higher quantities of IgG type antibodies than that of the mutant TMV (**Figure 1.21**); however, few of these titers were specifically generated against Tn (**Figure 1.24**). Based on these preliminary results described, it was tempting to conclude that the native TMV protein carrier was slightly superior to that of the mutant **TMV-1Cys** carrier. This conclusion was based on the fact that the two native TMV constructs generated a greater immune response, although few of the titers generated were Tn specific. Finally, these preliminary results also suggested that a significant amount of non-specific binding in the control populations was occurring.

We also thought it might be worth evaluating another promising platform, bacteriophage Qβ. Previous results published within the Huang group using CPMV,[34] indicated a strong humoral immune response. The protein coating of the wild-type Qβ has about 120 more subunits than CPMV, and each subunit contains about the same number of surface-accessible lysines as CPMV.[51] Thus, it seemed possible to elicit an even stronger immune response using Qβ as the Tn carrier.

1.8 Conjugation to Qβ and Immunological Studies

In this study, the noninfectious, self-assembled virus-like particle, *E. coli* bacteriophage Qβ encapsidating random cellular RNA was used.[52] This icosahedral virion is composed of 180 copies of the coat protein. The capsid protein is composed of 132 amino acids of a mostly antiparallel β-sheet structure.[53] A large non-covalent contact area within the capsid allows it to be unusually stable toward extreme temperature, pH, and chemical reagents. There are several benefits to using a virus scaffold toward vaccine development. A few of the many advantages in using virus scaffolds include ease of production and purification in large-scale, being well defined structurally at near atomic resolution, and can have their amino acid sequence engineered by recombinant DNA techniques.[54] The bioconjugation of this Qβ virion to our antigen constructs was carried out by our collaborators, Professor M. G. Finn and coworkers at the Scripps Research Institute. The method they used for bioconjugation can be seen below in **Scheme 1.16**.[51]

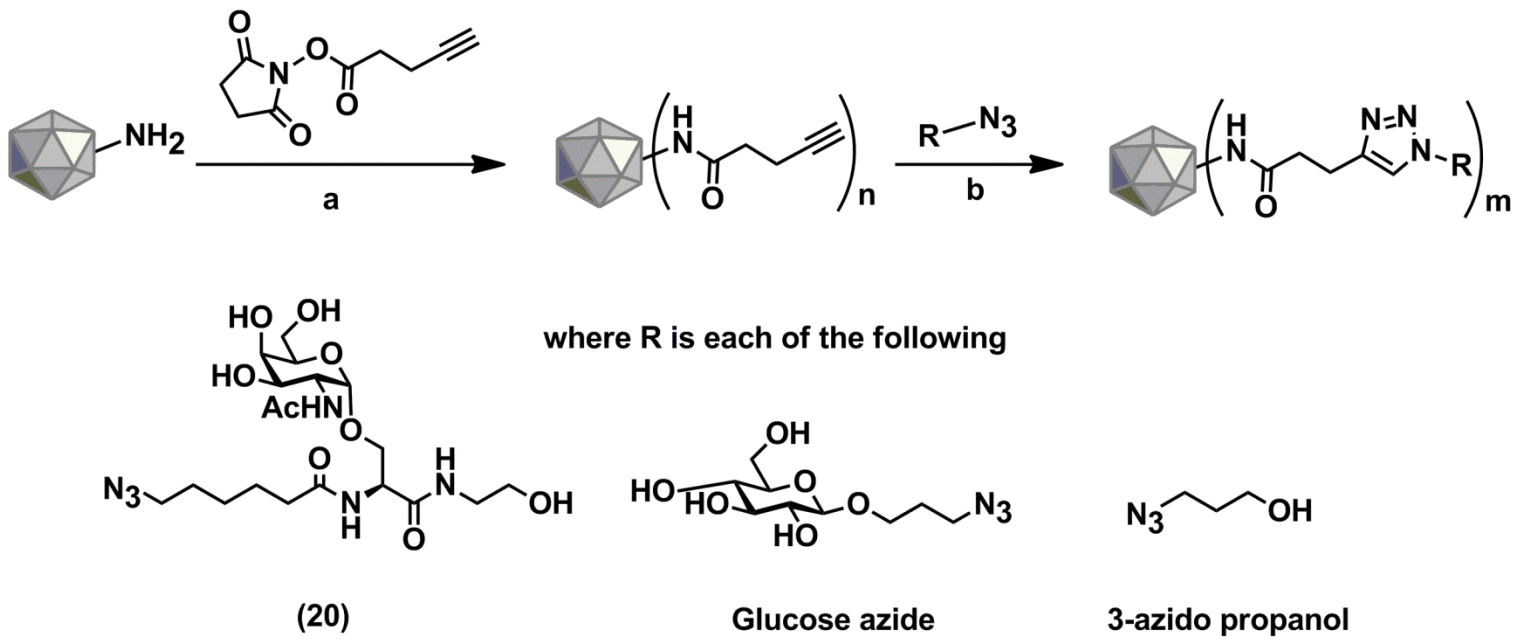

Scheme 1.17: Synthesis of azido conjugates using Qβ

This bioconjugation was accomplished by acylation of the surface lysine chains with alkynyl N-hydroxysuccinimide (NHS) ester, thus installing alkyne substituents on the surface. These alkyne substituents were then subjected to cycloaddition conditions with each of the azide compounds to be immunologically evaluated, affording each respective Qβ- bioconjugated vaccine construct.

These Qβ-vaccine constructs were then evaluated for their immunological properties. Five groups were assigned, three experimental and two controls. The experimental population, divided into three groups, was designed to test different concentrations of the Qβ-protein carrier conjugated to the Tn antigen after administration (**Qβ-Tn-N_3**, 0.45, 1.8, and 9 μg respectively). The first of the control groups was **Qβ-propanol**. This construct was designed to determine whether an immune response was generated against the carrier, in which antibodies produced, could bind non-specifically to our Tn antigen. The second control group, **Qβ-glucose**, was chosen to determine if an immune response could be elicited toward the construct; if so, could these antibodies bind non-specifically to GalNAc as well. One additional experiment that might be interesting to look into, in the future, would be to measure antibodies generated against glucose. Because it has been well established that glucose is a self antigen, it would seem highly improbable that an immune response could be generated against it. If there is a noticeable response, however, this might indicate that the construct was capable of overcoming immunological tolerance.

With the five vaccine constructs in hand, immunological studies were carried out using C57BL/6 female mice to evaluate the immunogenicity of these conjugates *in vivo*. The first, second and third groups: four, five, and four mice respectively were inoculated subcutaneously on day 0 with **Qβ-Tn-N_3** (corresponding to 17, 69, and 345 μg of the particle or 0.45, 1.8, 9.0 μg

GalNAc respectively) as a 1:1 emulsion in CFA. The fourth group included four mice each inoculated on day 0 with **Qβ-propanol** (220 μg equivalent to 2.4 μg propanol), as a 1:1 emulsion in CFA. And the fifth and final group, included three mice each inoculated on day 0 with **Qβ-glucose** (103 μg equivalent to 2.9 μg GalNAc), as a 1:1 emulsion in CFA. Booster injections were given subcutaneously to all mice on days 14 and 28 in the same doses as listed for day 0. The only difference is that IFA was used to generate the emulsions instead of CFA. Blood samples were collected from all groups on days 0, 7, and, 35 and serum was isolated. Antibody titers were analyzed by ELISA. To avoid measuring antibodies against the Qβ protein, the biotinated-Tn (**19**) was immobilized on a microtiter plate coated with NeutrAvidin. The serum was then added to each well and the total antibody titers (IgG + IgM) and titers of the IgG and IgM subtypes were measured photometrically using secondary IgG + IgM, IgG, and IgM antibodies conjugated to horseradish peroxidase (HRP).

The first few ELISA studies that were undertaken were designed to determine which mice had elicited the best immune responses. This was accomplished by measuring the IgG antibody titers for each mouse, in all five groups (**Figure 1.25**). As can be seen, the results from this study were rather alarming. While the titers generated against the **Qβ-Tn-N_3** were the same for all groups, more attention must be given to the two control groups. Both the **Qβ-propanol** and **Qβ-glucose** control groups yielded antibody titers as high as the experimental groups. In fact, the mouse with the highest antibody titer in the entire study, mouse 17, was from the **Qβ-propanol** control group.

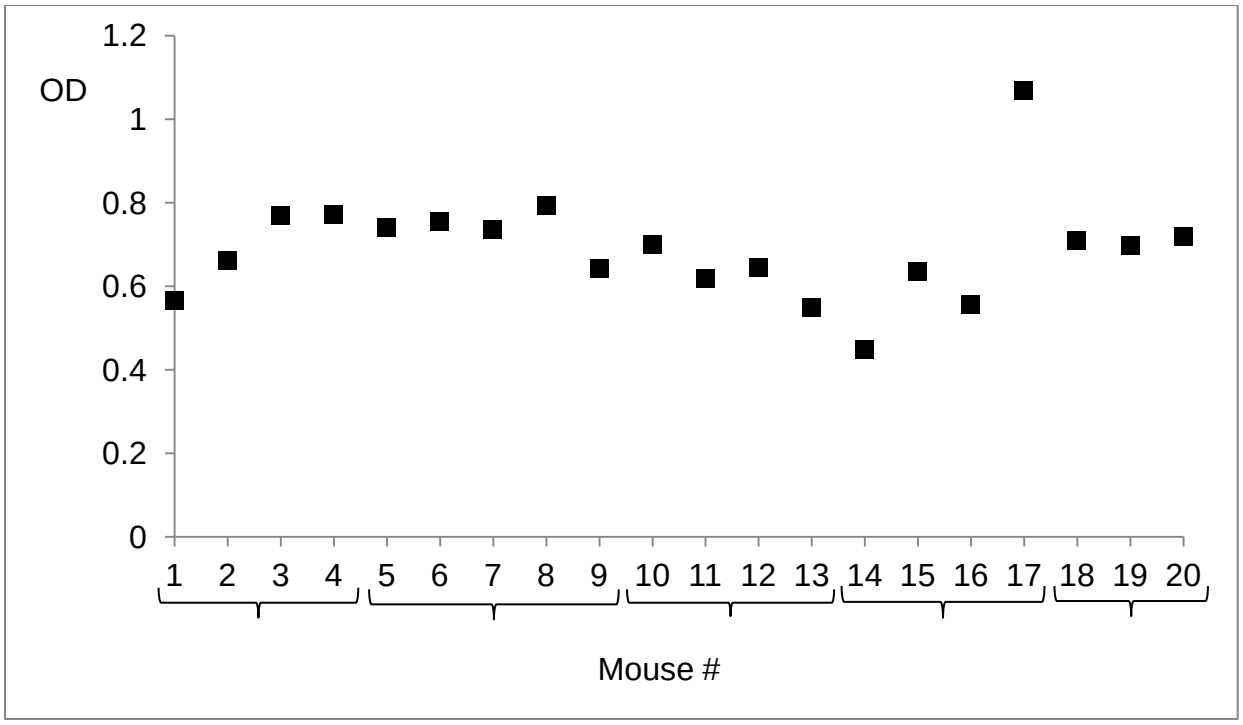

Figure 1.25: IgG Antibody Titers for Study 3: all mice
The results presented here show the alarming findings that both control populations have generated significant non-specific binding. Additionally, mouse 17, from the Qβ-propanol control group produced the highest titers. Mice 1-4: Qβ-Tn-N_3 (0.45 μg GalNAc); Mice 5-9: Qβ-Tn-N_3 (1.80 μg GalNAc); Mice 10-13: Qβ-Tn-N_3 (9.00 μg GalNAc); Mice 14-17: Qβ-propanol control; Mice 18-20: Qβ-glucose control

Based on the TMV studies, we had originally assumed that the high background in the control populations were likely due to non- specific binding. However, observing the results of this present study, it was becoming increasingly evident that something else was going on. There were a few key observations that led us to this conclusion. The first of which was alluded to in **Figure 1.22** and **Figure 1.23** but not discussed. The observation that both mice not injected throughout the course of the experiment (Study 2) had substantial IgG titers was perplexing. One would not expect to see a significant change over the course of the experiment especially considering that they were housed in a well maintained facility where the chance of

environmental antigen exposure was minimal. The second realization was that during many of the ELISA experiments that were run, very high background absorbance were detected. The final bit of evidence that clearly brought this issue to the forefront was in this third study in which **Qβ-propanol** and specifically the **Qβ-glucose** produced titers as high, if not higher, than the experimental groups. It seemed highly improbable that significant quantities of antibodies were being generated against a self antigen like glucose. With this realization, questions began to surface about possible explanations or experimental procedure that could explain this phenomenon. The first thing that we decided to investigate was each individual step of the ELISA protocol, as can be seen in **Figure 1.26**.

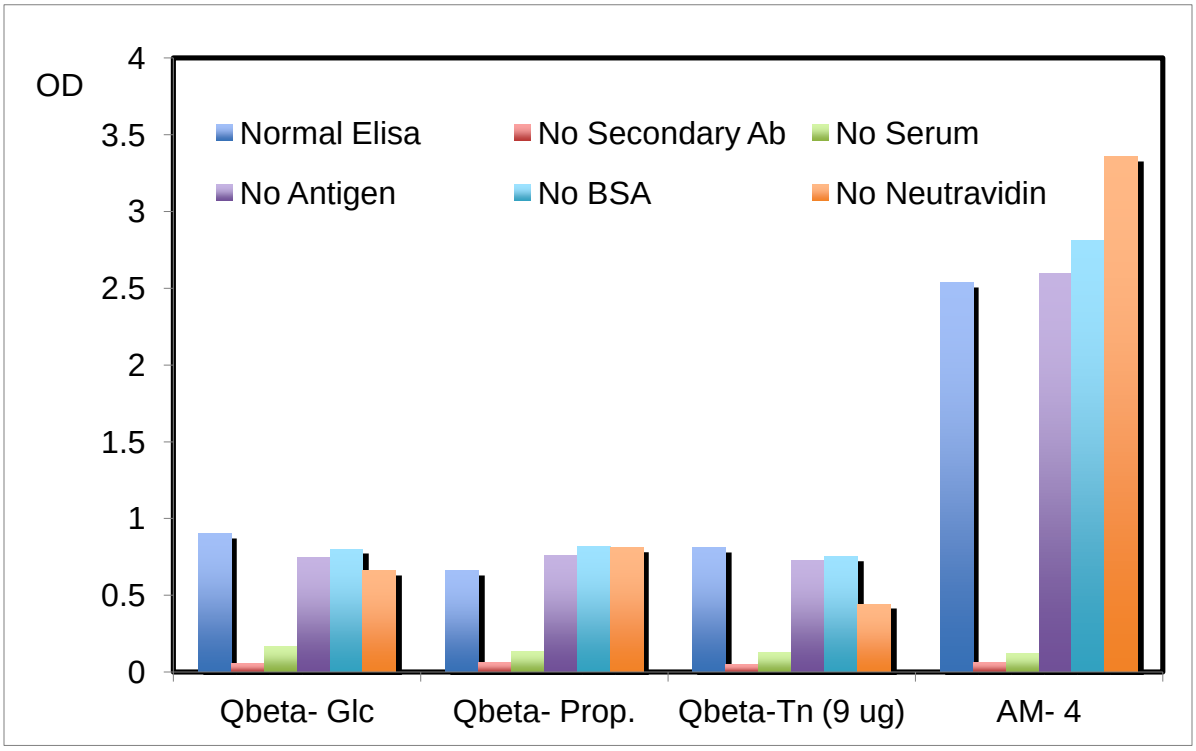

Figure 1.26: Evaluation of each step in the ELISA protocol
Qβ-Glc: Study 3, Mouse 20; Qβ-Prop: Study 3, Mouse 16; Qβ-Tn: Study 3. Mouse 13; AM-4

The idea for this study was that by removing one step from the procedure at a time, we could determine which step was resulting in the high background absorbance. The first step in the protocol was to coat the plate with NeutrAvidin which is capable of binding to our biotinated antigen. In the second step, biotinated antigen was added, which our serum antibodies should be able to recognize, if produced. Third, we used BSA as a small molecule blocker, which was supposed to prevent non- specific binding from occurring. We expected that by eliminating any one of these steps, with the exception of BSA blocking perhaps, there should be little to no antibody binding. This in turn should prevent the secondary HRP-coated antibody from binding. This ultimately meant that no absorbance should be recorded. However, as can be seen from the results, the absorbance measurements were all high. When the serum antibodies and HRP-coated secondary antibodies were omitted, the virtual lack of response in optical density was as expected. This high background absorbance strongly indicates that our serum antibodies were binding non-specifically, which further indicated that a change was required to the ELISA protocol.

After many adjustments to conditions, it was ultimately decided that a different means of antigen presentation needed to be tried. Ultimately, with the help of Dr. Zhaojun Yin, bovine serum albumin (BSA) was conjugated to the Tn antigen, This construct was used to replace the NeutrAvidin and biotinated- Tn antigen presenting steps in the ELISA protocol. This BSA system, was capable of carrying between 34-37 copies of the antigen on its surface, which is about 8-9 times more antigen density than NeutrAvidin. NeutrAvidin is known to be able to bind only four copies of biotin. By increasing the antigen density, perhaps the amount of non specific binding would be reduced and more importantly a reduction in the background absorbance would be detected.

With this modified system in hand, the results of the titers for all mice were repeated (**Figure 1.27**). Now when comparing the two control groups, **Qβ-propanol** and **Qβ-glucose**, the titers measured were negligible as was originally predicted. As for the experimental groups, there was a large discrepancy between individual mice within groups; however, this was the main reason for testing all mice at a given serum dilution (1: 6400), because not all mice should react to the vaccine in the same matter.

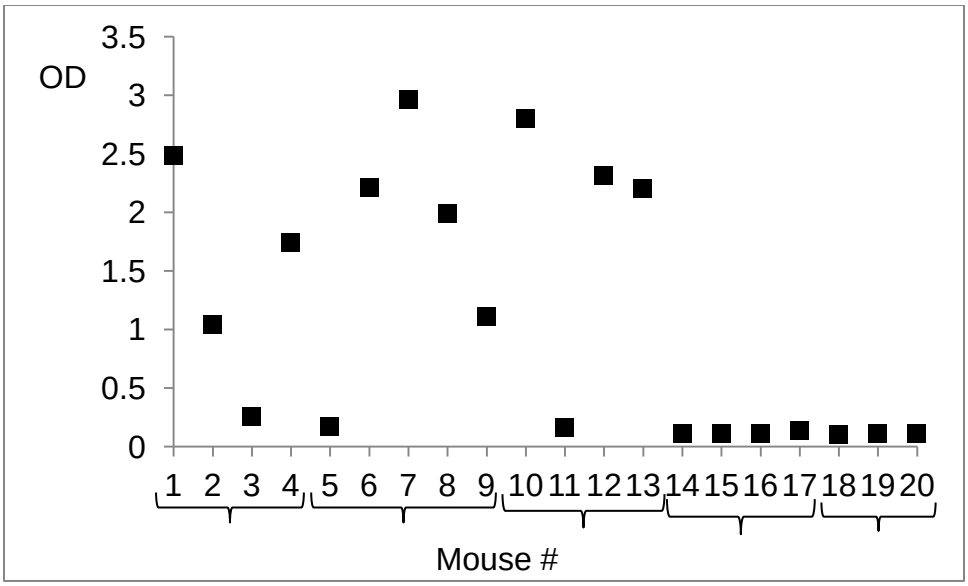

Figure 1.27: IgG Antibody Titers against BSA-Tn @ 1: 6400 serum dilutions for Study 3
All serum samples from Study 3 were analyzed at 1:6400 dilutions against BSA-Tn construct. All control mice gave background level absorbance's indicating that this new platform can greatly reduce the background absorbances. Mice 1-4: Qβ-Tn-N_3 (0.45 μg GalNAc); Mice 5-9: Qβ-Tn-N_3 (1.8 μg GalNAc); Mice 10-13: Qβ-Tn-N_3 (9.0 μg GalNAc); Mice 14-17: Qβ-propanol control; Mice 18-20: Qβ-glucose control

From these results, full ELISA determination was performed on the best mouse from each experimental group (**Figure 1.28**). Mouse 1 was chosen to represent **Qβ-Tn-N_3** (0.45 μg GalNAc) group, Mice 7 and 8 were chosen to represent **Qβ-Tn-N_3** (1.8 μg GalNAc), and Mouse

13 was chosen to represent **Qβ-Tn-N_3** (9.0 μg GalNAc). At this time, because no observable titers were detected in the single dilution study for **Qβ-propanol**, nor **Qβ-glucose**, full ELISA analysis has not been performed. It was interesting to determine how the Qβ conjugate compared to the native TMV construct that produced such high titers, it was decided to run full ELISAs on those as well.

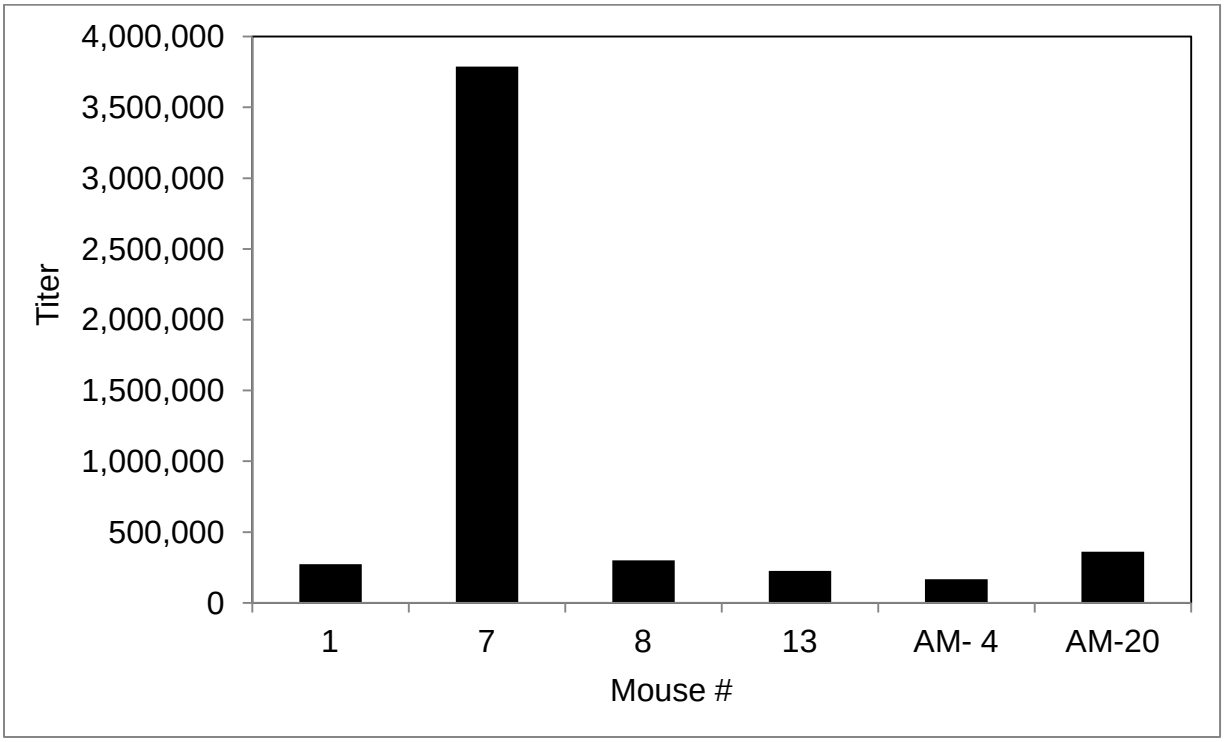

Figure 1.28: IgG titers for representative mice in Study 3 and native TMV-Tn-PEG-N_3
Based on our findings, it appears as though both the Qβ conjugates and the native TMV conjugates produces high quantities of IgG titers- Mouse 1: 272,000; Mouse 7: 3,787,000; Mouse 8: 300000; Mouse 13: 226,000; AM- 4: 166,000; AM- 20: 360,000

As it turned out, all the mice tested had very high IgG affinities; Mouse 7 had close to 3 million, whereas the rest all had closer to 300,000, which were still very impressive. With these interesting findings, we decided to determine the IgM antibody titers. Like IgG, all mice were

tested and the ones that produced the highest responses where used. We tested Mouse 1, Mouse 13, AM-4 and AM-20 using full dilution analysis.

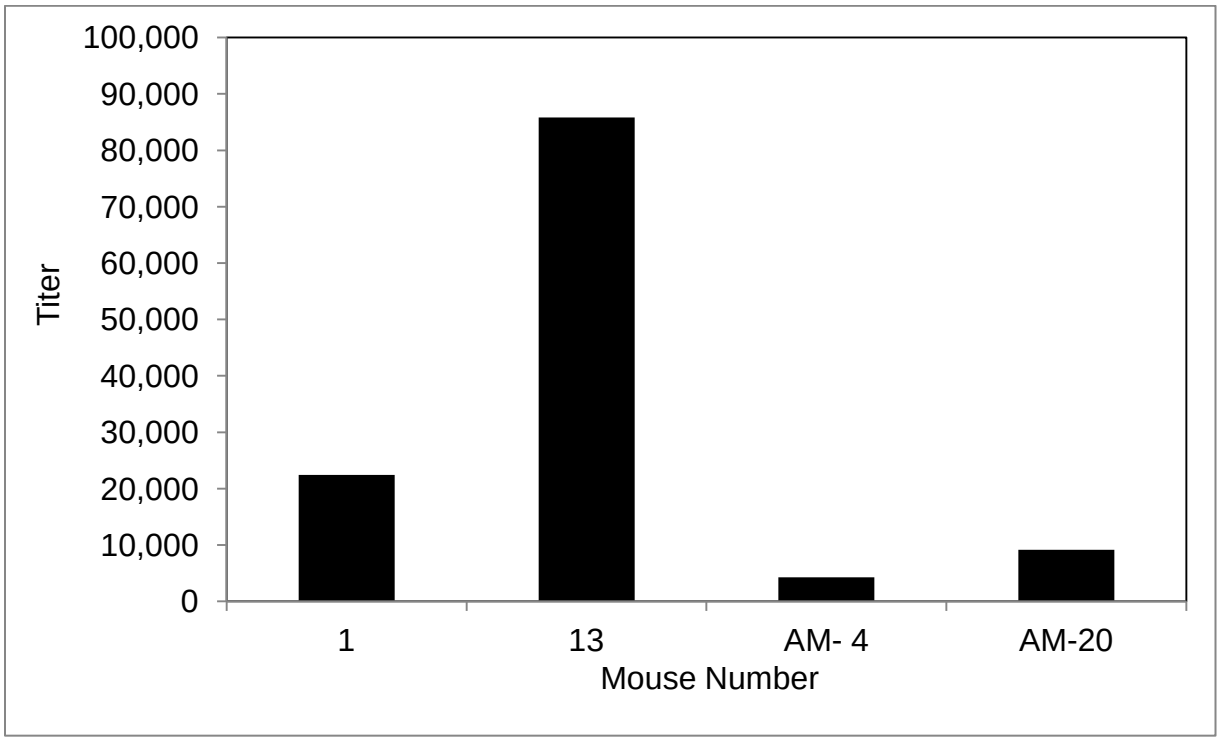

Figure 1.29: IgM titers for representative mice in Study 3 and native TMV-Tn-PEG-N_3
Respective titers- Mouse 1: 22,400; Mouse 13: 85,800; AM-4: 4,200; AM-20: 9,100

Excitedly, it seemed as though the number of high affinity IgG antibodies generated was significantly higher than the lower IgM affinity antibodies, which indicated that isotype class switching had occurred and the establishment of immunological memory was being produced.

Based on these conclusions, it would be interesting to know how specific these antibodies are toward the Tn antigen displayed in its native environment on the tumor cell surface. Preliminary FACS analyses have indicated that there is little specificity of these antibodies toward Tn in its natural environment on cancer cells, NCI-ADR-RES. However, it is now believed that the NCI-ADR-RES ovarian drug resistant cancer cell line that we have been using

may not express Tn but instead MUC1.[9] This issue is currently being investigated within the lab by testing other cell lines that have been proven to contain Tn on their surface. Additionally, a **Qβ-MUC1-N_3** vaccine serum is being tested against this MUC1 containing cell line (NCI-ADR-RES). It will be interesting to see what kind of specific binding these vaccine constructs can generate.

1.9 Re-evaluation of the TMV-1Cys Construct Using New ELISA Protocol

Having proven the effectiveness of the BSA conjugated Tn display for ELISA analysis, we thought it might be important to re-evaluate a few of the past **TMV-1Cys** samples. First, we re-evaluated all of the mice in study 1. Based on the original results (**Figure 1.20**), we observed a definitive increase from day 0 to day 35, however, the control groups were all surprising high as well, which we had originally just attributed to non- specific binding.

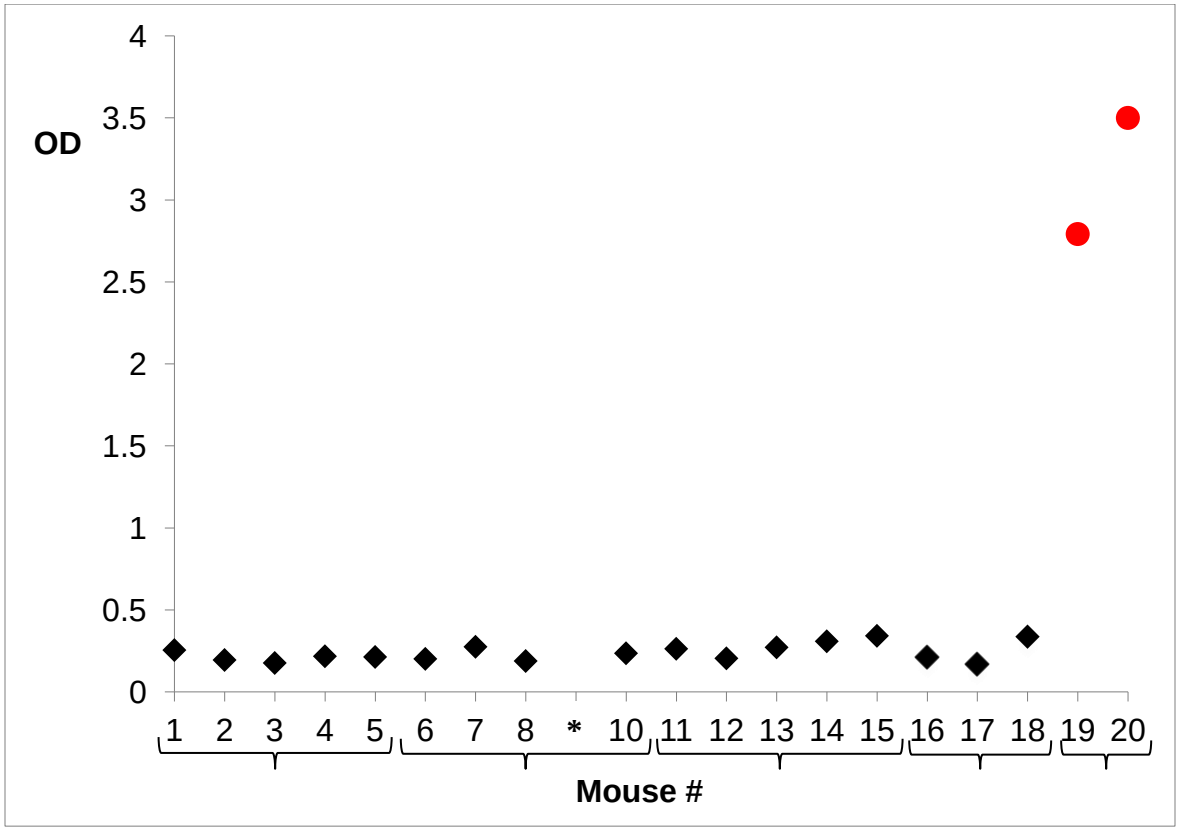

Figure 1.30: Antibody Titers for Study 1: all mice using BSA- Tn for ELISA
Antibody titers measured against the BSA-Tn construct show much lower titers than when the NeutrAvidin system was used. Mice 1-5: TMV-1Cys Control; Mice 6-10: TMV-1Cys-N_3 (137 ng GalNAc); Mice 11-15: TMV-1Cys-N_3 (2.1 μg GalNAc); Mice 16-18: TMV-1Cys-bromo (137 ng GalNAc). Number 19: AM-4; Number 20: AM-20
*mouse 9 died on Day 0 prior to first immunization

Although not shown, IgG titers of Study 2 were analyzed in an analogous fashion. Similar finding were observed. Based on these new realizations, it appeared that the native **TMV-Tn** construct had resulted in a better immune response than that of the mutant **TMV-1Cys** control. Additional ELISA analyses are currently underway to quantify the actual titers generated against these constructs, like the Qβ results already discussed.

1.10 Synthesis and Immunological Studies of a Triazole Linker

Having determined the antibody titers of the Qβ and TMV conjugated vaccines, we thought it would be interesting to quantify the amount of antibodies generated against the triazole linker. There has been a lot of debate in the literature about which linkers should and should not be used. However, few of these actually quantify the titers generated against the linker in question. To quantify antibody titers generated against the triazole linkers used in most of the vaccine constructs tested, two target compounds were needed. The first compound that was synthesized was needed to run a competition experiment analogous to those run using GalNAc to quantify titers against Tn. The second compound was needed to coat the ELISA plate to quantify antibody titers. The first compound was synthesized starting from the commercially available 3-chloro-propan-1-ol (**49**) (**Scheme 1.18**). Compound **49** was heated to 80 ^{o}C overnight for about 18 hours in the presence of sodium azide in water; thus causing an S_N2 displacement of chlorine generating 3-azido-propanol (**50**). **Note**: Since small molecular weight organic azides have been reported as potential explosives, extreme caution was used in the handing of this compound. Although this compound was concentrated to dryness, it was used immediately in the next step without further analysis due to the nature of the compound. Compound **50** then underwent a classic click reaction using commercially available propargyl amine, CuI, DIPEA in DMF. The reaction was heated for 16 hours at 50 ^{o}C resulting in **51** being generated in a 70 % yield over the two steps.

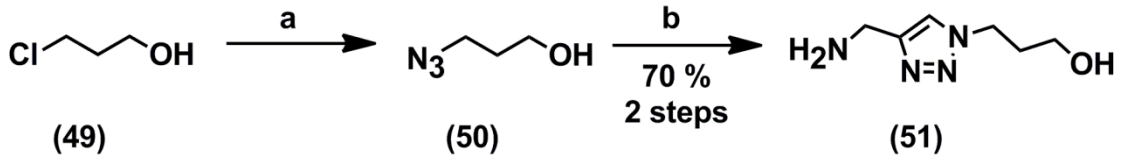

(49) (50) (51)

Reagents and conditions : a) NaN_3, H_2O, 80 ^{O}C, 18 h

b) propargyl amine, CuI, DIPEA, DMF, 50 ^{O}C, 16 h

Scheme 1.18: Synthesis of triazole linker (**51**)

Free amine, **51**, was less than desirable due to its strong nucleophilicity. It was thus decided to acetylate it for use in the competition experiments. The difficulty in acetylation, however, is that there is a primary amine and a primary alcohol. It seemed possible to use normal acetylating conditions to run this reaction as long as the temperature was kept low. We decided to use Ishihara and others[55] method in which they selectively acetylated a variety of primary alcohols in the presence of secondary alcohols. This method involved the reaction of **51** with 2, 4, 6- collidine, and acetyl chloride in DMF at -60 ^{O}C for two hours (**Scheme 1.19**). This reaction resulted in only a 53 % yield with no observable ester formation. The other major spot was starting material. There is a chance that adding more acetyl chloride might have pushed this yield higher however, it was decided against to avoid the risk of ester formation.

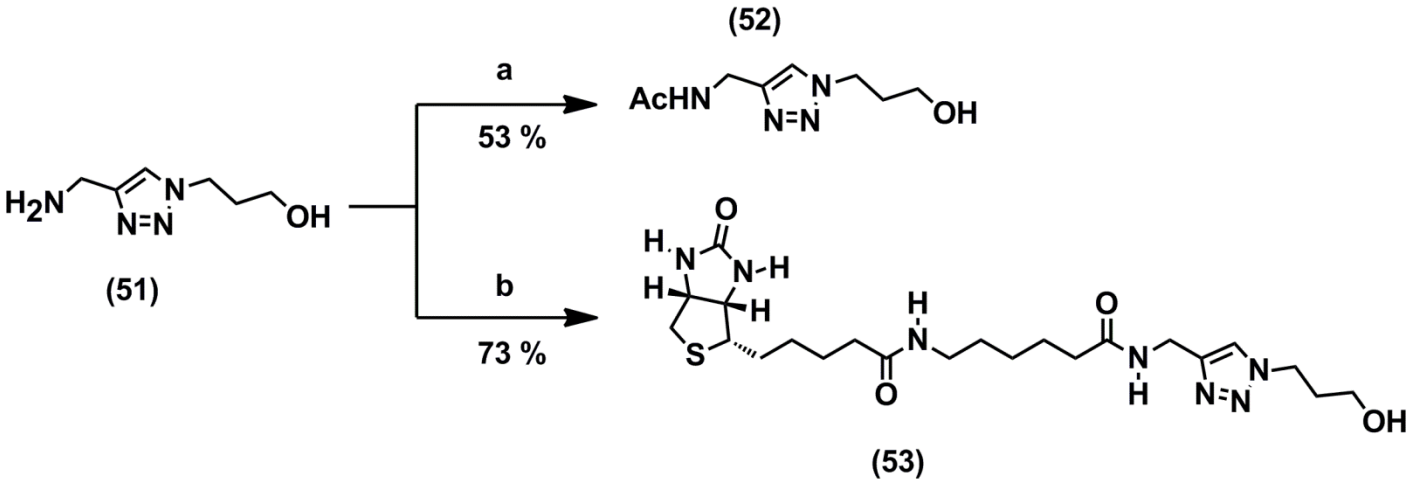

Reagents and conditions : a) 2,4,6-collidine, acetyl chloride, DMF, - 60 ^{o}C, 2 h

b) biotinated amino caproic acid NHS ester, DIPEA, NMP, r.t., 17 h

Scheme 1.19: Synthesis of triazole compounds for ELISA analysis

Finally, the last compound synthesized was biotinated triazole **53**. This compound was generated by addition of **51** to biotinated amino caproic acid NHS ester (**35**) and DIPEA to NMP. After 17 hours of stirring at room temperature, the biotinated product, **53**, was precipitated out using ice cold ether. Compound **53** was obtained in a 73 % yield. As it turned out, this biotinated- triazole synthesis was completed just prior to the discovery of the background issue discussed above. Consequently, a third construct needed to be synthesized for future ELISA experiments, to quantify the amount of antibodies generated against the triazole linker (**Figure 1.31**). This synthesis and conjugation, starting from **51** was carried out by Dr. Zhaojun Yin.

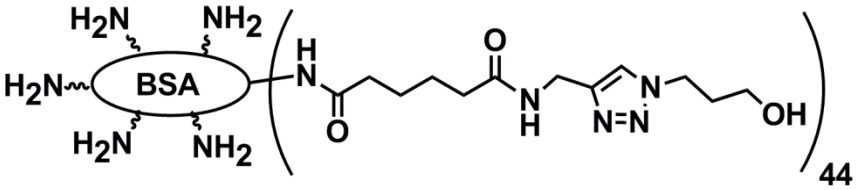

(54)

Figure 1.31: BSA conjugated triazole compound for ELISA analysis

Having synthesized our triazole compounds for ELISA analysis, we then tested each of the TMV conjugates to determine how much of an antibody response was generated against the linker. As can be seen in **Figure 1.32**, a mouse from the **TMV-1Cys-bromo** and both of the native TMV constructs have significant titers that have an affinity toward triazole.

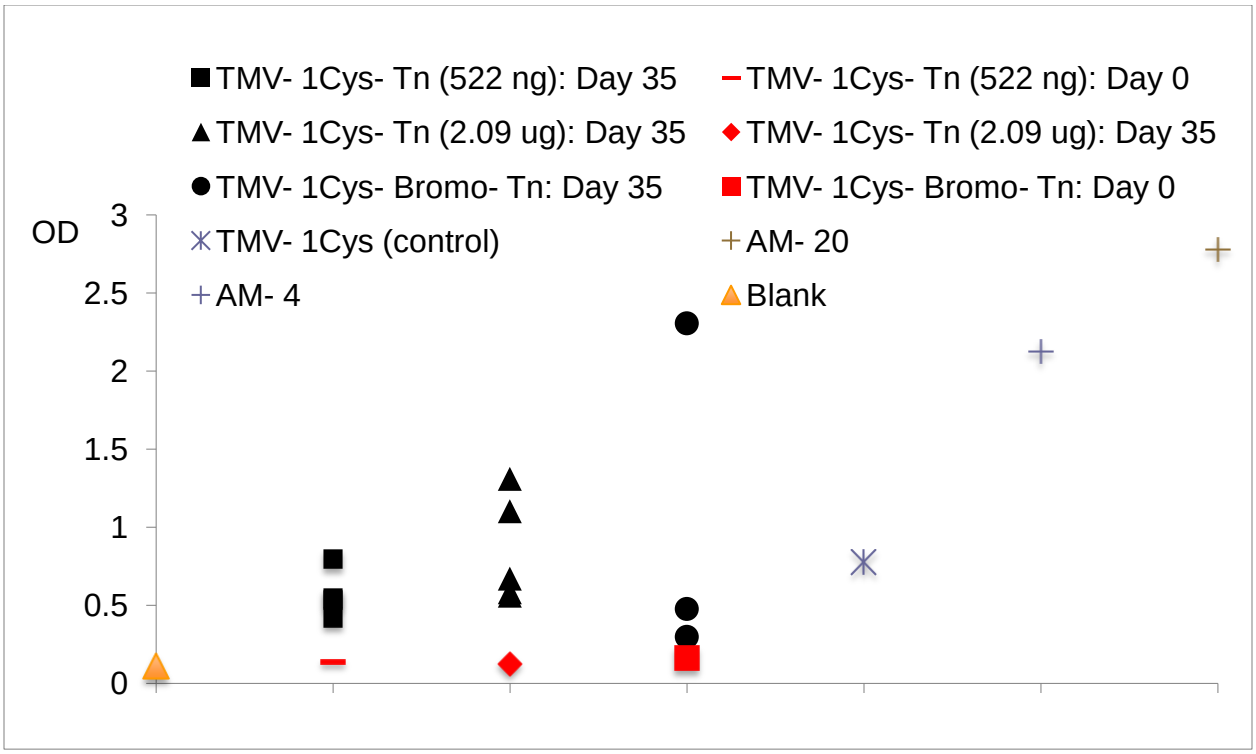

Figure 1.32: IgG antibodies measured against BSA-triazole in TMV study groups

As for the Qβ Study groups it appeared as though they all had high amounts of antibodies generated against the triazole linker (**Figure 1.33**). **Qβ-glucose** was the only group that had a lower level of antibodies generated against triazole, however, even one of the mice in that group showed significant antibodies against it.

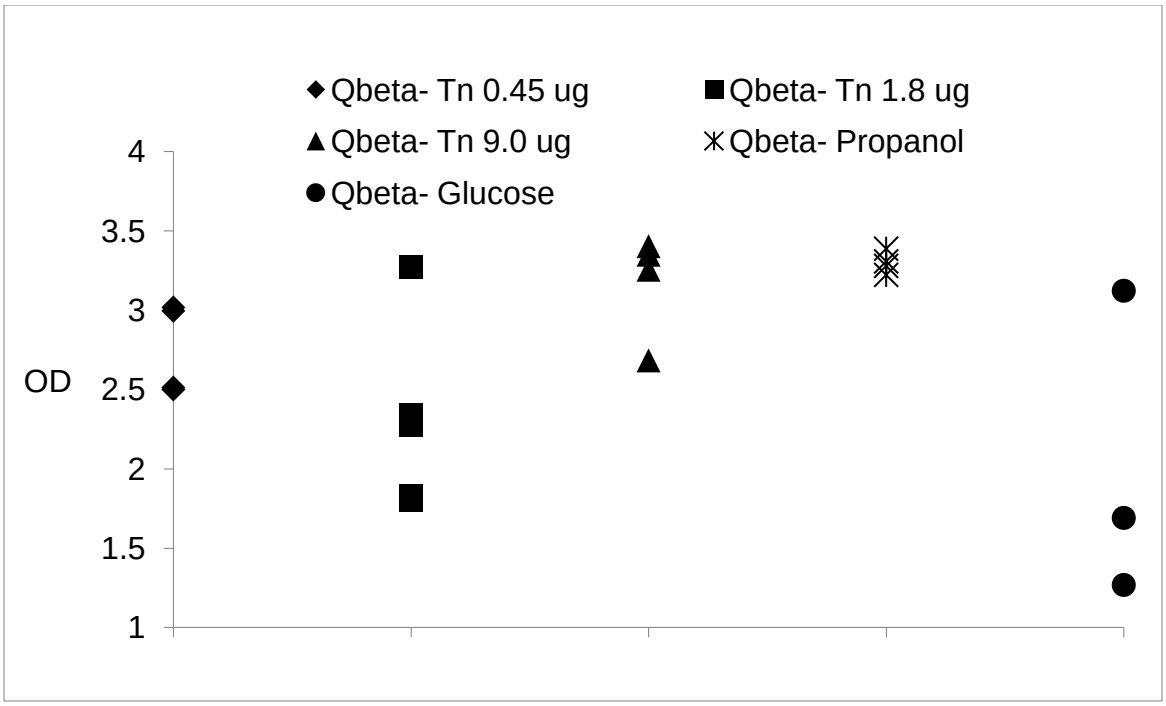

Figure 1.33: IgG antibodies measure against BSA- triazole in Qβ Study groups

Much work is still ongoing to get a better understanding of the role that linkers have in the immune response. It is believed that if a strong enough immune response is generated against the linker then there is likely a negative consequence to the response generated against the desired antigen.

1.11 Conclusions

Based on the findings presented herein, it seems as though many factors need to be considered when designing a successful vaccine. For instance, when comparing the native TMV to the mutant TMV-1Cys conjugates, it was predicted that modification of the protein surface would allow better expression of the carbohydrate antigen to the surroundings. However, after quantifying the antibody titers using the new BSA protocol, the native construct was shown to elicit the stronger response. This indicated that the location that the antigen is bound on the subunit of the antigen presenting cell is critical toward developing a successful immune response.

Probably one of the most interesting findings in the present work was the major setback caused using the biotinated antigen display for ELISA. The NeutrAvidin/ biotinated-Tn system was used successfully in our group in all past immunological evaluations and very impressive results were obtained.[34] After much thought on this issue, a few possible theories were developed. The first and most convincing, based on the evidence collected thus far, suggest that there may have been a significant difference in the 96-well ELISA plates used in past studies versus those used currently. This theory was suggested based on the findings using the AD-4 and AD-20 samples. Comparing past work carried out by Dr. Adeline Miermont within the group[49] to that of our present work, there was a large discrepancy between the data. She found that, not only was there a strong immune response generated, but the antibodies produced were highly specific toward the Tn antigen based on competitive ELISA. Using the same protocol as well as the serum samples she collected, in the current work little specificity toward the Tn antigen was observed (**Figure 1.24**). The only unknown variable between the current work and past work is the 96-well plates that were used. There is a chance that the plates used in her case

may have been able to bind more NeutrAvidin/ biotinated- Tn thus resulting in a higher density of antigen expression than the plates currently used. A second theory may be that antibodies generated against a certain vaccine have different sensitivities to antigen density. For instance, when using CPMV, excellent results were obtained.[34] Perhaps the antibodies generated, using this construct, were sensitive to the lower density antigen expressed using the NeutrAvidin system. On the other hand, when the TMV and Qβ constructs were used, potentially the antibodies generated were not as sensitive to the low density antigen presented by the NeutrAvidin system thus could not bind. Whereas, once the higher antigen density system utilizing BSA was applied, these antibodies could bind. This is an extremely interesting idea, because if true, this potentially means that antibodies generated against the TMV or Qβ constructs may be more selective towards cancer cells, which have high density antigen presentation, and less sensitive to normal cells which express low density antigens. This will be a theory that I am sure will be actively investigated in the near future as soon as the results from the FACS experiments begin to push forward.

1.12 Experimental Section

General Experimental Procedures.

All reactions were carried out under nitrogen or argon with anhydrous solvents in oven-dried glassware. All glycosylation reactions were performed in the presence of molecular sieves, which were flame dried immediately prior to the reaction under high vacuum. Glycosylation solvents were dried using a solvent purification system and used directly without further drying. Chemicals used were reagent grade as supplied except where noted. Analytical thin-layer chromatography was performed using silica gel 60 F254 glass plate. Compound spots were visualized by UV light (254 nm) and by staining with a yellow solution containing $Ce(NH_4)_2(NO_3)_6$ (0.5 g) and $(NH_4)_6Mo_7O_{24}$ * $4H_2O$ (24.0 g) in 6% H_2SO_4 (500 mL) or a solution of Ninhydrin (1.5g) in n-butanol (100mL) and acetic acid (3mL). Flash column chromatography was performed on silica gel 60 (230–400 Mesh). NMR spectra were referenced using Me_4Si (0 ppm), residual $CHCl_3$ (δ ^{1}H-NMR 7.24 ppm, ^{13}C-NMR 77.0 ppm), H_2O (δ ^{1}H-NMR 4.63ppm), CH_3OH (δ ^{1}H-NMR 3.30 ppm, ^{13}C-NMR 49.0 ppm), and $(CH_3)_2CO$ (δ ^{1}H-NMR 2.04 ppm, ^{13}C-NMR 29.84 ppm). Peak and coupling constant assignments were based on ^{1}H-NMR, ^{1}H–^{1}H gCOSY and (or) ^{1}H–^{13}C gHMQC and ^{1}H–^{13}C gHMBC experiments. ESI mass spectra were recorded in positive ion mode.

O-(2-Acetamido-2-deoxy-α-D-galactopyranosyl)-L-serine ethanolamide (34)

Compound **33** (206.8 mg, 0.296 mmol) was dissolved in a 7N* solution of ammonia in methanol (10 mL) (*Note: using $\leq$ 7N solutions, reaction will not work) and the reaction was

stirred at 0 ^{o}C and gradually allowed to warm to room temperature overnight. The reaction mixture was allowed to stir for 15 hours. Completion of the reaction was confirmed using a DCM: MeOH: NH_4OH (4: 4: 1) TLC elution mixture. The reaction was then concentrated to dryness and the residue was then purified via column chromatography using a DCM: MeOH: NH_4OH (5: 3: 1) elution mixture. The desired product was obtained as a white solid with a 92% yield. ^{1}H NMR (500 MHz, CD_3OD) δ 2.00 (s, 3H), 3.34 (t, *J* = 5.5 Hz, 2H), 3.56 (dd, *J* = 5.0, 10.1 Hz, 1H), 3.59 – 3.63 (m, 2H), 3.67- 3.72 (m, 2H), 3.74 (t, *J* = 5.6 Hz, 1H), 3.76 – 3.80 (m, 1H), 3.80 – 3.85 (m, 1H), 3.87 (d, *J* = 3.0 Hz, 1H), 3.91 (dd, *J* = 4.3, 10.1 Hz, 1H), 4.28 (dd, *J* = 3.7, 10.9 Hz, 1H), 4.78 (d, *J* = 3.7 Hz, 1H) ^{13}C-NMR (150 MHz, CD_3OD), δ 22.8, 43.0, 51.4, 55.7, 61.4, 62.9, 69.7, 70.3, 70.4, 72.9, 99.6, 173.8, 174.1. [HRMS] $[M+H]^+$ m/z: calc. for $C_{13}H_{26}N_3O_8$: 352.1720, found 352.1707.

6-*N*-Biotinamido-hexanoyl-*O*-(2-acetamido-2-deoxy-α-D-galactopyranosyl)-L-serine ethanolamide (19)

Compound **34** (29 mg, 0.083 mmol), compound **35** (29.7 mg, 0.138 mmol, 1.66 eq) were dissolved in N-methylpyrrolidinone (4 mL). The reaction mixture was stirred at room temperature for 15 hours. Completion of the reaction was confirmed using a DCM: MeOH: H_2O (60: 34: 6) TLC elution mixture. A large excess of ether was added to the reaction to precipitate out the product. The solid residue was collected via vacuum filtration and then purified via column chromatography using the same solvent elution mixture used for TLC. The compound was then re-dissolved in water and lyophilized. The desired product was obtained as a white

solid with a 57% yield. Comparison with literature data[34] confirmed its identity. ^{1}H NMR (600 MHz, D_2O) δ 1.14 – 1.31 (m, 4H), 1.34 – 1.64 (m, 8H), 1.90 (s, 3H), 2.10 (t, *J* = 7.2 Hz, 2H), 2.20 (t, *J* = 7.5 Hz, 2H), 2.63 (d, *J* = 13.2 Hz, 1H), 2.85 (dd, *J* = 5.1, 12.9 Hz, 1H), 3.99 – 2.08 (m, 2H), 3.16 – 3.26 (m, 3H), 3.47 – 3.54 (m, 2H), 3.57 – 3.63 (m, 2H), 3.65 (dd, *J* = 5.4, 10.8 Hz, 1H), 3.71 - 3.75 (m, 2H), 3.77 (dd, *J* = 5.4, 10.8 Hz, 1H), 3.83 (d, *J* = 3.0 Hz, 1H), 4.02 (dd, *J* = 3.6, 10.8 Hz, 1H), 4.28 (dd, *J* = 4.8, 7.8 Hz, 1H), 4.41 – 4.50 (m, 2H), 4.75 (d, *J* = 3.6 Hz, 1H) ^{13}C-NMR (125 MHz, $CDCl_3$), δ 22.2, 25.0, 25.3, 25.8, 27.8, 28.0, 28.2, 35.4, 35.7, 39.2, 39.9, 41.7, 49.9, 53.9, 55.6, 60.0, 60.4, 61.3, 62.3, 67.4, 67.8, 68.6, 71.5, 98.0, 165.5, 171.8, 174.6, 176.8, 177.3. [HRMS] $[M+H]^+$ m/z: calc. for $C_{29}H_{51}N_6O_{11}S$: 691.3337, found 691.3347.

Azido-caproic-amido-*O*-(2-acetamido-2-deoxy-α-D-galactopyranosyl)-L-serine ethanolamide (20)

Compound **34** (47.5 mg, 0.135 mmol), compound **37** (29.7 mg, 0.189 mmol, 1.4 eq), BOP (72.6 mg, 0.164 mmol, 1.22 eq), HOBT (22.8 mg, 0.168 mmol, 1.24 eq), and DIPEA (45 μL, 0.266 mmol, 1.97 eq) were dissolved in N-methylpyrrolidinone (4 mL). The reaction mixture was stirred at room temperature for 15 hours. Completion of the reaction was confirmed using a DCM: MeOH: NH_4OH (12: 5: 1) TLC elution mixture. A large excess of ether was added to the reaction to precipitate out the product. The solid residue was collected via vacuum filtration and then purified via column chromatography using the same solvent elution mixture used for TLC. This is to remove any starting material **34** that may have co-precipitated out with the product. The compound was then re-dissolved in water and lyophilized. The desired product

was obtained as a white solid with a 94% yield. ^{1}H NMR (600 MHz, D_2O) δ 1.20 – 1.30 (m, 2H), 1.43 – 1.55 (m, 4H), 1.90 (s, 3H), 2.22 (t, *J* = 7.4 Hz, 2H), 3.19 (t, *J* = 6.8 Hz, 2H), 3.22 (t, *J* = 4.8 Hz, 2H), 3.49 – 3.53 (m, 2H), 3.59 – 3.63 (m, 2H), 3.63 – 3.68 (dd, *J*= 5.4, 10.8, 1H), 3.72 – 3.76 (m, 2H), 3.78 (dd, *J* = 5.4, 10.8 Hz, 1H), 3.84 (d, *J* = 3.6 Hz, 1H), 4.02 (dd, *J* = 3.6, 10.8 Hz, 1H), 4.45 (t, *J* = 5.4 Hz, 1H), 4.76 (d, *J* = 3.6 Hz, 1H) ^{13}C-NMR (150 MHz, $CDCl_3$), δ 24.6, 27.3, 28.1, 30.3, 37.8, 44.2, 52.4, 53.5, 56.3, 62.4, 63.7, 69.9, 70.3, 71.0, 73.9, 100.4, 174.2, 177.0, 179.7. [HRMS] $[M+H]^+$ m/z: calc. for $C_{19}H_{35}N_6O_9$: 491.2466, found 491.2485.

N-(Prop-2-yn-1-yl)acrylamide (41)

Propargyl amine (**40**) (3.98 g, 72.26 mmol) and DIPEA (12.5 mL, 71.99 mmol, 0.996 eq), were dissolved in dichloromethane (132 mL). The reaction mixture was cooled to 0 ^{o}C. Once chilled, acryloyl chloride (4.65 mL, 57.49 mmol, 0.80 eq) was added dropwise slowly (~30 mins). The reaction was then allowed to slowly warm to room temperature overnight. Stirring was continued for 20 hours after which the reaction mixture was washed with brine and water, dried over anhydrous sodium sulfate, and concentrated under vacuum. The product was obtained as an amorphous light yellow solid in an 84% yield after purification by column chromatography using an EtOAc/ Hex (2:1) mixture. Comparison with literature data[43] confirms its identity. ^{1}H NMR (500 MHz, $CDCl_3$) δ 2.22 (t, *J* = 2.5 Hz, 1H), 4.09 – 4.13 (dd, *J* = 2.5, 5.0 Hz, 2H), 5.63 – 5.69 (dd, *J* = 3.0, 10.5 Hz, 1H), 6.00 (broad s, 1H), 6.10 (dd, *J* = 10.5, 17.0 Hz, 1H), 6.29 (dd, *J* = 3.0, 17.0 Hz, 1H) ^{13}C-NMR (150 MHz, $CDCl_3$), δ 29.2, 71.7, 79.3, 127.3, 130.1, 165.2. [HRMS] $[M+H]^+$ m/z: calc. for C_6H_8NO: 110.0606, found 110.0611.

N-(3-(Trimethylsilyl)prop-2-yn-1-yl)acrylamide (42)

To a suspension of silver chloride (332.8 mg, 2.32 mmol, 0.25 eq) in dichloromethane (65 mL), compound (**41**) (1.01 g, 9.26 mmol), and DBU (6.85 mL, 45.80 mmol, 4.87 eq) were added. The reaction was allowed to stir at room temperature for 20 minutes, after which time, chlorotrimethylsilane (12.5 mL, 98.49 mmol, 10.64 eq) was added. After stirring the reaction at room temperature for 1.5 hours the reaction was heated to 45 ^{o}C for 22 hours. The reaction was then diluted with 200 mL of dichloromethane. The organic phase was washed with saturated sodium bicarbonate (2x 100mL), followed by 1% hydrochloric acid solution (2x 100mL), and water (1x 100mL). The organic phase was then dried over anhydrous sodium sulfate, filtered, and concentrated under vacuum. The product was obtained as an amorphous white solid in a 57% yield after purification by column chromatography using an EtOAc/ Hex (1:3) mixture. Comparison with literature data[43] confirms its identity. ^{1}H NMR (600 MHz, $CDCl_3$) δ 0.14 (s, 9H), 4.13 (d, *J* = 5.1 Hz, 2H), 5.65 (dd, *J* = 1.2, 10.3 Hz, 1H), 5.85 (broad s, 1H), 6.09 (dd, *J* = 10.3, 17.0 Hz, 1H), 6.28 (dd, *J* = 1.2, 17.0 Hz, 1H), ^{13}C-NMR (150 MHz, $CDCl_3$), δ -0.2, 30.3, 88.7, 100.9, 127.1, 130.2, 164.9. [HRMS] $[M+H]^+$ m/z: calc. for $C_9H_{16}NOSi$: 182.1001, found 182.0998.

3-(4-(Aminomethyl)-1H-1,2,3-triazol-1-yl)propan-1-ol (51)

Step 1: 3-azido-propan-1-ol (**50**) needed to be freshly synthesized. Due to the low molecular weight of this azide, caution must be taken during the concentration step for this compound. This reaction was accomplished by addition of commercially available 3-chloropropan-1-ol (**49**) (1.5 g, 15.87 mmol, 1.0 eq.) to sodium azide (2.06g, 31.69 mmol, 2.0 eq.) and water (40 mL).

This reaction was then heated to 80 ^{o}C and left to react for 18 hours. After which time, the aqueous phase was extracted with EtOAc 3 to 4 times (40 mL). The organic layers were washed with brine (30 mL) and then dried over anhydrous sodium sulfate, filtered, and concentrated under close supervision under reduced pressure. This colorless oil (**50**) was used directly in the next step. **Step 2**: 3-Azido-propan-1-ol (**50**) (1.6 g, 15.82 mmol, 2.5 eq) synthesized in the previous step, propargyl amine (0.4 mL, 6.25 mmol, 1 eq), copper (I) iodide (1.00 g, 5.25 mmol, 0.84 eq.), and DIPEA (2.0 mL, 13.31 mmol, 2.13 eq.) were mixed together in a reaction flask containing DMF (50 mL). The reaction was then heated to 50 ^{o}C and continued overnight. After 16 hours, the product was isolated in a 70 % yield after both steps. Comparison with literature data[55] confirms its identity. ^{1}H NMR (600 MHz, D_2O) δ 1.92 – 2.03 (m, 2H), 3.42 (t, *J* = 6.3 Hz, 2H), 3.74 (t, *J* = 7.1 Hz, 2H), 4.35 (t, *J* = 7.0 Hz, 2H), 7.75 (s, 1H), ^{13}C NMR (150 MHz, D_2O) δ 31.93, 35.68, 47.29, 58.29, 123.39, 148.30. ESI-MS $[M+H]^{+}$ m/z: calc. for $C_6H_{12}NaN_4O_0$: 57.11 found 157.11.

N-((1-(3-Hydroxypropyl)-1H-1,2,3-triazol-4-yl)methyl)acetamide (**52**)

Compound (**51**) (202.3mg, 1.30 mmol, 1eq.) was first dissolved in DMF (10 mL). The reaction mixture was then cooled to -60 ^{o}C at which point 2, 4, 6- collidine (511 μL, 4.63 mmol, 3.56 eq) was added. This mixture was allowed to stir for 20 mins to ensure the reaction mixture was at -60 ^{o}C. Then, acetyl chloride (91 μL, 1.05 mmol, 0.8 eq.) was added dropwise to the chilled solution. Once added, the reaction was allowed to stir for 2 hours. At this point, it was warmed to -30 ^{o}C, diluted with EtOAc (10 mL) and washed with 1M HCl (10 mL), followed by

saturated sodium bicarbonate (10mL), and brine (10mL). The organic phase was then dried over anhydrous sodium sulfate, filtered, and concentrated under vacuum. The product was obtained in a 53 % yield, as a light yellow solid, after purification by column chromatography using a DCM/ MeOH/ H_20 (33: 15: 2) mixture. Comparison with literature data[56] confirms its identity. ^{1}H NMR (600 MHz, D_2O) δ 1.87 (s, 3H), 1.97 (p, *J*= 6.6 Hz, 2H), 3.42 (t, *J* = 6.6 Hz, 2H), 4.29 (s, 2H), 4.35 (t, *J*= 6.6 Hz, 2H), 7.75 (s, 1H), ^{13}C-NMR (150 MHz, $CDCl_3$), δ 21.9, 31.9, 34.7, 47.4, 58.3, 123.9, 144.7, 174.3. [HRMS] $[M+H]^+$ m/z: calc. for $C_8H_{15}N_4O_2$: 199.1195, found 199.1202.

N-((1-(3-Hydroxypropyl)-1H-1,2,3-triazol-4-yl)methyl)-6-(5-((3aS,4S,6aR)-2-oxohexahydro-1H-thieno[3,4-d]imidazol-4-yl)pentanamido)hexanamide (**53**)

Compound (**51**) (25.5 mg, 0.16 mmol, 1 eq.) and biotinated amino caproic acid N-hydroxysuccinimide ester (**35**) (80.2 mg, 0.18 mmol, 1.1 eq.) were dissolved in NMP (2 mL). Then DIPEA (26.4 μL, 0.16 mmol, 1 eq.) was added and the reaction allowed to stir at room temperature for 17 hours. Once reaction had gone to completion as monitored my TLC using a DCM/ MeOH/ H_2O (33: 15: 2) solvent mixture, reaction was cooled to 0 ^oC and then the product was precipitated out using ice cold ether. Product was then filtered and then re-dissolved in H_2O. Product (**53**) was then lyophilized under high vacuum producing a pure white product in a 73 % yield. ^{1}H NMR (600 MHz, D_2O) δ 1.31 – 1.38 (m, 2H), 1.39 – 1.50 (m, 3H), 1.52 – 1.59 (m, 2H), 1.59 – 1.83 (m, 7H), 2.15 – 2.22 (m, 2H), 2.30 (t, *J* = 7.2 Hz, 2H), 2.33 – 2.39 (m, 2H), 2.79 – 2.87 (m, 1H), 3.04 (dd, *J* = 13.1, 5.0 Hz, 1H), 3.16 – 3.28 (m, 2H), 3.35 – 3.42 (m, 1H),

3.63 (t, *J* = 6.2 Hz, 2H), 4.48 (dd, *J* = 7.9, 4.5 Hz, 1H), 4.51 (s, 2H), 4.57 (t, *J* = 7.0 Hz, 2H), 4.64 – 4.69 (m, 1H), 7.96 (s, 1H), ^{13}C-NMR (150 MHz, $CDCl_3$), δ 25.0, 25.3, 25.6, 27.8, 28.0, 28.1, 32.0, 34.5, 35.59, 35.64, 39.2, 39.8, 47.4, 55.5, 58.3, 60.4, 62.2, 124.0, 144.8, 165.5, 176.8, 177.0. [HRMS] $[M+H]^+$ m/z: calc. for $C_{22}H_{38}N_7O_4S$: 496.2706, found 496.2719.

General procedure for colorimetric determination of carbohydrate concentration.

Serial dilutions of known carbohydrate (i.e., GalNAc, Gal) concentrations in PBS were made, ranging from 2 mg/ mL down to 4 μg/ mL. Then, 200 μL of each solution were pipetted into either a 96-well plate or Eppendorf tubes depending on the number of samples to be measured. Next, 50 μL of an 80 % phenol solution in H_2O was added to each tube. After this point, 1 mL of concentrated H_2SO_4 was added rapidly to each to allow good mixing. The mixtures were then allowed to stand at r.t. for 10 minutes before being placed for an additional 15 minutes in a water bath set at 30 ^{o}C. After this time, the solutions should develop a yellow color which can be measured at 480 nm.

General procedure for vaccine emulsion preparation.

Samples were combined with Freunds adjuvant (complete for first inject, and incomplete for all booster injections) in a 1: 1 ratio by volume. Samples were then vortexed on high overnight (≥15-20 hours prior to immunizations). Note: all samples were calculated and prepared assuming one extra mouse more than what was used during the study to account for volume loss due to the formation of this emulsion and for loss in the syringe. After stirring overnight, emulsions were thick, white, and homogeneous.

Study 1: Immunization of mice with TMV-1 Cys conjugates

Pathogen-free C57BL/6 female mice age 6-10 weeks were obtained from Jackson Laboratory (Bar Harbor, ME, USA) and maintained in the Animal Care Facility at the biochemistry building of Michigan State University. All animal care procedures and experimental protocols have been approved by the Institutional Animal Care and Use Committee (IACUC) Michigan State University.

Vaccine Injections:

Group 1- Control: Five C57BL/6 mice were injected subcutaneously (90 μL) under the scruff on day 0 with 240 μg of TMV-1Cys as an emulsion in CFA (0.1 mL, Fisher). Booster injections (90 μL) were given subcutaneously under the scruff on days 14 and 21 with 240 μg of TMV-1Cys as emulsions in IFA (0.1 mL, Fisher)**.**

Group 2: Five C57BL/6 mice were injected subcutaneously (90 μL) under the scruff on day 0 with 60 μg of TMV-1Cys-Tn-N_3 (containing 522 ng of GalNAc) as an emulsion in CFA. Booster (90 μL) injections were given subcutaneously under the scruff on days 14 and 21 with 60 μg of TMV-1Cys-Tn-N_3 (containing 522 ng of GalNAc) as emulsions in IFA.

Group 3: Five C57BL/6 mice were injected subcutaneously (90 μL) under the scruff on day 0 with 240 μg of TMV-1Cys-Tn-N_3 (containing 2.1 μg of GalNAc) as an emulsion in CFA. Booster injections (90 μL) were given subcutaneously under the scruff on days 14 and 21 with 240 μg of TMV-1Cys-Tn-N_3 (containing 2.1 μg of the GalNAc) as emulsions in IFA.

Group 4: Three C57BL/6 mice were injected subcutaneously (90 μL) under the scruff on day 0 with 53 μg of TMV-1Cys-Tn-bromoacetamide (containing 137 ng of GalNAc) as an emulsion in CFA. Booster injections (90 μL) were given subcutaneously under the scruff on days 14 and 21

with 53 μg of TMV-1Cys-Tn-bromoacetamide (containing 137 ng of GalNAc) as emulsions in IFA.

Blood Collections:

Blood (~ 0.2 mL/mouse) was collected from all groups of mice on days 0, 7, 28 and 35. Sera from each group of mice were allowed to clot at 0 ^{o}C overnight and then centrifuged at 3,000 RPM for 10 minutes (longer time may be required, but it is recommended not to increase centrifugal rate as red blood cells will lyse). Sera was then extracted from the red blood cell clot and stored at -20 ^{o}C until needed for ELISA analysis

Study 2: Immunization of mice with TMV-1 Cys conjugates reproduced

Pathogen-free C57BL/6 female mice age 6-10 weeks were obtained from Jackson Laboratory (Bar Harbor, ME, USA) and maintained in the Animal Care Facility at the biochemistry building of Michigan State University. All animal care procedures and experimental protocols have been approved by the Institutional Animal Care and Use Committee (IACUC) Michigan State University.

Vaccine Injections:

Group 1: Four C57BL/6 mice were injected subcutaneously (90 μL) under the scruff on day 0 with 240 μg of TMV-1Cys-Tn-N_3 (containing 2.1 μg of GalNAc) as an emulsion in CFA (0.1 mL, Fisher). Booster injections (90 μL) were given subcutaneously under the scruff on days 14 and 28 with 240 μg of TMV-1Cys-Tn-N_3 (containing 2.1 μg of GalNAc) as emulsions in IFA (0.1 mL, Fisher).

Group 2- Control: Four C57BL/6 mice were injected subcutaneously (90 μL) under the scruff on day 0 with 240 μg of TMV-1Cys as an emulsion in CFA. Booster injections (90 μL) were given subcutaneously under the scruff on days 14 and 28 with 240 μg of TMV-1Cys as emulsions in IFA**.**

Group 3- Control: Two C57BL/6 mice were NOT injected during the course of this study to test ensure that the mice antibody titers remain low throughout the course of the experiment.

Blood Collections:

Blood (~ 0.2 mL/mouse) was collected from all groups of mice on days 0, 7, and 35. Sera from each group of mice were allowed to clot at 0 ^{o}C overnight and then centrifuged at 3,000 RPM for 10 minutes (longer time may be required, but it is recommended not to increase centrifugal rate as red blood cells will lysis can occur). Sera was then extracted from the red blood cell clot and stored at -20 ^{o}C until needed for ELISA analysis

Study 3: Immunization of mice with Qβ conjugates

Pathogen-free C57BL/6 female mice age 6-10 weeks were obtained from Jackson Laboratory (Bar Harbor, ME, USA) and maintained in the Animal Care Facility at the biochemistry building of Michigan State University. All animal care procedures and experimental protocols have been approved by the Institutional Animal Care and Use Committee (IACUC) Michigan State University.

Vaccine Injections:

Group 1: Four C57BL/6 mice were injected subcutaneously (90 μL) under the scruff on day 0 with 17 μg of Qβ-Tn-N_3 (containing 450 ng of GalNAc) as an emulsion in CFA (0.1 mL,

Fisher). Booster injections (90 μL) were given subcutaneously under the scruff on days 14 and 28 with 17 μg of Qβ-Tn-N_3 (containing 450 ng of GalNAc) as emulsions in IFA (0.1 mL, Fisher).

Group 2: Five C57BL/6 mice were injected subcutaneously (90 μL) under the scruff on day 0 with 69 μg of Qβ-Tn-N_3 (containing 1.8 μg of GalNAc) as an emulsion in CFA. Booster injections (90 μL) were given subcutaneously under the scruff on days 14 and 28 with 68.97 μg of Qβ-Tn-N_3 (containing 1.8 μg of GalNAc) as emulsions in IFA.

Group 3: Four C57BL/6 mice were injected subcutaneously (90 μL) under the scruff on day 0 with 345 μg of Qβ-Tn-N_3 (containing 9 μg of GalNAc) as an emulsion in CFA. Booster injections (90 μL) were given subcutaneously under the scruff on days 14 and 28 with 345 μg of Qβ-Tn-N_3 (containing 9 μg of GalNAc) as emulsions in IFA.

Group 4- Control: Four C57BL/6 mice were injected subcutaneously (90 μL) under the scruff on day 0 with 220 μg of Qβ-propanol (containing 2.4 μg of propanol) as an emulsion in CFA. Booster injections (90 μL) were given subcutaneously under the scruff on days 14 and 28 with 220 μg of Qβ-propanol (containing 2.4 μg of propanol) as emulsions in IFA.

Group 5- Control: Three C57BL/6 mice were injected subcutaneously (90 μL) under the scruff on day 0 with 103 μg of Qβ-glucose (containing 2.9 μg of Glc) as an emulsion in CFA. Booster injections (90 μL) were given subcutaneously under the scruff on days 14 and 28 with 103 μg of Qβ-glucose (containing 2.9 μg of Glc) as emulsions in IFA.

Blood Collections:

Blood (~ 0.2 mL/mouse) was collected from all groups of mice on days 0, 7, and 35. Sera from each group of mice were allowed to clot at 0 ^{o}C overnight and then centrifuged at 3,000 RPM for 10 minutes (longer time may be required, but it is recommended not to increase centrifugal rate as red blood cells will lyse). Sera was then extracted from the red blood cell clot and stored at -20 ^{o}C until needed for ELISA analysis

General procedure for ELISA with NeutrAvidin

To each well of a 96-well microtiter plate (Thermo scientific Nunc Immuno 96-well solid plates (clear, passive surfaces) flat-bottomed; Maxisorp: pinchbar; 400 μL/ well), 100 μL of a NeutrAvidin solution (8 μg / mL in PBS) was added and the plate was allowed to incubate overnight at 4 ^{o}C (cover with aluminum foil). The next morning (~15 hours), the NeutrAvidin solution was thrown away and the plate washed with 200 μL PBST (0.5 % tween 20 in PBS) three times. Wells were dried by tapping over absorbent pads and residual air bubbles were carefully removed. Next, 200 μL of 1% BSA/PBS was added as a blocking agent and the plate was allowed to incubate for 1 hour at room temperature. After the hour had passed, the blocking solution was thrown away and the plate washed again three times with 200 μL PBST like above. Wells were dried by tapping over absorbent pads and residual air bubbles were carefully removed. Then, 200 μL of biotinated antigen (5 μg/ mL in 0.1 % BSA/ PBS) was added to each well. It was then incubated at 37 ^{o}C for 1 hour. During this wait time, 1:4 serial dilutions of the diluted serum samples (serum to 0.1 % BSA/PBS 1:10 ratio) were prepared. After the incubation was complete, the plate was washed three times with PBST and the wells dried

thoroughly. 100 μL of the freshly prepared serum samples was added to each well and incubated at 37 ^{o}C for 2 hours. The plate was again washed three times with PBST and dried. Next, 100 μL of a 1: 2000 dilution (secondary antibody (Ab) to 0.1 % BSA/PBS) of horseradish peroxidase (HRP)-conjugated goat anti-mouse IgG + IgM, IgG, or IgM (Jackson ImmunoResearch Laboratory IgG + IgM catalog # 115-035-068, IgG catalog # 115-035-071, or IgM catalog # 115-035-075) antibody was added to each well. This secondary antibody was incubated at 37 ^{o}C for 1 hour. During the last 10 minutes of this wait period, a solution of 3, 3', 5, 5'-tetramethylbenzidine (TMB) was prepared (5 mg of TMB was dissolved in 2 mL of DMSO and then diluted to 20 mL using citrate phosphate buffer). Immediately prior to adding the TMB solution to the plate, 20 μL of H_2O_2 was added. After incubation the plate was washed three times with PBST and dried. The freshly prepared TMB solution was then added (200 μL/ well). Color (blue) was allowed to develop for 10-20 minutes. At this time, 50 μL of a 0.5 M H_2SO_4 solution was added to quench the reaction (blue color changes to yellow). Note: if the color became too intense, the reaction should be quenched sooner. The optical density (OD) was then measured using a plate reader at 450 nm. Each experiment was repeated three to four times and the average was used to calculate the titers. Antibody titers were defined as the maximum folds of dilution resulting in a 0.1 OD unit higher than the average absorbance after greater than one hundred thousand folds of dilution.

General procedure for ELISA with BSA

To each well of a 96-well microtiter plate (Thermo scientific Nunc Immuno 96-well solid plates (clear, passive surfaces) flat-bottomed; Maxisorp; pinchbar; 400 μL/ well), 100 μL of a

BSA- Tn (10 μg / mL in PBS) was added and the plate was allowed to incubate overnight at 4 ^{o}C. The next morning (~15 hours), the BSA- Tn solution was thrown away and the plate washed with 200 μL PBST (0.5 % tween 20 in PBS) three times. Wells were dried by tapping over absorbent pads and residual air bubbles were carefully removed. Next, 200 μL of 1% BSA/PBS was added as a blocking agent and the plate was allowed to incubate for 1 hour at room temperature. During this wait time, 1:4 serial dilutions of the diluted serum samples (serum to 0.1 % BSA/PBS 1:10 ratio) were prepared. After the hour had passed, the blocking solution was thrown away and the plate washed again three times with 200 μL PBST like above. 100 μL of the freshly prepared serum samples was added to each well and incubated at 37 ^{o}C for 2 hours. The plate was again washed three times with PBST and dried. Next, 100 μL of a 1: 2000 dilution (secondary antibody (Ab) to 0.1 % BSA/PBS) of horseradish peroxidase (HRP)-conjugated goat anti-mouse IgG + IgM, IgG, or IgM (Jackson ImmunoResearch Laboratory IgG + IgM catalog # 115-035-068, IgG catalog # 115-035-071, or IgM catalog # 115-035-075) antibody was added to each well. This secondary antibody was incubated at 37 ^{o}C for 1 hour. During the last 10 minutes of this wait period, a solution of 3, 3', 5, 5'- tetramethylbenzidine (TMB) was prepared (5 mg of TMB was dissolved in 2 mL of DMSO and then diluted to 20 mL using citrate phosphate buffer). Immediately prior to adding the TMB solution to the plate, 20 μL of H_2O_2 was added. After incubation the plate was washed three times with PBST and dried. The freshly prepared TMB solution was then added (200 μL/ well). Color (blue) was allowed to develop for 10-20 minutes. At this time, 50 μL of a 0.5 M H_2SO_4 solution was added to quench the reaction (blue color changes to yellow). Note: if the color became too intense, the reaction

should be quenched sooner. The optical density (OD) was then measured using a plate reader at 450 nm. Each experiment was repeated three to four times and the average was used to calculate the titers. Antibody titers were defined as the maximum folds of dilution resulting in a 0.1 OD unit higher than the average absorbance after greater than one hundred thousand folds of dilution.

General procedure for competitive ELISA

The protocol for competitive ELISA was almost identical to that of the normal ELISA protocol mentioned previously. The only difference occurred after incubation with the biotinated antigen and wash. A 0.1 M GalNAc solution (dissolved in 0.1 % BSA/PBS) was used to dilute the serum samples (instead of 0.1 % BSA/ PBS like before). Note: The serum was allowed to incubate for 1 hour before addition to the plate as well as being directly added to the plate. No significant difference was noticed between the two methods.

General Procedure for FACS

NCI/ ADR- RES ovarian cancer cells were obtained from Professor Paul Erhardt, the University of Toledo, and were grown in serum containing RPMI-1640 containing 2.0 mM L-glutamine supplemented with 10% FBS, and incubated at 37 ^{o}C and 5% CO_2. On the day of the experiment, 100,000 cells/ mL were transferred to eppendorf tubes, and the tubes were labeled corresponding to the serum sample being tested. The cells were than washed with FACS buffer (1% BSA, 0.1% NaN_3/PBS) using centrifugation. The cells were then re-suspended in 1:10 diluted test sera (75 μL), and incubated at 4 ^{o}C for 30 minutes. The cells were then washed

twice with FACS buffer (1 mL). All tubes, including the control tube which does not contain serum, received 100 μL of a 1:100 diluted goat antimouse IgG labeled with FITC (Jackson ImmunoResearch Laboratory, catalog #115-095-164). Tubes were incubated with this secondary antibody at 4 ^{o}C for 30 minutes. The cells were washed again with FACS buffer (1 mL) and then resuspended in FACS buffer (200 μL). Fluorescence was then accessed immediately on a Vantage FACS to determine the percentage of positive cells.

APPENDICES

Appendix 1 – Spectral Data

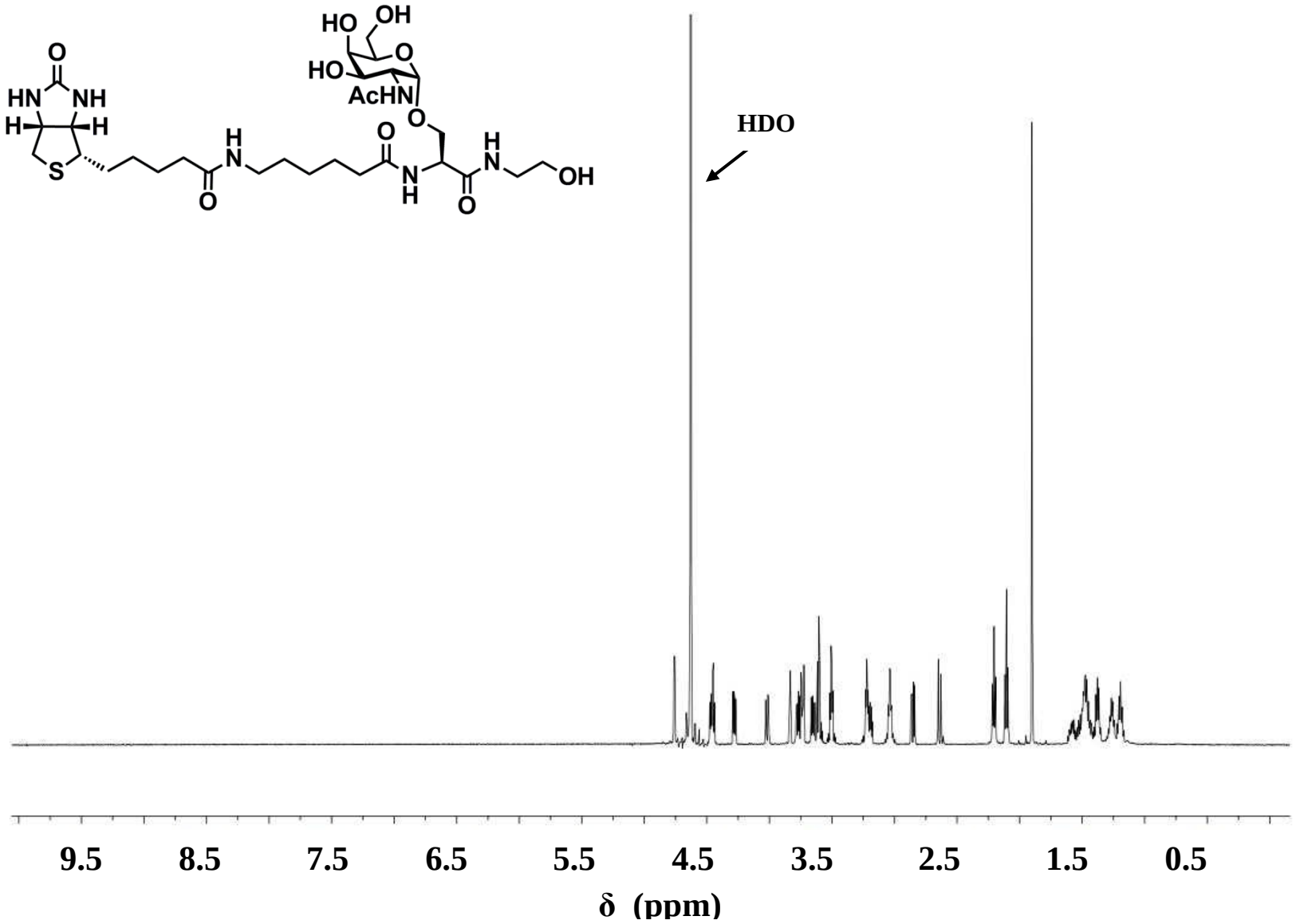

Figure 1.34: 600 MHz (D_2O), ^1H NMR of **19**

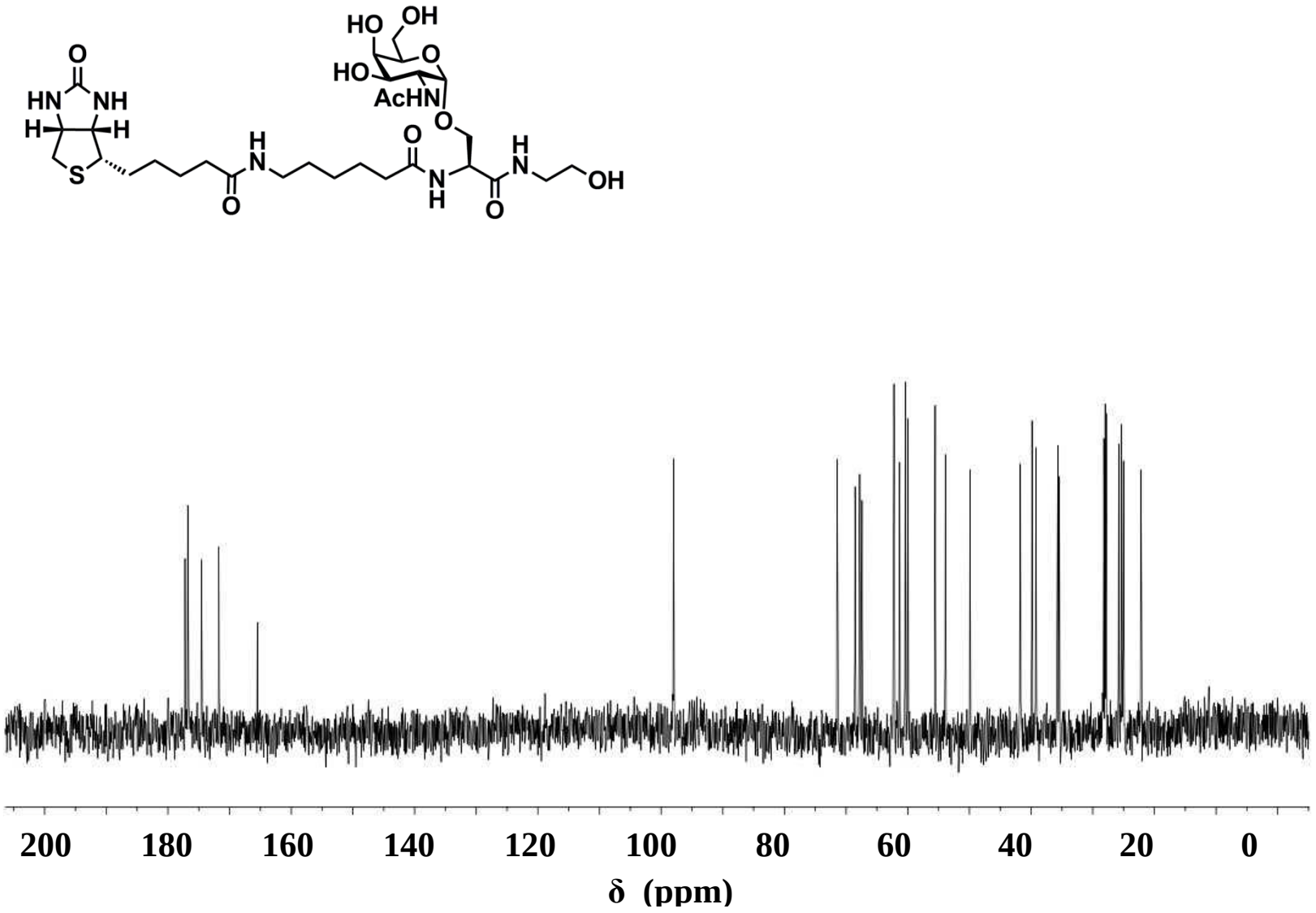

Figure 1.35: 125 MHz (D_2O), ^{13}C NMR of **19**

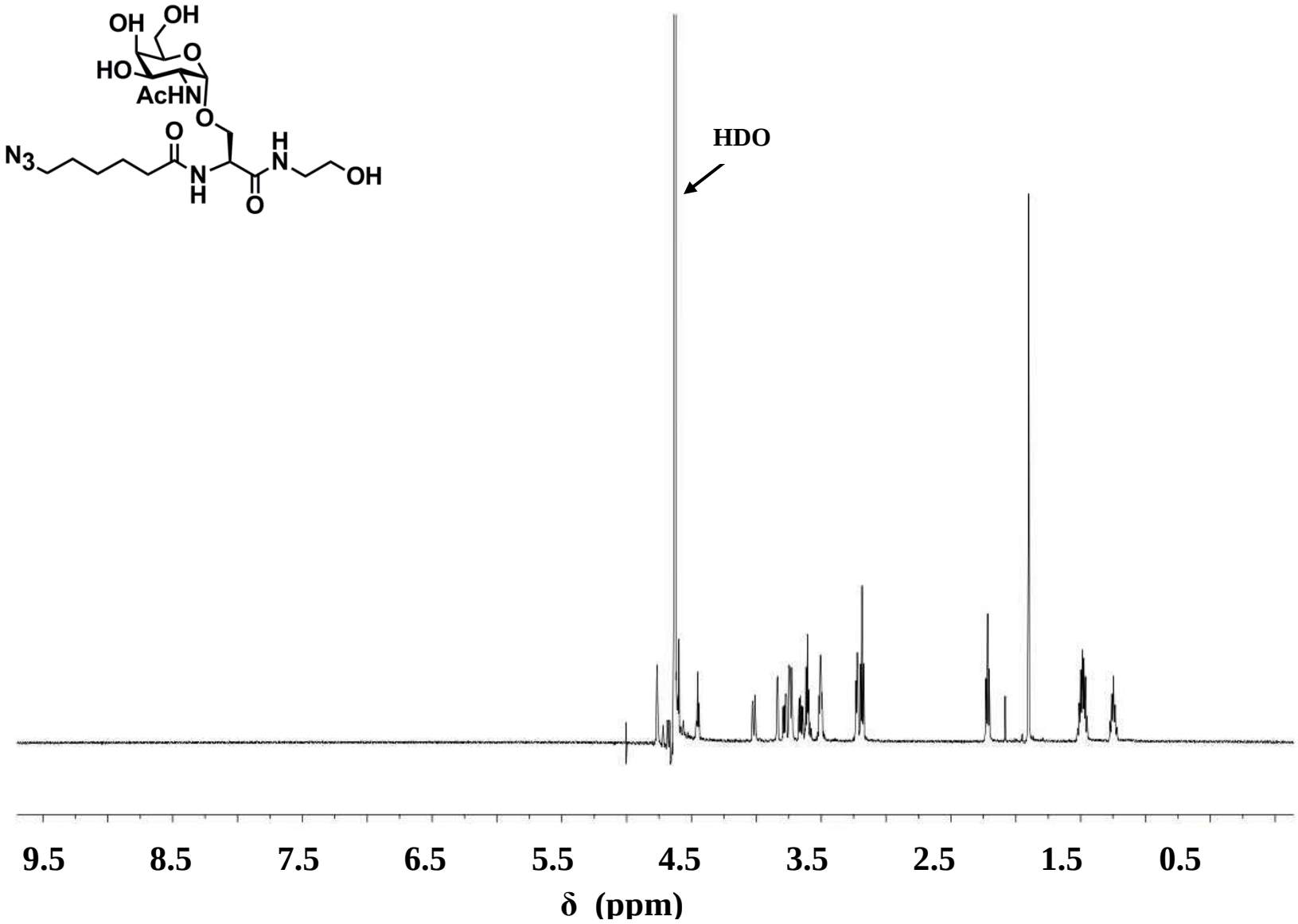

Figure 1.36: 600 MHz (D_2O), ^1H NMR of **20**

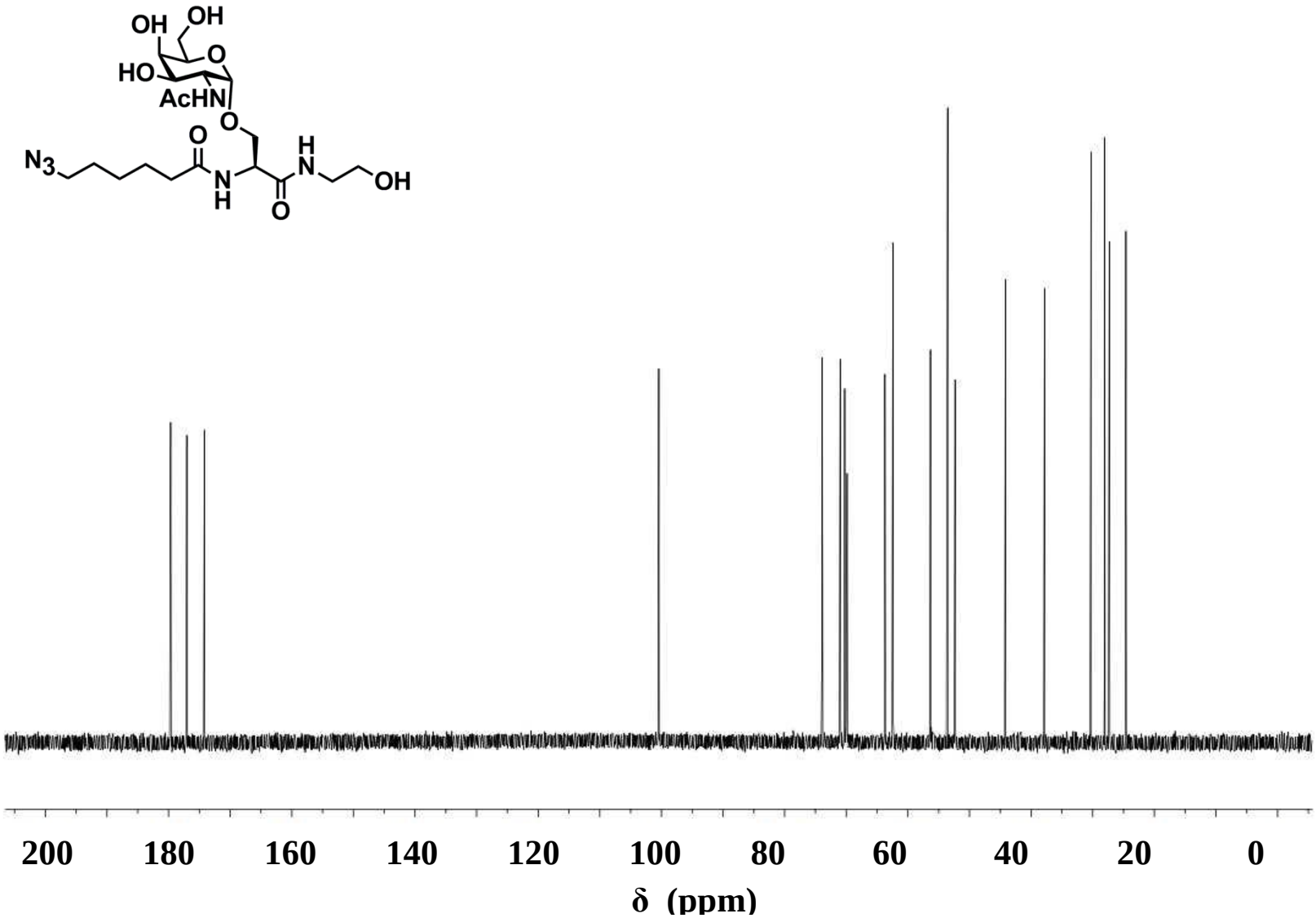

Figure 1.37: 150 MHz (D_2O), ^1H NMR of **20**

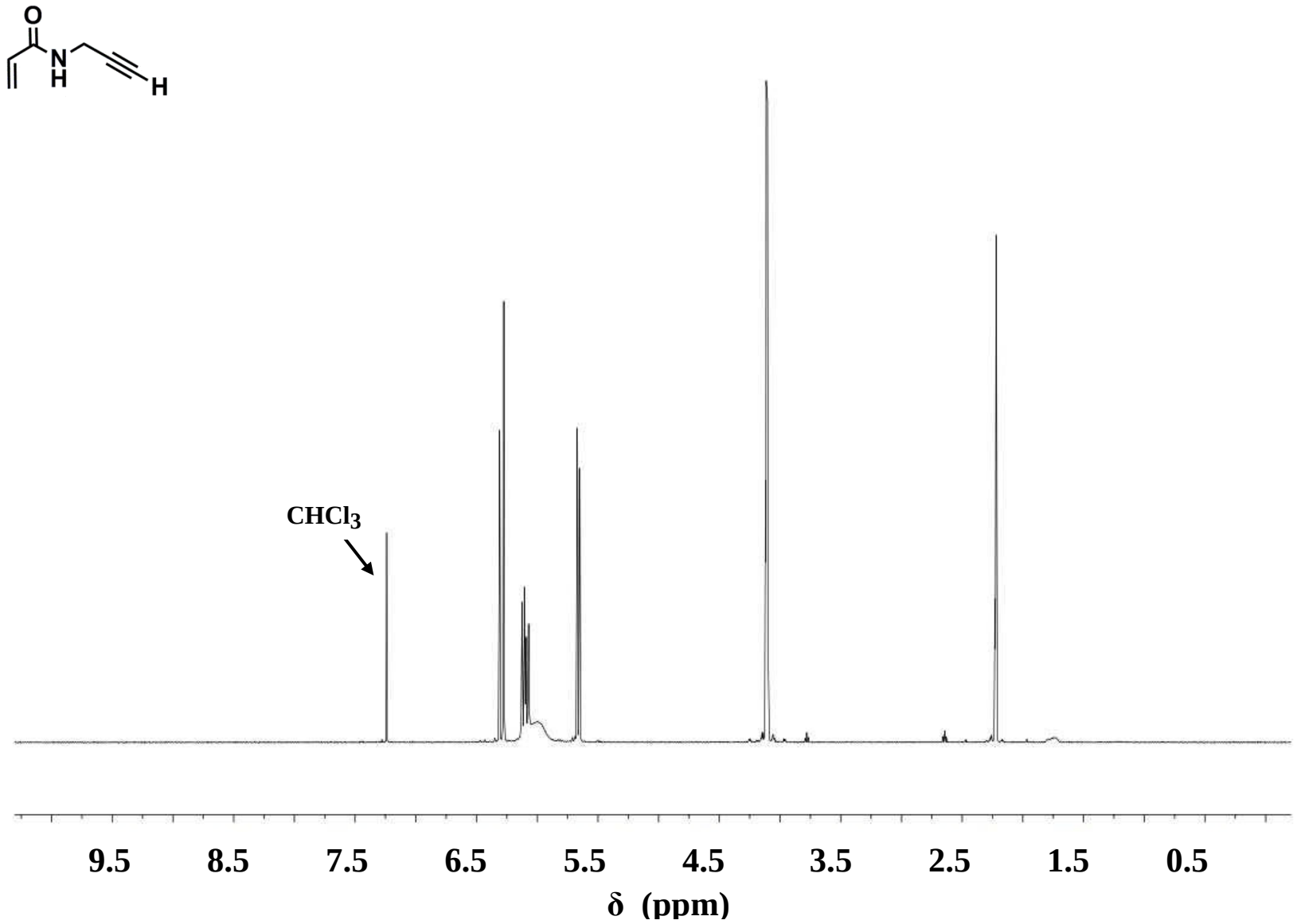

Figure 1.38: 500 MHz, ($CDCl_3$), ^1H NMR of **41**

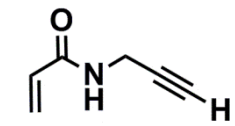

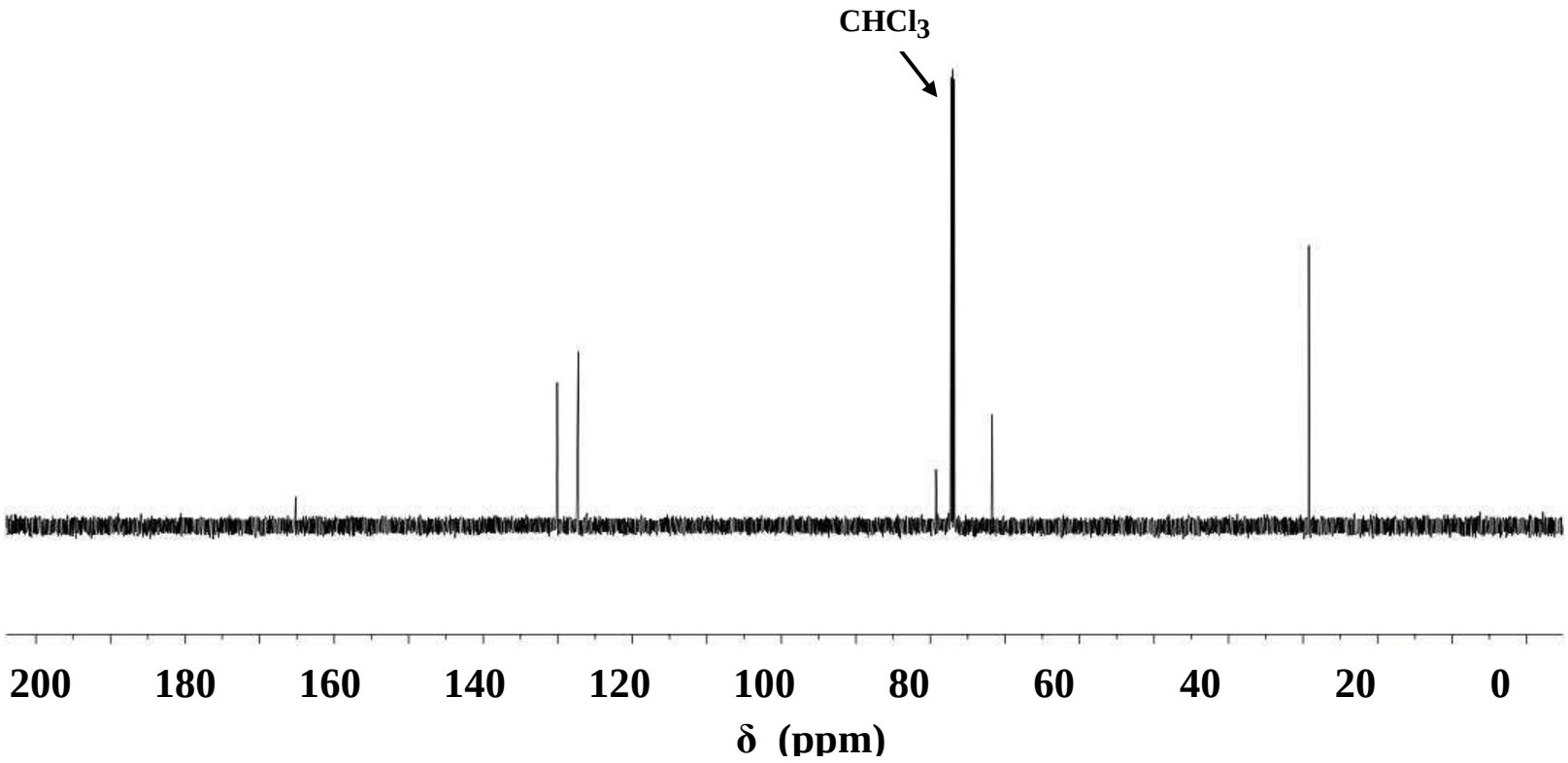

Figure 1.39: 150 MHz, ($CDCl_3$), ^{13}C NMR of **41**

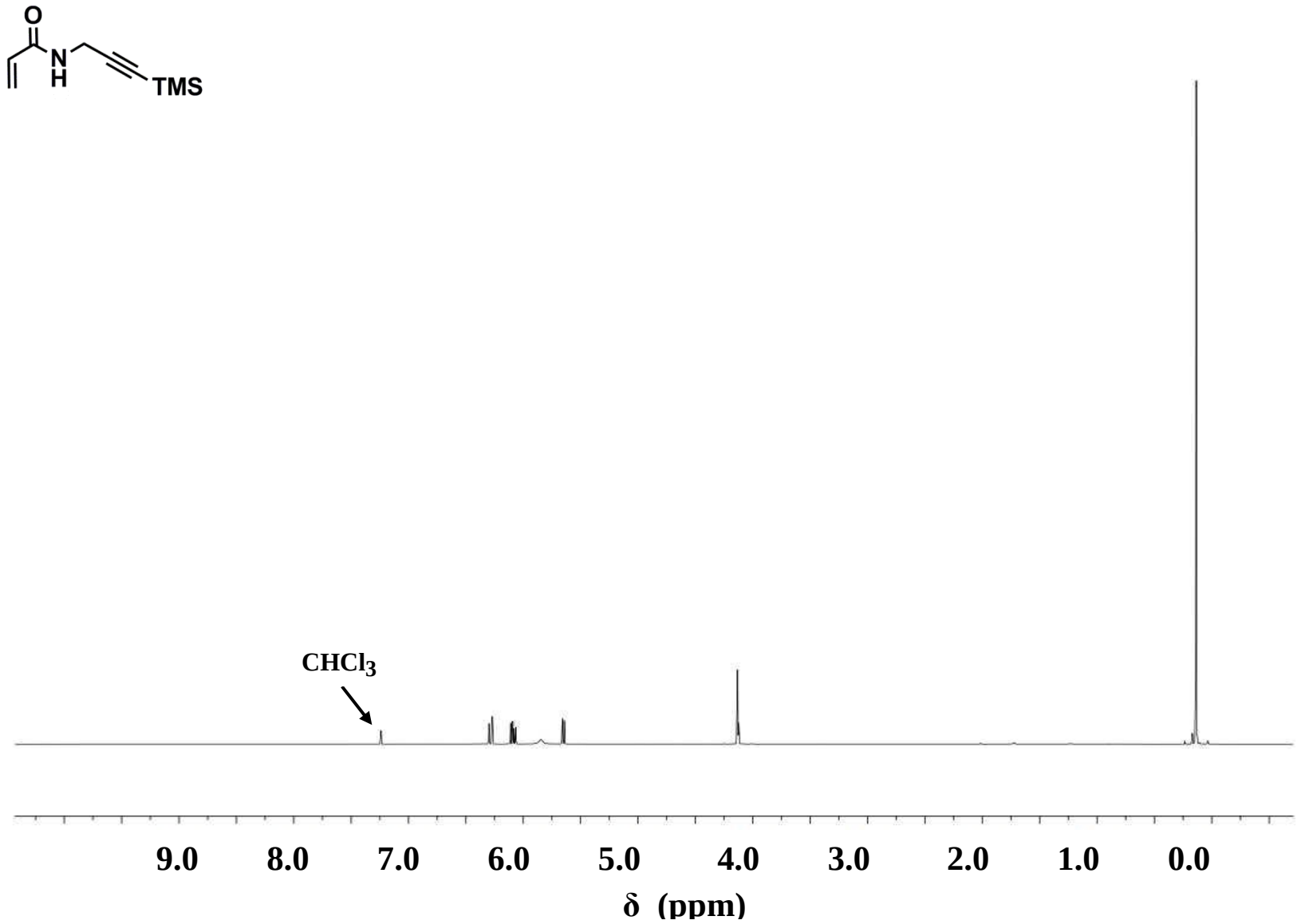

Figure 1.40: 600 MHz, ($CDCl_3$), ^1H NMR of **42**

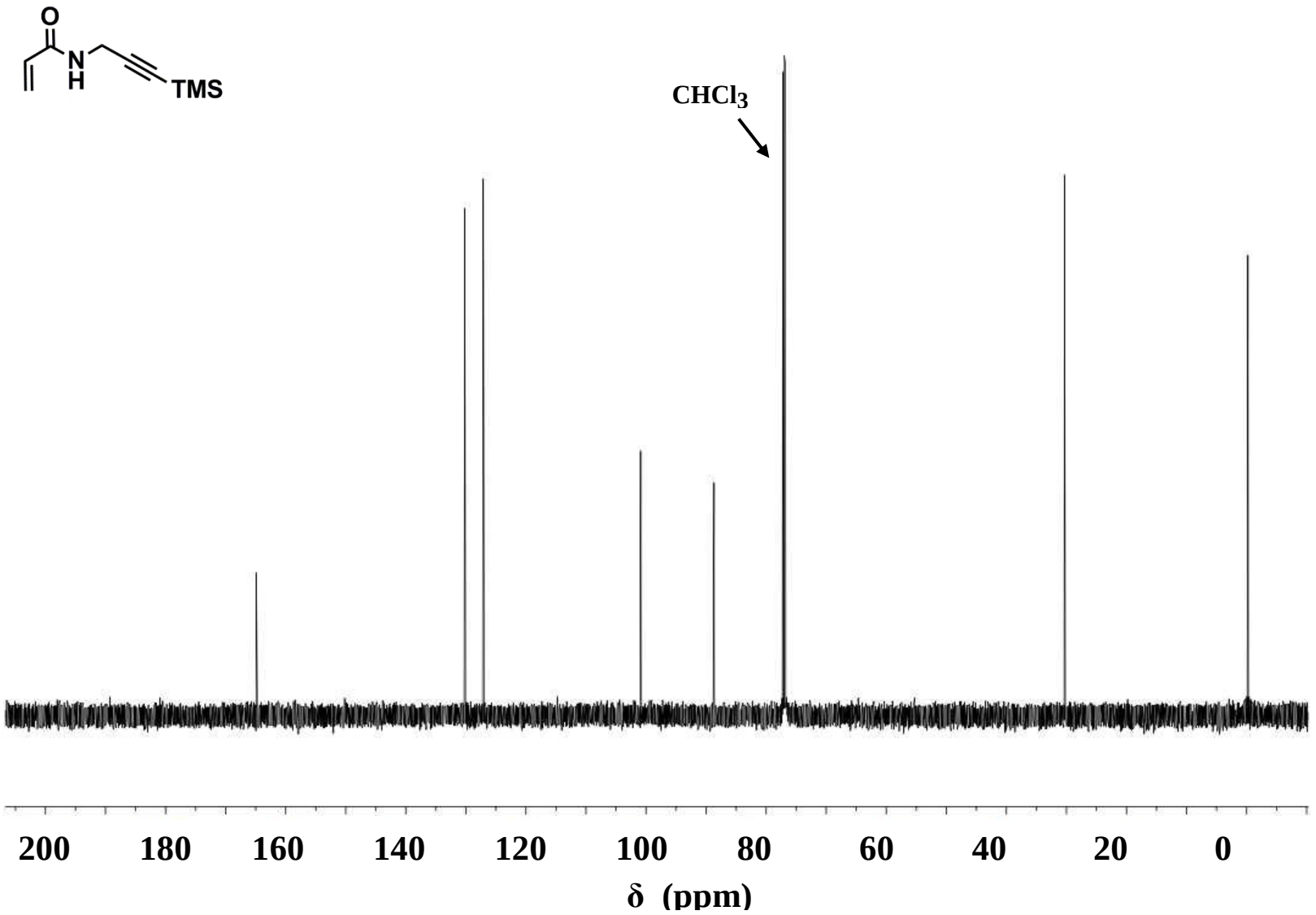

Figure 1.41: 150 MHz, ($CDCl_3$), ^{13}C NMR of **42**

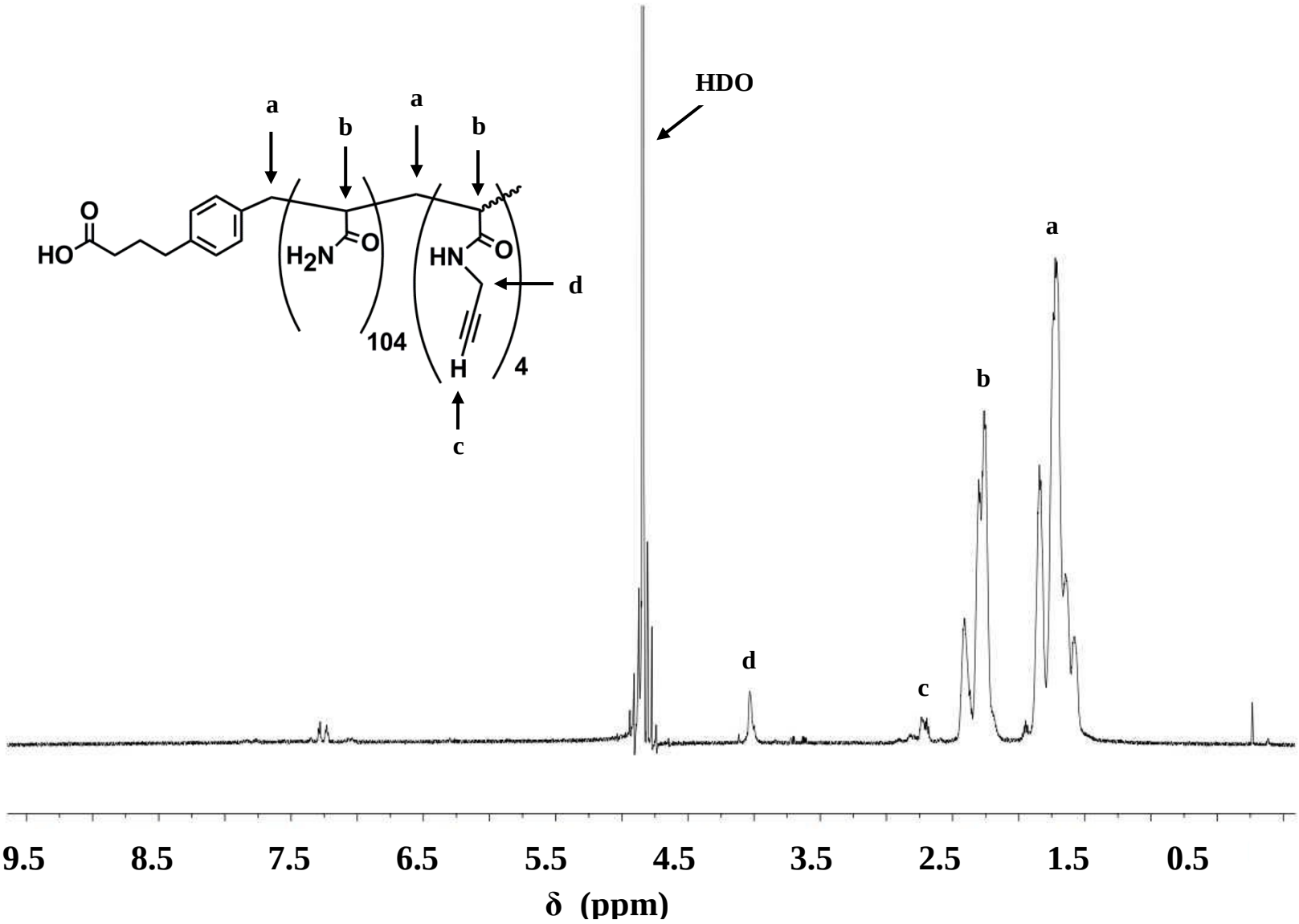

Figure 1.42: 600 MHz, (D_2O), ^1H NMR of **46A**

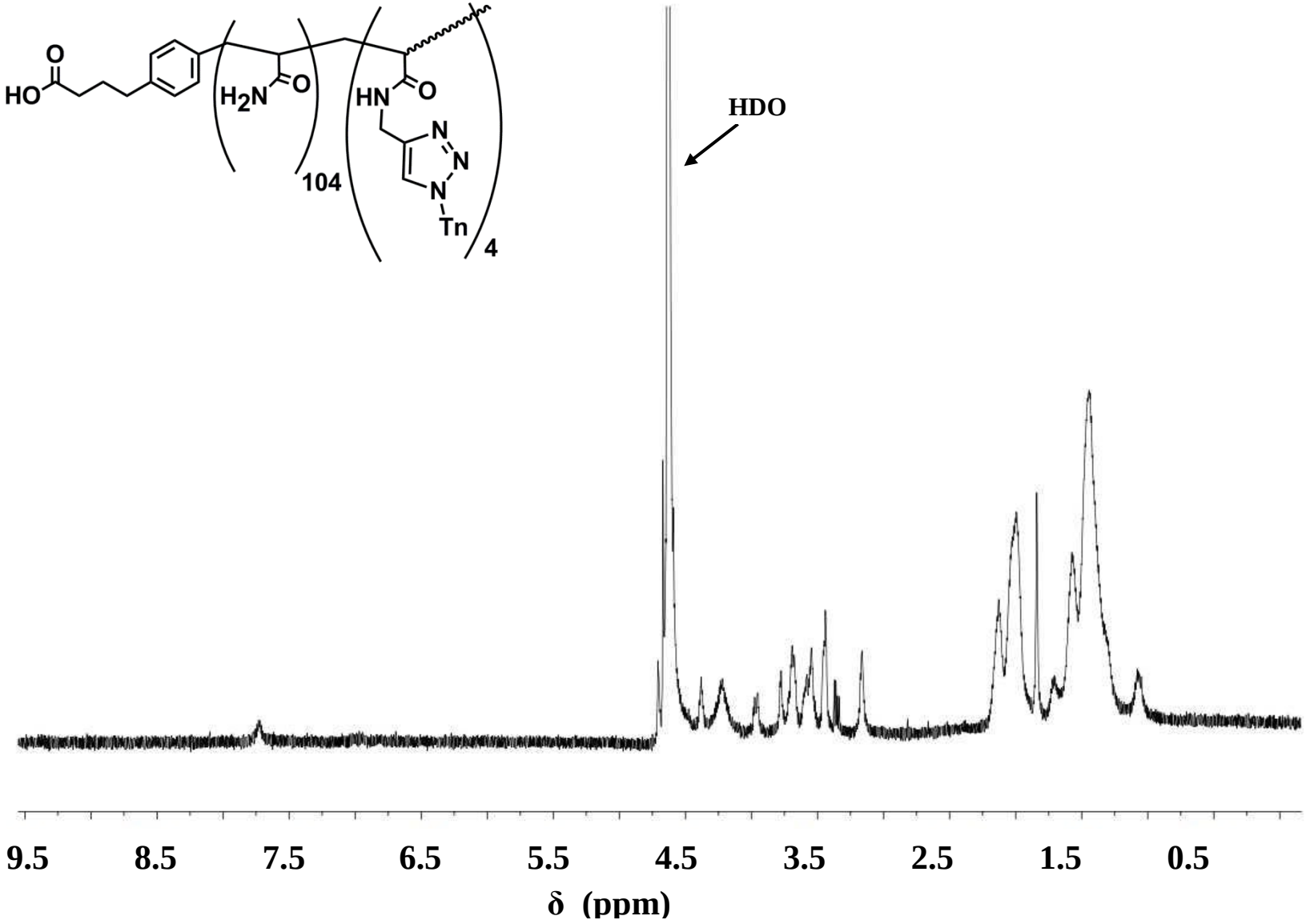

Figure 1.43: 500 MHz, (D_2O), ^1H NMR of **47A**

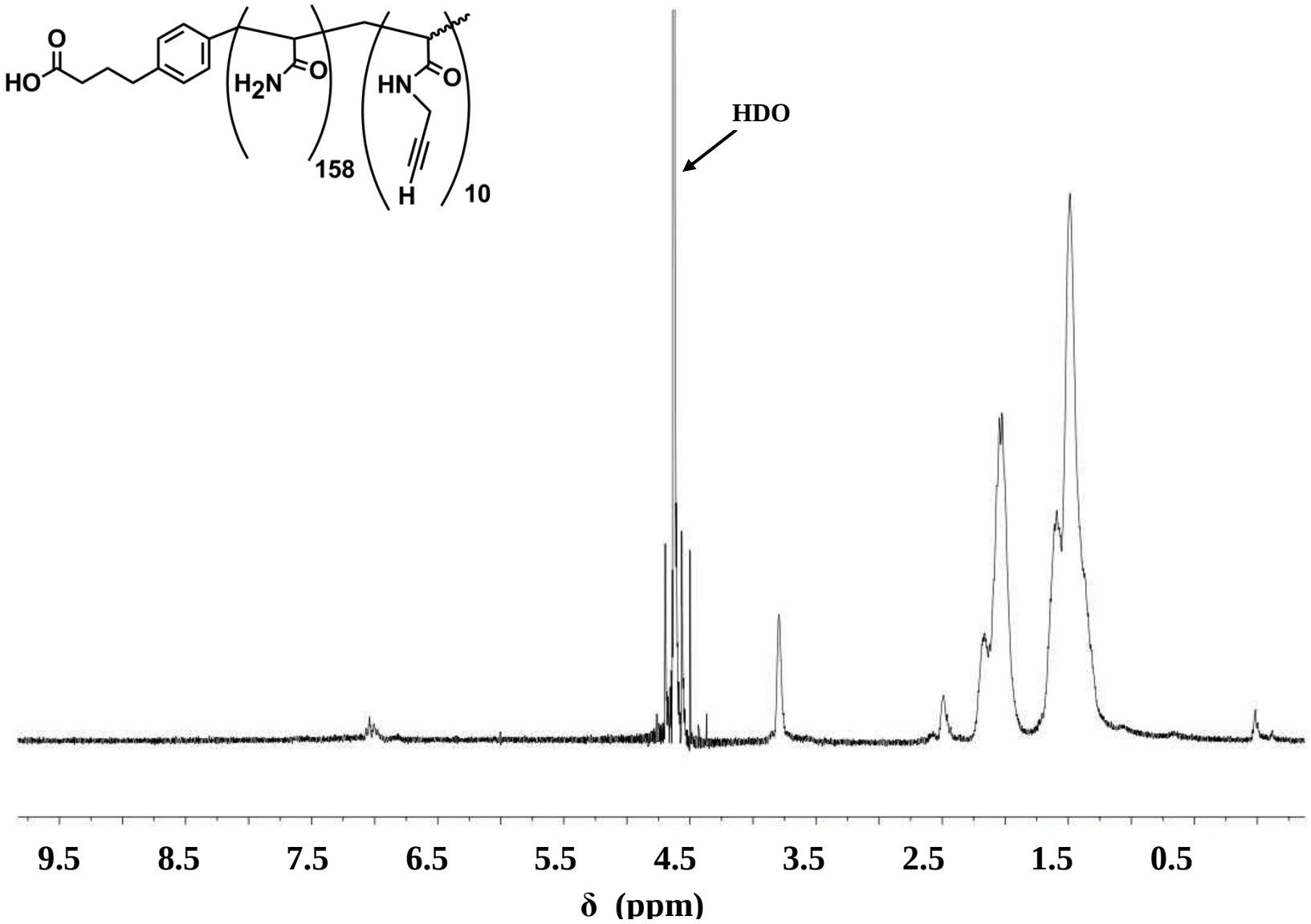

Figure 1.44: 300 MHz, (D_2O), ^1H NMR of **46B**

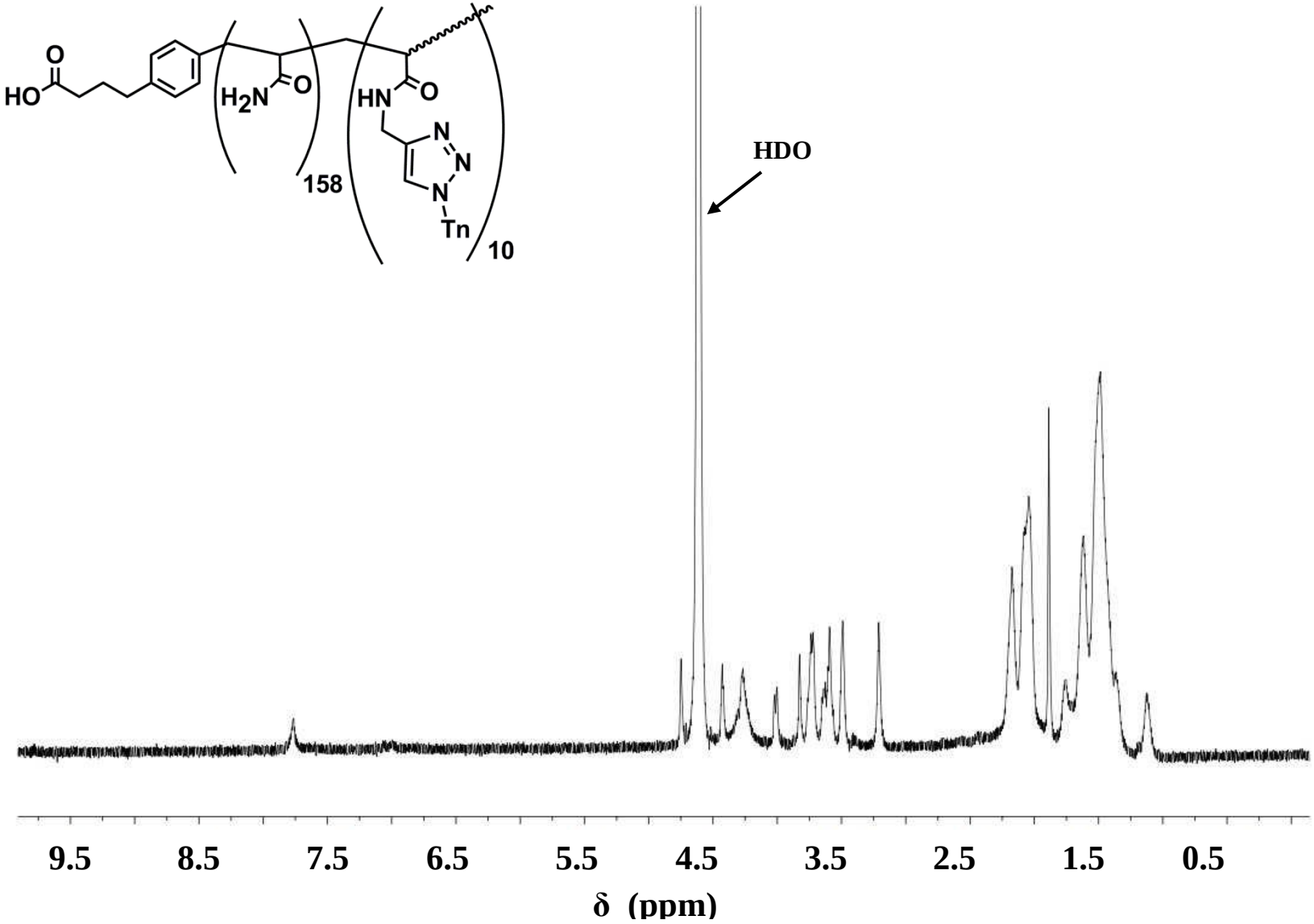

Figure 1.45: 600 MHz, (D_2O), ^1H NMR of **47B**

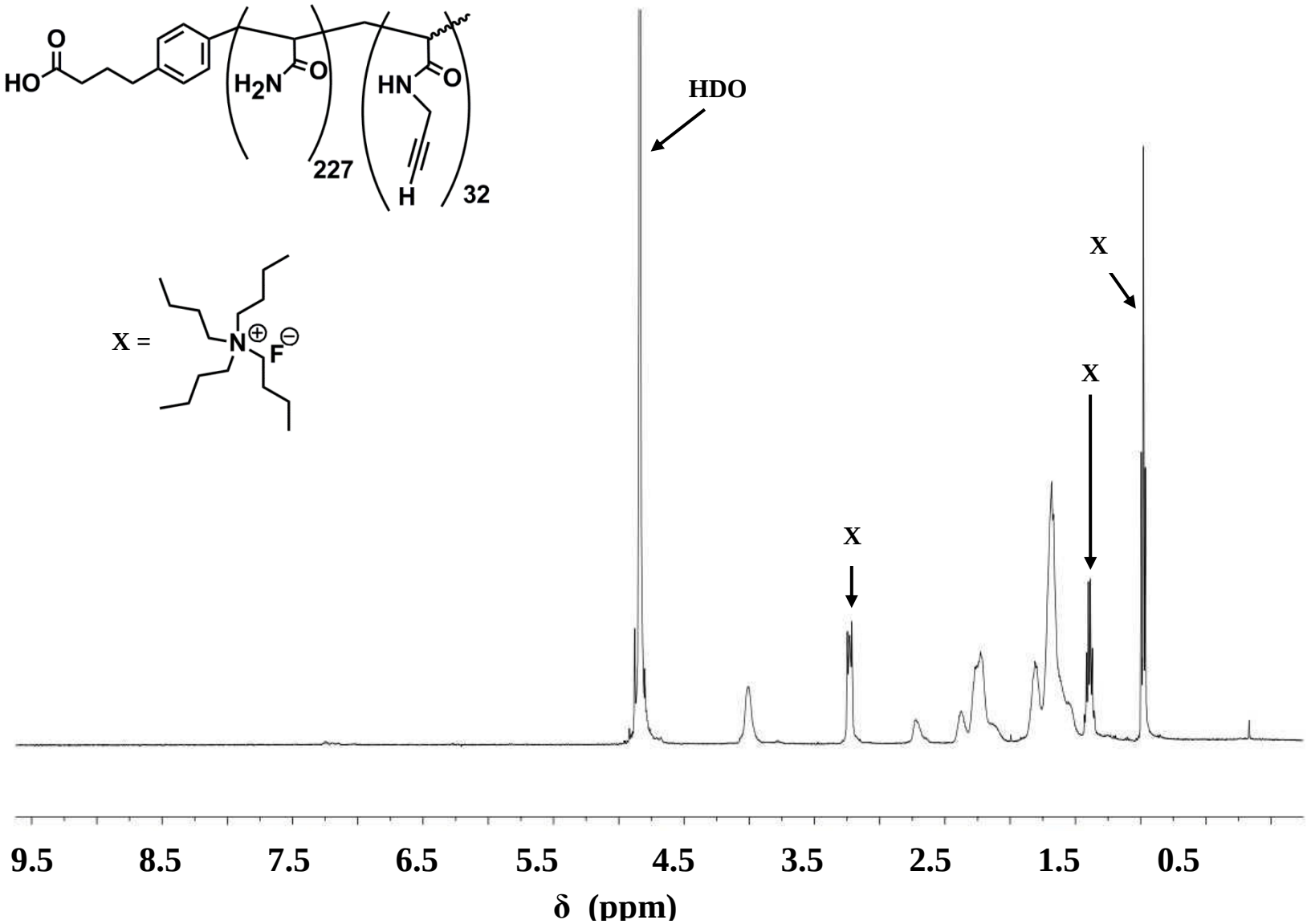

Figure 1.46: 500 MHz, (D_2O), ^1H NMR of **46C**

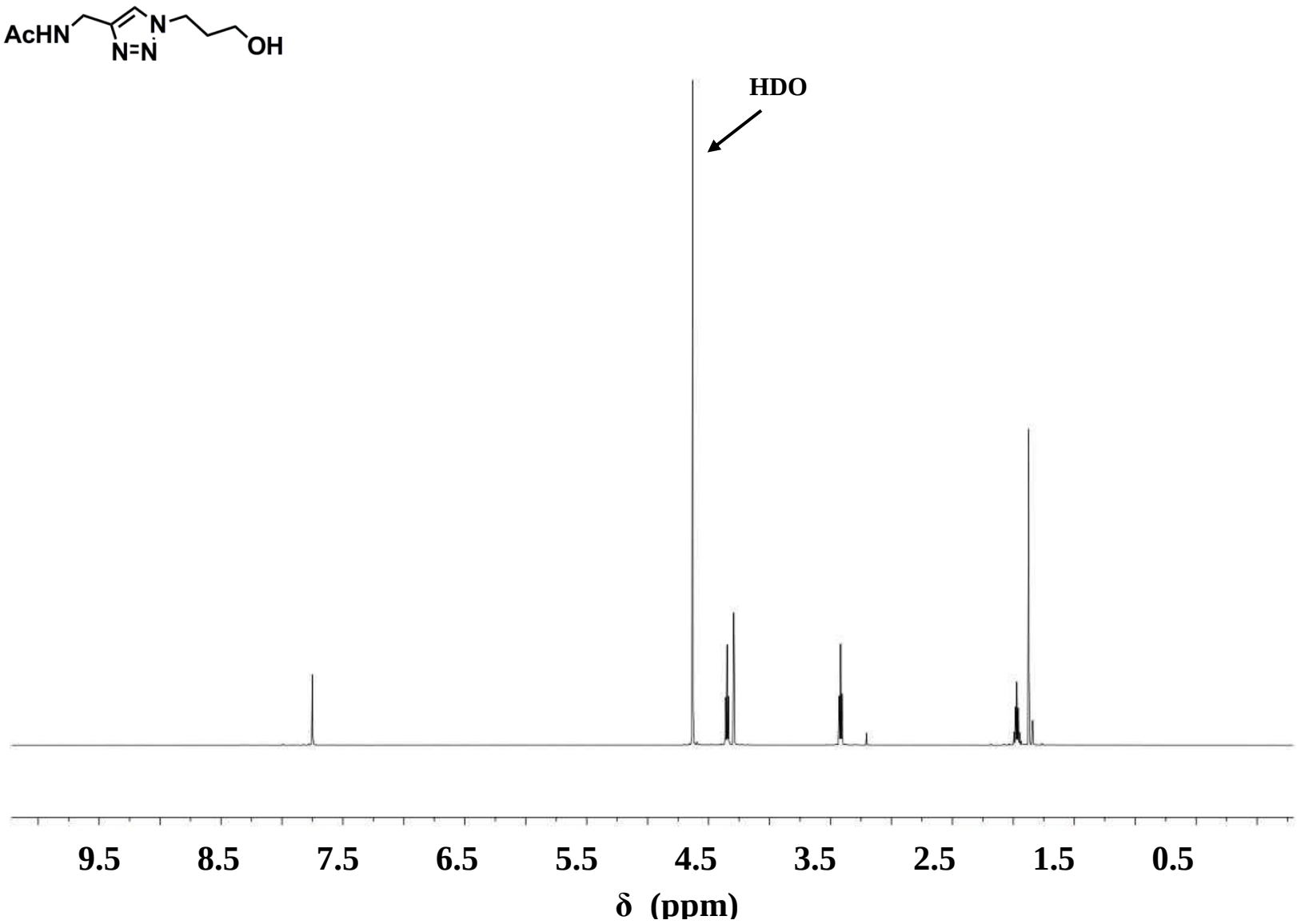

Figure 1.47: 600 MHz (D_2O), ^1H NMR of **52**

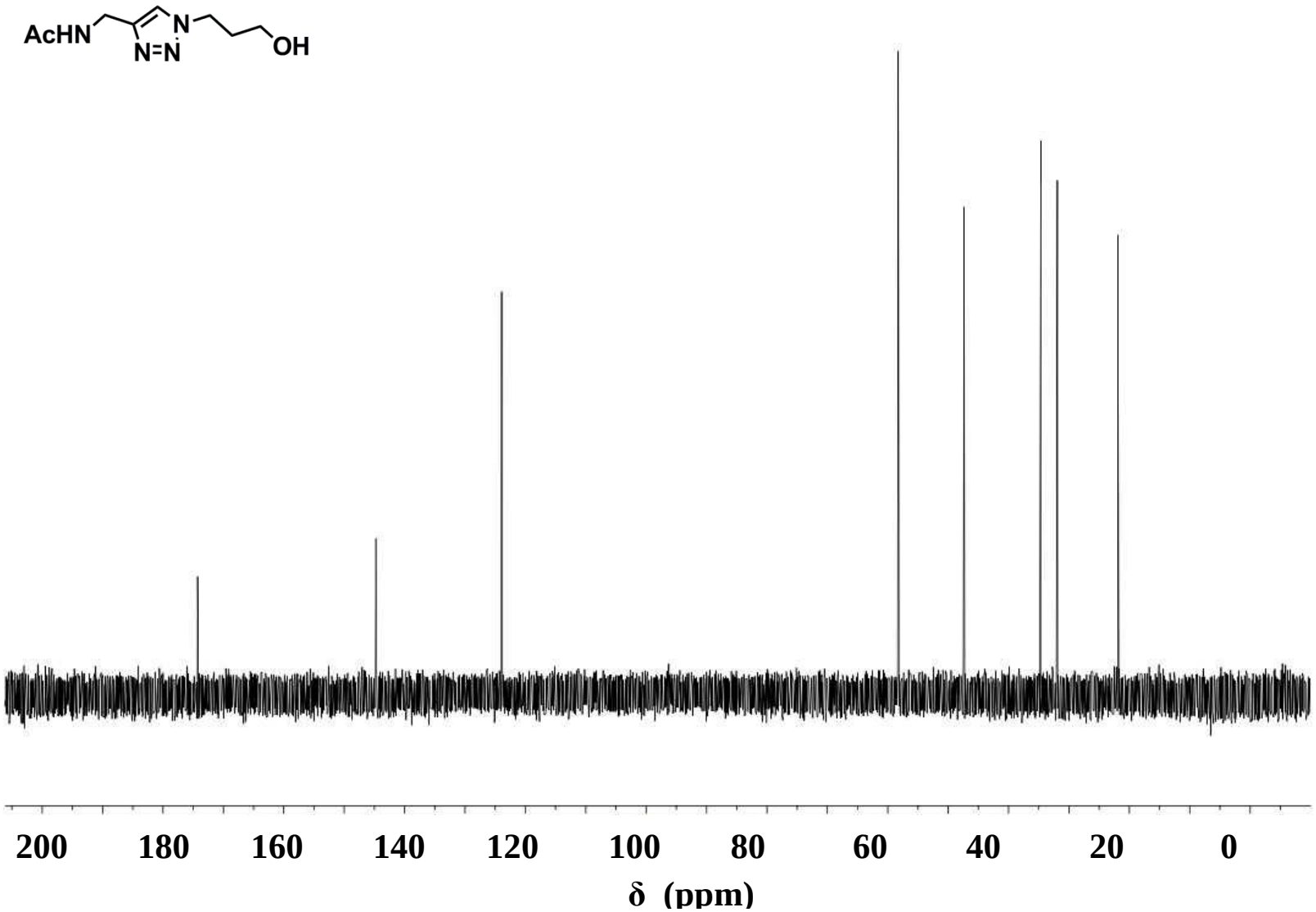

Figure 1.48: 600 MHz (D_2O), ^{13}C NMR of **52**

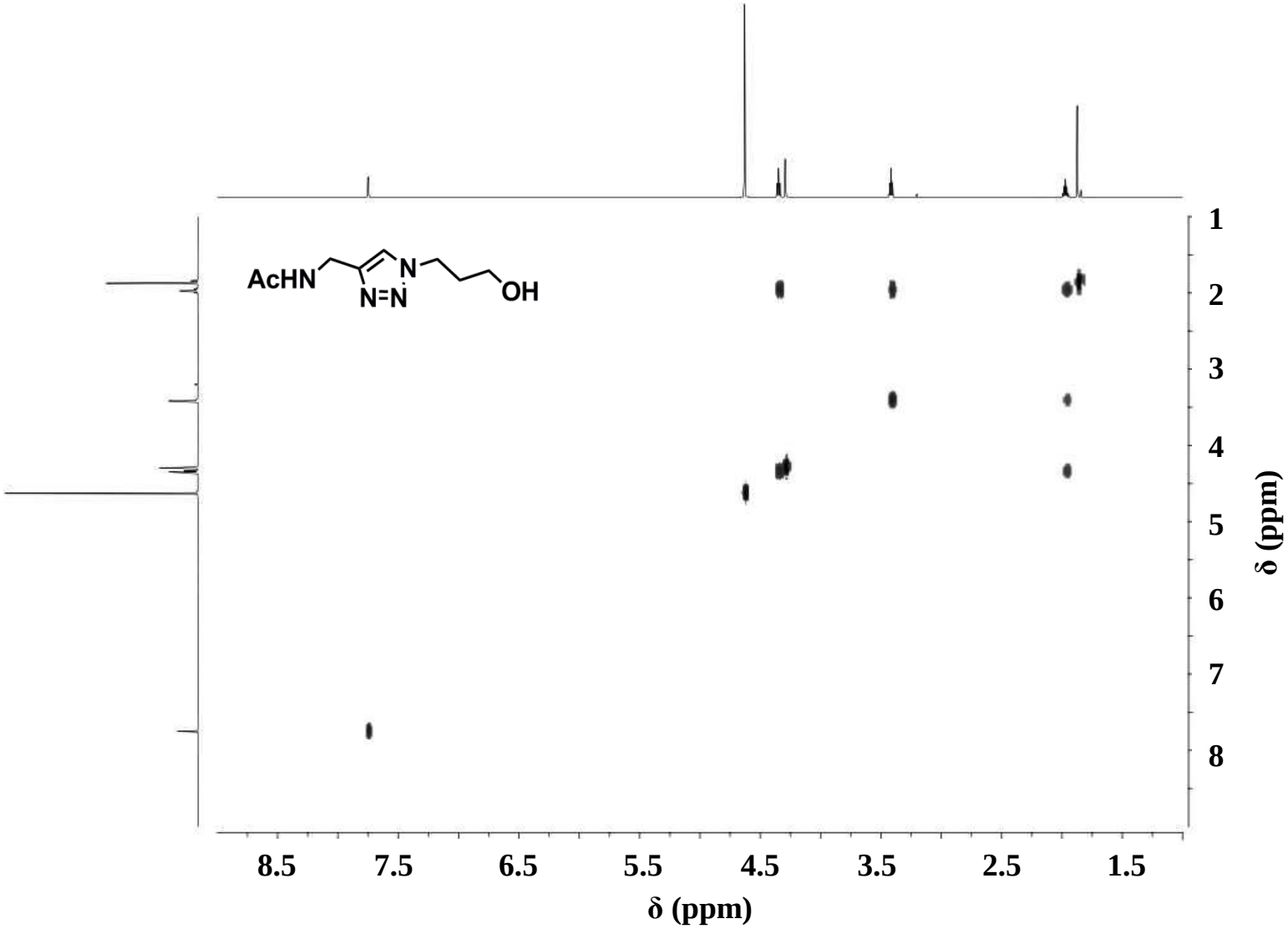

Figure 1.49: 600 MHz (D_2O), gCOSY NMR of **52**

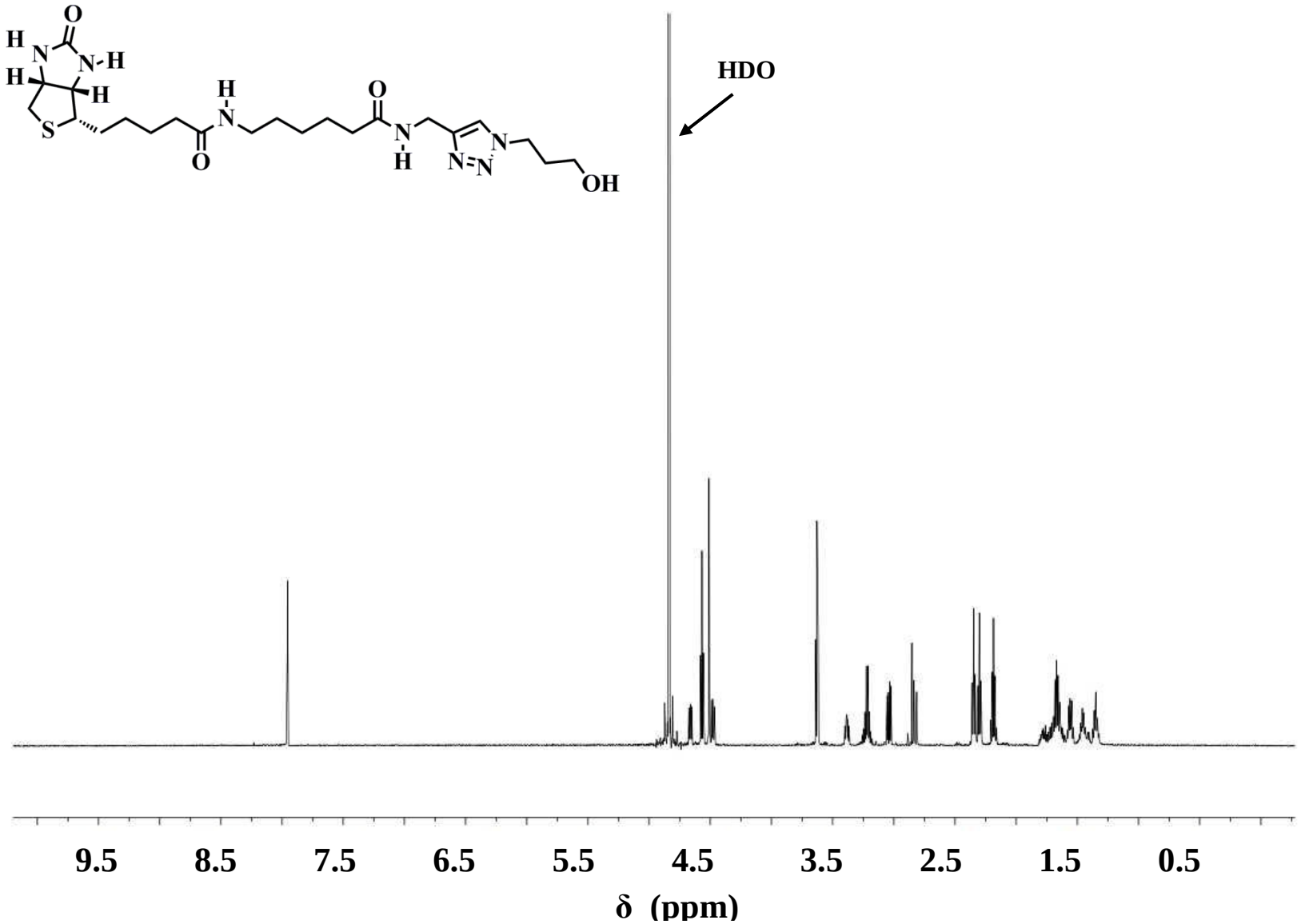

Figure 1.50: 600 MHz (D_2O), ^1H NMR of **53**

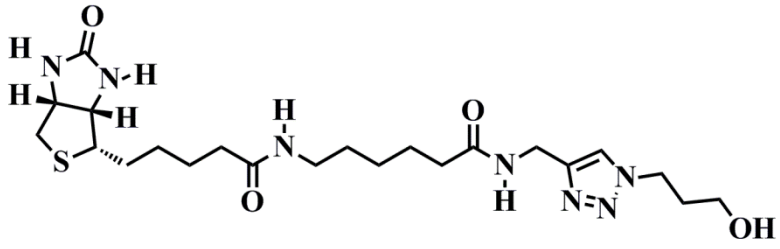

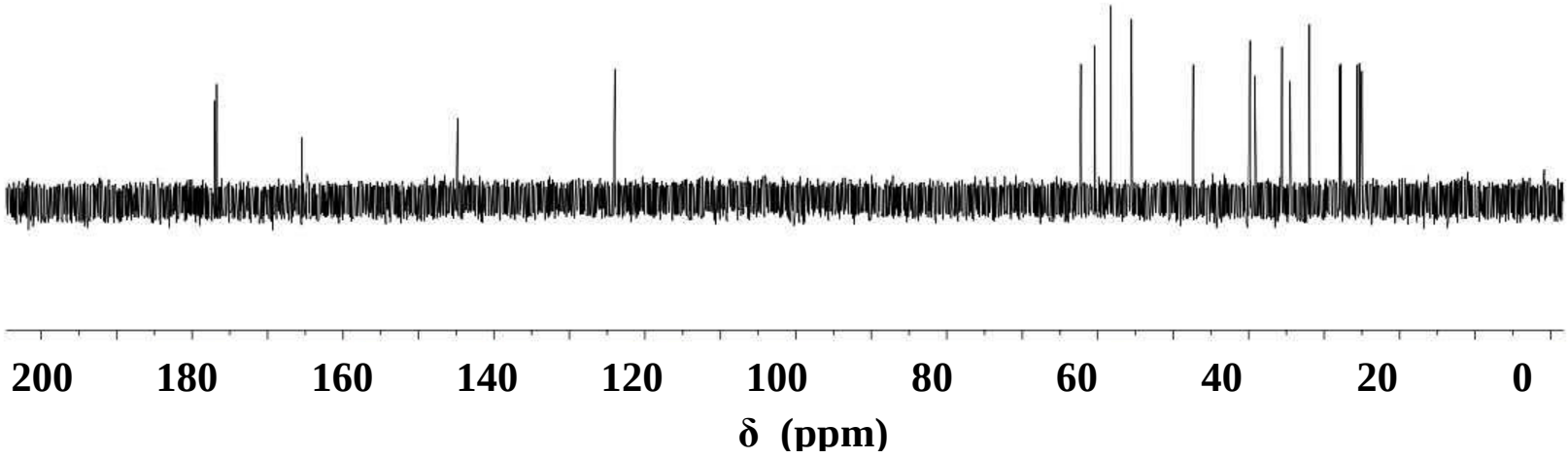

Figure 1.51: 150 MHz (D_2O), ^{13}C NMR of **53**

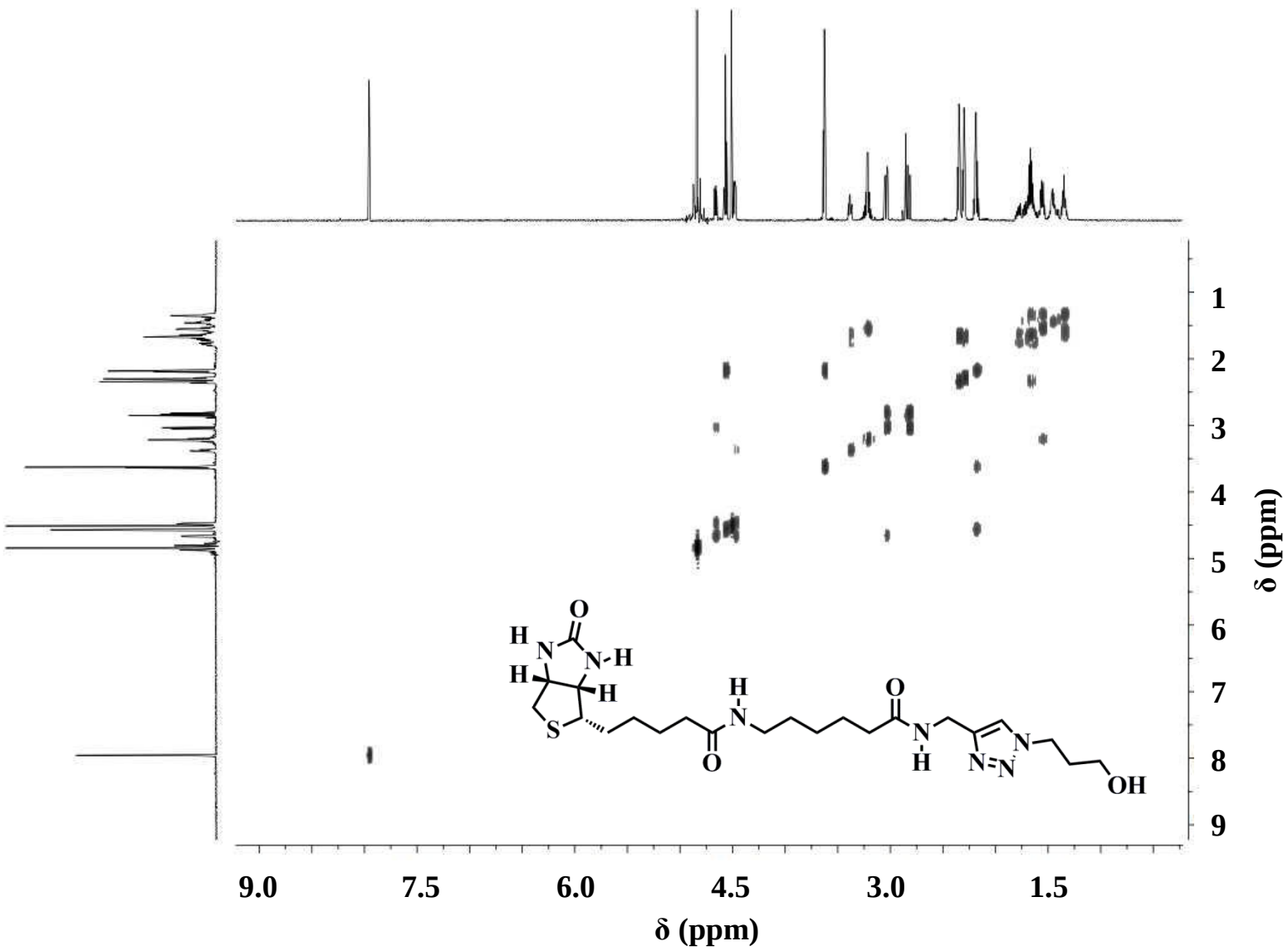

Figure 1.52: 600 MHz (D_2O), COSY NMR of **53**

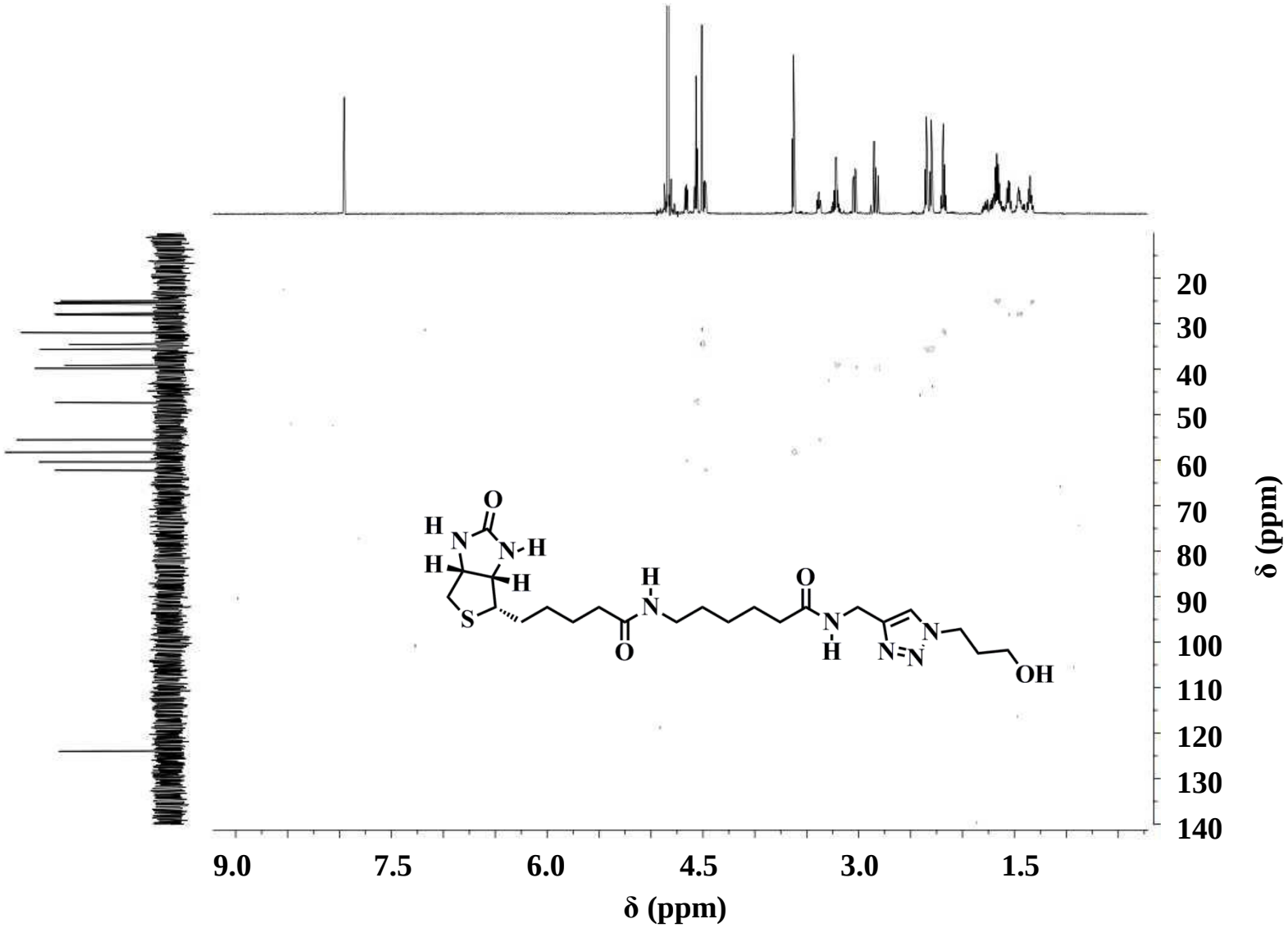

Figure 1.53: 600 MHz (D_2O), HMQC NMR of **53**

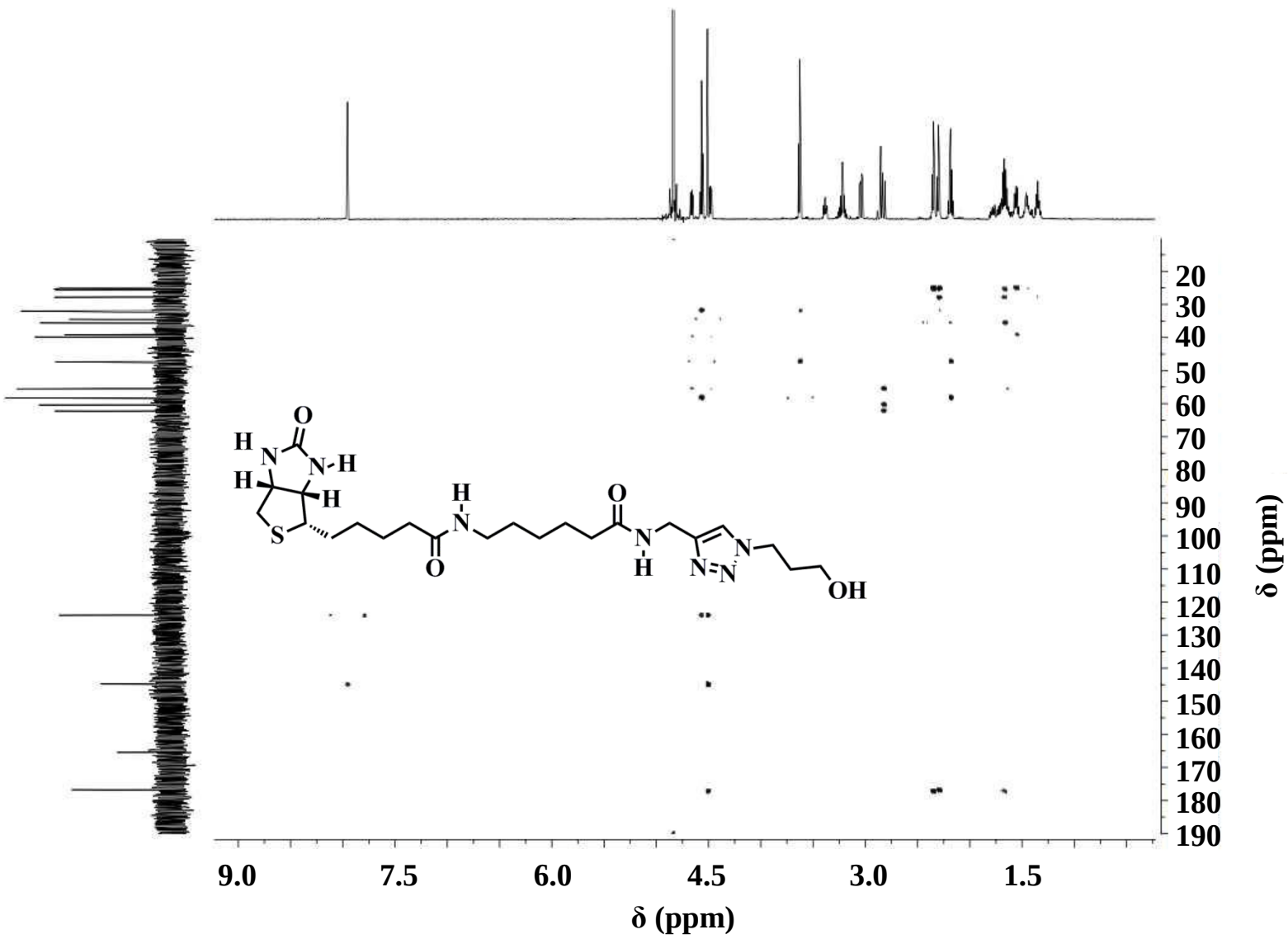

Figure 1.54: 600 MHz (D_2O), HMBC NMR of **53**

REFERENCES

References

1. *In Cancer Facts & Figures 2008,* American Cancer Society, Ed., Atlanta: American Cancer Society: 2008, 52.

2. Globocan 2008. *International Agency for Research on Cancer.* **2010**.

3. Gajewski, T. F.; Meng, Y.; Blank, C.; Brown, I.; Kacha, A.; Kline, J.; Harlin, H., Immune Resistance Orchestrated by the Tumor Microenvironment. *Immun. Rev.* **2006,** 213, 131-145.

4. Parham, P., *The Immune System*. Third Ed. ed.; Garland Science, Taylor & Francis Group, LLC: 2009; p 506.

5. Danishefsky, S. J.; Allen, J. R., From the Laboratory to the Clinic: A Retrospective on Fully Synthetic Carbohydrate-Based Anticancer Vaccines. *Angew. Chem. Int. Ed.* **2000,** 39, 836-863.

6. Bernstein, M. A.; Hall, L. D., A General Synthesis of Model Glycoproteins: Coupling of Alkenyl Glycosides to Proteins, Using Reductive Ozonolysis Followed by Reductive Amination with Sodium cyanoborohydride. *Carbohydr. Res.* **1980,** 78, C1-C3.

7. Lemieux, R. U., Haworth Memorial Lecture. Human Blood Groups and Carbohydrate Chemistry. *Chem. Soc. Rev.* **1978,** 7, 423-452.

8. Kuduk, S. D.; Schwarz, J. B.; Chen, X.-T.; Glunz, P. W.; Sames, D.; Ragupathi, G.; Livingston, P. O.; Danishefsky, S. J., Synthetic and Immunological Studies on Clustered Modes of Mucin-Related Tn and TF O-Linked Antigens: The Preparation of a Glycopeptide-Based Vaccine for Clinical Trials against Prostate Cancer *J. Am. Chem. Soc.* **1998,** 120, 12474-12485.

9. Kagan, E.; Ragupathi, G.; Yi, S. S.; Reis, C. A.; Gildersleeve, J.; Kahne, D.; Clausen, H.; Danishefsky, S. J.; Livingston, P. O., Comparison of Antigen Constructs and Carrier Molecules for Augmenting the Immunogenicity of the Monosaccharide Epithelial Cancer Antigen Tn. *Cancer Immunol. Immunother.* **2005,** 54, 424-430.

10. Ragupathi, G.; Coltart, D. M.; Williams, L. J.; Koide, F.; Kagan, E.; Allen, J.; Harris, C.; Glunz, P. W.; Livingston, P. O.; Danishefsky, S. J., On the Power of Chemical Synthesis: Immunological Evaluation of Models for Multiantigenic Carbohydrate-Based Cancer Vaccines. *Proc. Natl. Acad. Sci. U.S.A.* **2002,** 99, 13699.

11. Coltart, D. M.; Royyuru, A. K.; Williams, L. J.; Glunz, P. W.; Sames, D.; Kuduk, S. D.; Schwarz, J. B.; Chen, X.-T.; Danishefsky, S. J.; Live, D. H., Principles of Mucin Architecture: Structural Studies on Synthetic Glycopeptides Bearing Clustered Mono-, Di-, Tri-, and Hexasaccharide Glycodomains. *J. Am. Chem. Soc.* **2002,** 124, 9833-9844.

12. Ragupathi, G.; Koide, F.; Livingston, P. O.; Cho, Y. S.; Endo, A.; Wan, Q.; Spassova, M. K.; Keding, S. J.; Allen, J.; Ouerfelli, O.; Wilson, R. M.; Danishefsky, S. J., Preparation and Evaluation of Unimolecular Pentavalent and Hexavalent Antigenic Constructs Targeting Prostate and Breast Cancer: A Synthetic Route to Anticancer Vaccine Candidates. *J. Am. Chem. Soc.* **2006,** 128, 2715-2725.

13. Zhu, J.; Wan, Q.; Lee, D.; Yang, G.; Spassova, M. K.; Ouerfelli, O.; Ragupathi, G.; Damani, P.; Livingston, P. O.; Danishefsky, S. J., From Synthesis to Biologics: Preclinical Data on a Chemistry Derived Anticancer Vaccine. *J. Am. Chem. Soc.* **2009,** 131, 9298-9303.

14. Buskas, T.; Li, Y.; Boons, G.-J., Synthesis of a Dimeric Lewis Antigen and the Evaluation of the Epitope Specificity of Antibodies Elicited in Mice. *Chem. Eur. J.* **2005,** 11, 5457-5467.

15. Buskas, T.; Li, Y.; Boons, G.-J., The Immunogenicity of the Tumor-Associated Antigen Lewis^{y} May Be Suppressed by a Bifunctional Cross-Linker Required for Coupling to a Carrier Protein. *Chem. Eur. J.* **2004,** 10, 3517-3524.

16. Keil, S.; Claus, C.; Dippold, W.; Kunz, H., Towards the Development of Antitumor Vaccines: A Synthetic Conjugate of a Tumor-Associated MUC1 Glycopeptide Antigen and a Tetanus Toxin Epitope. *Angew. Chem. Int. Ed.* **2001,** 40, 366-369.

17. Dziadek, S.; Hobel, A.; Schmitt, E.; Kunz, H., A Fully Synthetic Vaccine Consisting of a Tumor-Associated Glycopeptide Antigen and a T-Cell Epitope for the Induction of a Highly Specific Humoral Immune Response. *Angew. Chem. Int. Ed.* **2005,** 44, 7630-7635.

18. Buskas, T.; Ingale, S.; Boons, G.-J., Towards a Fully Synthetic Carbohydrate-Based Anticancer Vaccine: Synthesis and Immunological Evaluation of a Lipidated Glycopeptide Containing the Tumor-Associated Tn Antigen. *Angew. Chem. Int. Ed.* **2005,** 44, 5985-5988.

19. Ingale, S.; Wolfert, M. A.; Gaekwad, J.; Buskas, T.; Boons, G.-J., Robust Immune Responses Elicited by a Fully Synthetic Three-Component Vaccine. *Nat. Chem. Biol.* **2007,** 3, 663-667.

20. Grigalevicius, S.; Chierici, S.; Renaudet, O.; Lo-Man, R.; Dériaud, E.; Leclerc, C.; Dumy, P., Chemoselective Assembly and Immunological Evaluation of Multiepitopic Glycoconjugates Bearing Clustered Tn Antigen as Synthetic Anticancer Vaccines. *Bioconjugate Chem.* **2005,** 16, 1149-1159.

21. Moreau, R.; Dausset, J.; Bernard, J.; Moullec, J., Anémie Hémolytique Acquise Avec Polyagglutinabilité des Hématies par un Nouveau Facteur Présent dans le Sérum Humain Normal (Anti-Tn). *Bull. Soc. méd. HÔp., paris* **1957,** 73, 569-587.

22. Dausset, J.; Moullec, J.; Bernard, J., Acquired Hemolytic Anemia with Polyagglutinability of Red Blood Cells Due to a New Factor Present in Normal Human Serum (Anti-Tn). *Blood* **1959,** 14, 1079-1093.

23. Eric G, B., Tn-syndrome. *Biochimica et Biophysica Acta (BBA) - Molecular Basis of Disease* **1999,** 1455, 255-268.

24. Berger, E. G.; Thurnher, M.; Dinter, A., The cell-specific expression of glycan antigens exemplified by the deficiency of β1, 3 galactosyltransferase in the Tn-syndrome. *Transfus. Clin. Biol.* **1994,** 1, 103-108.

25. Springer, G. F.; Desai, P. R.; Banatwala, I., Blood Group MN Specific Substances and Precursors in Normal and Malignant Human Breast Tissues. *Naturwissenschaften* **1974,** 61, 457-458.

26. Springer, G. F., T and Tn, General Carcinoma Autoantigens *Science* **1984,** 224, 1198-1206.

27. Dabelsteen, E., Cell Surface Carbohydrates as Prognostic Markers in Human Carcinomas. *J. Pathol.* **1996,** 179, 358-369.

28. Goddard-Borger, E. D.; Stick, R. V., An Efficient, Inexpensive, and Shelf-Stable Diazotransfer Reagent: Imidazole-1-sulfonyl Azide Hydrochloride. *Org. Lett.* **2007,** 9, 3797-3800.

29. Koeller, K. M.; Smith, M. E. B.; Wong, C.-H., Chemoenzymatic Synthesis of PSGL-1 Glycopeptides: Sulfation on Tyrosine Affects Glycosyltransferase-Catalyzed Synthesis of the O-glycan. *Bioorg. Med. Chem.* **2000,** 8, 1017-1025.

30. Huang, Y.; Dey, S.; Zhang, X.; Sönnichsen, F.; Garner, P., The α-Helical Peptide Nucleic Acid Concept: Merger of Peptide Secondary Structure and Codified Nucleic Acid Recognition. *J. Am. Chem. Soc.* **2004,** 126, 4626-4640.

31. Grundler, G.; Schmidt, R. R., Glycosylimidate, 13. Anwendung des Trichloracetimidat-Verfahrens auf 2-Azidoglucose- und 2-Azidogalactose-Derivate. *Liebigs Ann. Chem.* **1984,** 1984, 1826-1847.

32. Karplus, M., Vicinal Proton Coupling in Nuclear Magnetic Resonance. *J. Am. Chem. Soc.* **1963,** 85, 2870-2871.

33. Karplus, M., Contact Electron- Spin Coupling of Nuclear Magnetic Moments. *J. Chem. Phys.* **1959,** 30, 11-15.

34. Miermont, A.; Barnhill, H.; Strable, E.; Lu, X.; Wall, K. A.; Wang, Q.; Finn, M. G.; Huang, X., Cowpea Mosaic Virus Capsid: A Promising Carrier for the Development of Carbohydrate Based Antitumor Vaccines. *Chem. Eur. J.* **2008,** 14, 4939-4947.

35. Matyjaszewski, K.; Xia, J., Atom Transfer Radical Polymerization. *Chemical Reviews* **2001,** 101, 2921-2990.

36. Bernard, J.; Hao, X.; Davis, T. P.; Barner-Kowollik, C.; Stenzel, M. H., Synthesis of Various Glycopolymer Architectures via RAFT Polymerization: From Block Copolymers to Stars. *Biomacromolecules* **2006,** 7, 232-238.

37. Chiefari, J.; Chong, Y. K.; Ercole, F.; Krstina, J.; Jeffery, J.; Le, T. P. T.; Mayadunne, R. T. A.; Meijs, G. F.; Moad, C. L.; Moad, G.; Rizzardo, E.; Thang, S. H., Living Free- Radical Polymerization by Reversible Addition- Fragmentation Chain Transfer: The RAFT Process. *Macromolecules* **1998,** 31, 5559-5562.

38. Hawker, C. J.; Bosman, A. W.; Harth, E., New Polymer Synthesis by Nitroxide Mediated Living Radical Polymerizations. *Chem. Rev.* **2001,** 101, 3661-3688.

39. Baskaran, S.; Grande, D.; Sun, X.-L.; Yayon, A.; Chaikof, E. L., Glycosaminoglycan-Mimetic Biomaterials. 3. Glycopolymers Prepared from Alkene-Derivatized Mono- and Disaccharide-Based Glycomonomers. *Bioconjugate Chem.* **2002,** 13, 1309-1313.

40. Grande, D.; Baskaran, S.; Baskaran, C.; Gnanou, Y.; Chaikof, E. L., Glycosaminoglycan-Mimetic Biomaterials. 1. Nonsulfated and Sulfated Glycopolymers by Cyanoxyl-Mediated Free-Radical Polymerization. *Macromolecules* **2000,** 33, 1123-1125.

41. Grande, D.; Baskaran, S.; Chaikof, E. L., Glycosaminoglycan Mimetic Biomaterials. 2. Alkene- and Acrylate-Derivatized Glycopolymers via Cyanoxyl-Mediated Free-Radical Polymerization. *Macromolecules* **2001,** 34, 1640-1646.

42. Sun, X.-L.; Grande, D.; Baskaran, S.; Hanson, S. R.; Chaikof, E. L., Glycosaminoglycan Mimetic Biomaterials. 4. Synthesis of Sulfated Lactose- Based Glycopolymers That Exhibit Anticoagulant Activity. *Biomacromolecules* **2002,** 3, 1065-1070.

43. Malkoch, M.; Thibault, R. J.; Drockenmuller, E.; Messerschmidt, M.; Voit, B.; Russell, T. P.; Hawker, C. J., Orthogonal Approaches to the Simultaneous and Cascade Functionalization of Macromolecules Using Click Chemistry. *J. Am. Chem. Soc.* **2005,** 127, 14942-14949.

44. Carpita, A.; Mannocci, L.; Rossi, R., Silver(I)- Catalysed Protiodesilylation of 1-(Trimethylsilyl)-1-alkynes. *Eur. J. Org. Chem.* **2005,** 2005, 1859-1864.

45. Tornøe, C. W.; Christensen, C.; Meldal, M., Peptidotriazoles on Solid Phase: [1,2,3]-Triazoles by Regiospecific Copper(I)-Catalyzed 1,3-Dipolar Cycloadditions of Terminal Alkynes to Azides. *J. Org. Chem.* **2002,** 67, 3057-3064.

46. Hermanson, G. T., *Bioconjugate Techniques*. second ed.; Academic Press, Inc: 2008; p 1202.

47. DuBois, M.; Gilles, K. A.; Hamilton, J. K.; Rebers, P. A.; Smith, F., Colorimetric Method for Determination of Sugars and Related Substances. *Anal. Chem.* **1956,** 28, 350-356.

48. Jahnel, J. B.; Ilieva, P.; Frimmel, F. H., HPAE-PAD- A Sensitive Method for the Determination of Carbohydrates. *Fresenius J. of Anal. Chem.* **1998,** 360, 827-829.

49. Miermont, A. Syntheses and Immunological Studies of Tumor Associated Carbohydrate Antigens. Ph.D. Dissertation, University of Toledo. Toledo, OH, 2008.

50. McCormick, A. A.; Corbo, T. A.; Wykoff-Clary, S.; Nguyen, L. V.; Smith, M. L.; Palmer, K. E.; Pogue, G. P., TMV- Peptide Fusion Vaccines Induce Cell- Mediated Immune Responses and Tumor Protection in Two Murine Models. *Vaccine* **2006,** 24, 6414-6423.

51. Kaltgrad, E.; O'Reilly, M. K.; Liao, L.; Han, S.; Paulson, J. C.; Finn, M. G., On-Virus Construction of Polyvalent Glycan Ligands for Cell-Surface Receptors. *J. Am. Chem. Soc.* **2008,** 130, 4578-4579.

52. Overby, L. R.; Barlow, G. H.; Doi, R. H.; Jacob, M.; Spiegelman, S., Comparison of Two Serologically Distinct Ribonucleic Acid Bacteriophages I. Properties of the Viral Particles. *J. Bacteriol.* **1966,** 91, 442-448.

53. Strable, E.; Prasuhn, D. E.; Udit, A. K.; Brown, S.; Link, A. J.; Ngo, J. T.; Lander, G.; Quispe, J.; Potter, C. S.; Carragher, B.; Tirrell, D. A.; Finn, M. G., Unnatural Amino Acid Incorporation into Virus-Like Particles. *Bioconjugate Chem.* **2008,** 19, 866-875.

54. Prasuhn, D. E.; Singh, P.; Strable, E.; Brown, S.; Manchester, M.; Finn, M. G., Plasma Clearance of Bacteriophage Qβ Particles as a Function of Surface Charge. *J. Am. Chem. Soc.* **2008,** 130, 1328-1334.

55. Ishihara, K.; Kurihara, H.; Yamamoto, H., An Extremely Simple, Convenient, and Selective Method for Acetylating Primary Alcohols in the Presence of Secondary Alcohols. *J. Org. Chem.* **1993,** 58, 3791-3793.

56. Jlalia, I.; Beauvineau, C.; Beauvière, S.; Önen, E.; Aufort, M.; Beauvineau, A.; Khaba, E.; Herscovici, J.; Meganem, F.; Girard, C., Automated Synthesis of a 96 Product- Sized Library of Triazole Derivatives Using a Solid Phase Supported Copper Catalyst. *Molecules* **2010,** 15, 3087-3120.

Chapter 2 – Synthesis of an Alzheimer's Disease Imaging Agent

2.1 Introduction

Currently, Alzheimer's Disease (AD) is attributed to the sixth leading cause of death in the United States and the fifth leading cause of death in Americans over the age of 65.[1] As the average age of the current population increases, the number of people affected by this disease is projected to soar. The cost surrounding the disease is staggering. It is estimated that $148 billion is spent annually in direct and indirect costs. This disease can be characterized by a progressive loss of cognitive function, memory decline, and altered behavior. In the later stages of this disease, motor function deteriorates and global amnesia sets in. What makes this disease so difficult to detect and treat, is that the only absolute definitive diagnosis for the disease is during postmortem neuropathological examinations. Because of this, it is absolutely essential that a new method for detection be developed allowing earlier detection. Earlier detection would also be a great assisting tool in attempts directed toward treatment of the disease. One such option was developed by Barrio and coworkers in which they developed the hydrophobic, fluorescent molecular-imaging probe 2-(1-(6-[(2-[^{18}F]fluoroethyl)(methyl)amino]-2-naphthyl)ethylidene malononitrile ([^{18}F] FDDNP) and its analog, 1-(6-[(2-[^{18}F]fluoroethyl)(methyl)amino]naphthalene-2-yl)ethanone ([^{18}F] FFENE) both of which were found to be capable of crossing the blood- brain barrier (**Figure 2.1**). These two compounds were found to have K_d values of 0.12 and 0.16 nM for high- affinity binding sites for FDDNP and FENE respectively, and K_d values of 1.86 and 71.2 nM for low-affinity sites.

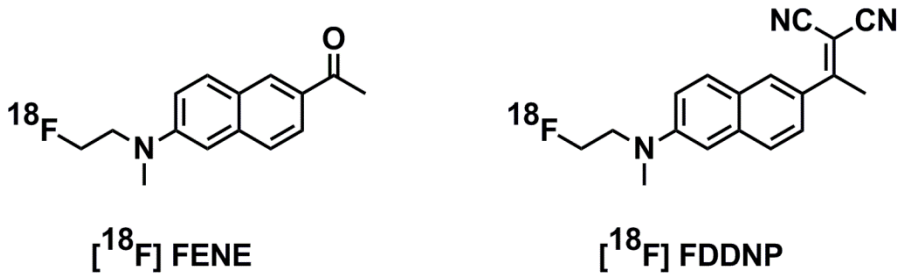

[18F] FENE [18F] FDDNP

Figure 2.1: Structures of FENE and FDDNP

These two compounds have previously been used to label senile plaques and neurofibrillary tangles (two hallmark pathologies accompanying the neurodegeneration involved in the diseased state) in the living brains of patients using positron emission tomography (PET). One of the biggest limitations to these current compounds is that they require the use of radio-labeled fluorine. Many locations (i.e., hospitals/ clinics), do not have the ability nor the expertise to work with such compounds. Design of a more universal analog would therefore be highly advantageous. Realizing that these current compounds have demonstrated success, the goal of our project was to design and synthesize an analog that would be capable of being attached to a nanoparticle. Once conjugated to the nanoparticle scaffold, these compounds could then be observed using magnetic resonance imaging (MRI). The original direction of our design was to synthesize a compound in which we installed an amine linker in place of the radio- labeled fluorine in [^{18}F] FENE. Once demonstrated as proof of concept in MRI, the [^{18}F] FDDNP compound would also be synthesized in an analogous fashion.

2.2 Synthesis of Alzheimer's Imaging Agent

A paper published in a 1999 symposium abstract by J.R. Barrio and coworkers made mention of the Bucherer reaction[2] in the reversible conversion of aromatic alcohols with secondary amines. After looking into this named reaction, literature precedence[3] indicated that this reaction might be an excellent starting point in our synthesis. To perform this reaction, a 2-naphthol compound needed to be synthesized that would allow the synthesis of the 2, 6 - substitution pattern that we desired. It was decided to start from commercially available 1-(6-methoxynaphthalen-2-yl)ethanone (**1**) which could easily be converted into **2** in the presence of concentrated hydrochloric acid (**Scheme 2.1**). This reaction was completed after two hours and the product was isolated in an 85-90% yield.

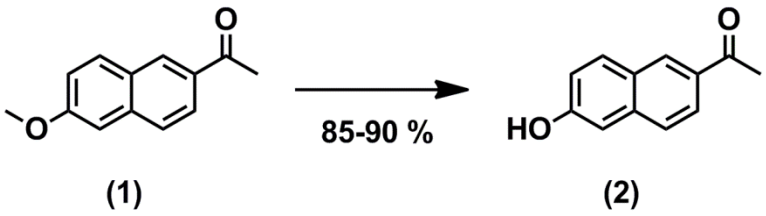

(1) (2)

Reagents and conditions : conc. HCl, minimal DCM, reflux, 2 h

Scheme 2.1: Synthesis of 2-6 -substituted aromatic alcohol **2**

With the desired aromatic alcohol in hand, it was time to determine if the Bucherer reaction could couple the secondary amine to the aromatic alcohol. Compound **2** was placed in a Schlenk tube, along with 2-methylaminoethanol, sodium bisulfite, and water. The flask was sealed and then heated to approximately 140 ^{o}C for four days (**Scheme 2.2**). After work-up and purification, it was determined that the reaction had proceeded in a 70 %.

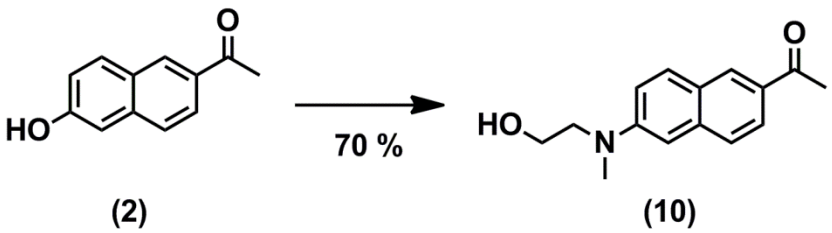

(2) (10)

Reagents and conditions : 2-methylaminoethanol, $NaHSO_3$, H_2O, 140 ^oC, 3 d

Scheme 2.2: Synthesis of **10** utilizing the Bucherer reaction

This reaction mechanism had been elucidated by Seeboth in 1967 (**Scheme 2.3**).[4] It is believed that the aromatic alcohol will first pick up a proton from its surroundings forming intermediate **3**. Then, when the resonance form intermediate **4** interacts with sodium bisulfite, intermediate **5** could be generated. Intermediate **5** can then undergo tautermerization to form intermediate **6**. This cyclic ketone can interact with the secondary amine generating intermediate **7**. Next, intermediate **7** would undergo a proton transfer from the amine to the alcohol, which could subsequently undergo dehydration forming intermediate **8**. Next a molecule of sodium bisulfite could eliminate a proton from the 5- position generating intermediate **9**. And finally, syn-elimination of sodium sulfite from intermediate **9** would produce the desired compound **10**.

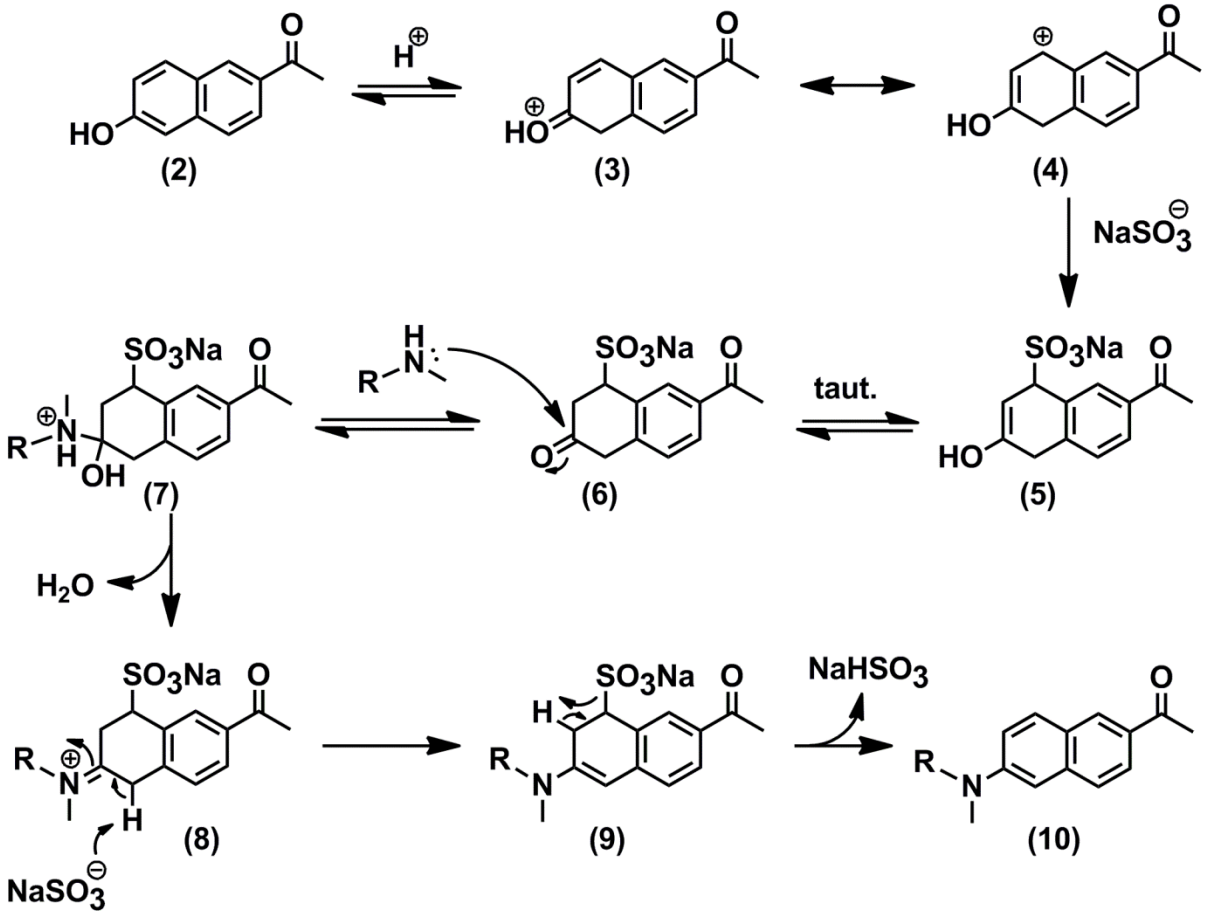

Scheme 2.3: Predicted mechanism for the synthesis of **10** using the Bucherer reaction

With this compound in hand, the rest of the reaction steps are quite straight forward (**Scheme 2.4**). Based on literature precedence in which they converted a primary alcohol to a primary amine,[5] primary alcohol (**10**) was reacted with *p*- toluenesulfonyl chloride in dichloromethane, with DMAP and pyridine. This reaction was allowed to stir at room temperature overnight at which point, the reaction was found to contain two major products. As it turned out, beside the desired tosylate compound (**11**), a significant amount of the chloro-substituted compound was observed (**12**). The ratio of **11** to **12** varied anywhere from 1:1 to 5:1 respectively. This by-product is likely a result of the chloride anion generated during the reaction of the primary alcohol with Tos-Cl acting as a nucleophile and displacing the tosylate leaving group via an S_N2 mechanism. Although these compounds could be separated via column chromatography, it was decided to use them both directly in the next step. The only disadvantage to having the chloro- compound in the reaction mixture was that it is, of course, not as good a leaving group as the tosylate compound. Thus, it caused the reaction time to be increased. Both **11** and **12** were combined with sodium azide, DMF, and a few drops of water to help with the solubility of the sodium azide. After 15 hours of stirring at 55 ^{o}C azide compound **13** was isolated in a 68 % yield over the past two steps. The final step was a straight forward hydrogenation of azide compound **13** to the desired primary amine target (**14**) using standard conditions. This reaction resulted in a 71 % yield of an extremely fluorescent yellow solid. Unfortunately however, it appears as though this compound is extremely unstable because even after very short periods of storage or use (i.e., NMR analysis, mass measurements) decomposition appears to occur.

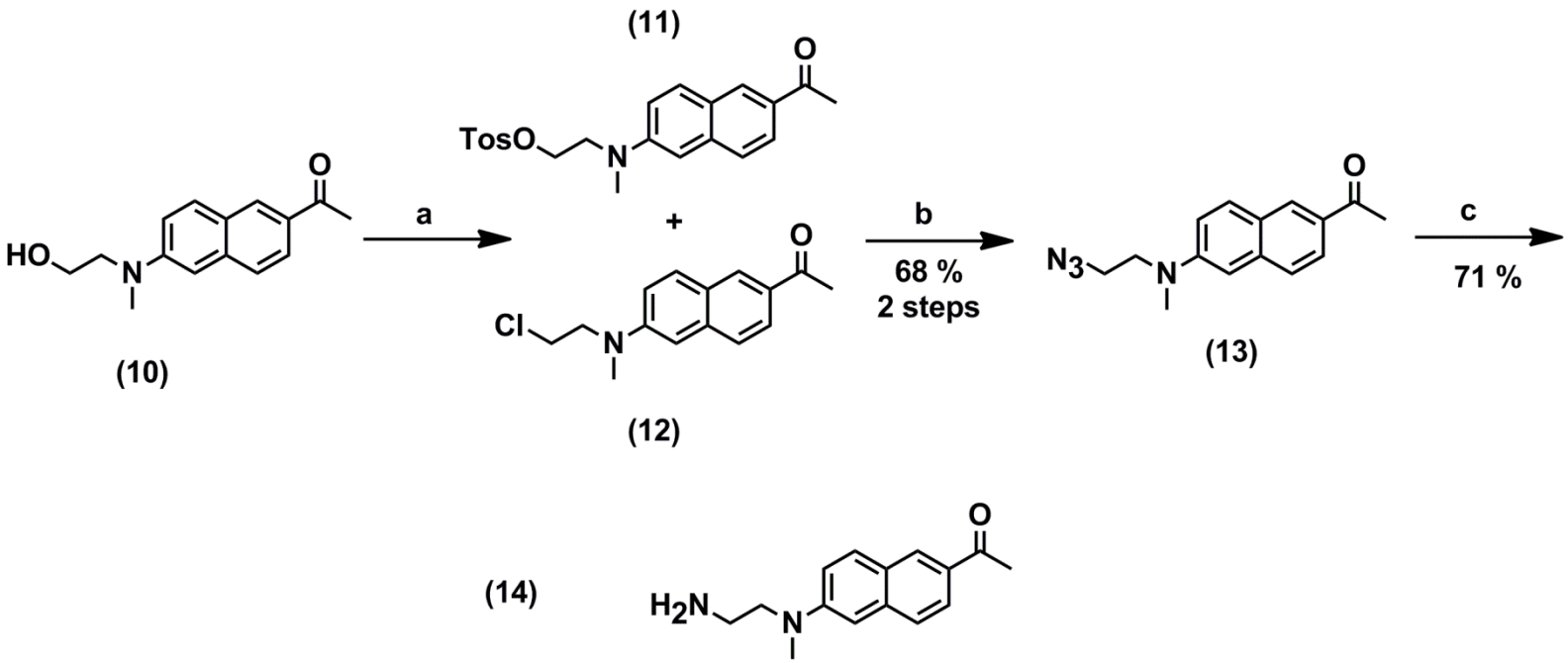

Reagents and conditions : a) Tos-Cl, DMAP, py , DCM, 0 ^{O}C, 15 h

b) NaN_3, DMF, 55 ^{O}C, 15 h

c) H_2, Pd/C, EtOAc, r.t., 15 h

Scheme 2.4: Synthesis of the desired FDDNP imaging agent (**14**)

With this unfortunate occurrence, it was decided that it would be more advantageous to synthesis a free acid instead of this free amine. This might prevent the compound from being quite so sensitive to decomposition. Since the nanoparticles can be synthesized to express either acid or amine functionality, it does not make a difference which our compound includes. It was decided to perform a one pot reduction of azide (**13)** which subsequently reacted with succinic anhydride generating the free acid compound (**15**) (**Scheme 2.5**).

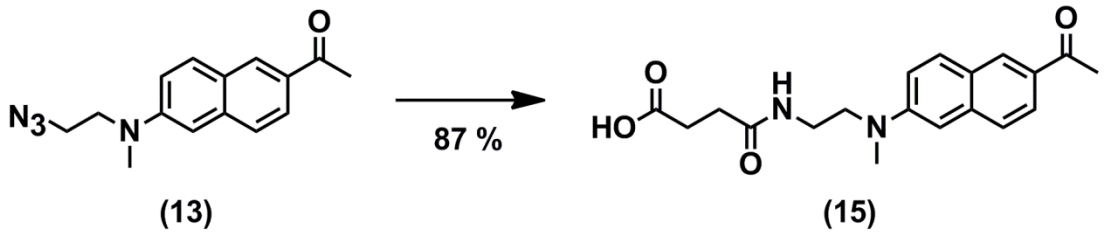

(13) **(15)**

Reagents and conditions : succinic anhydride, H_2, 10 % Pd/C, THF, r.t., 5 h

Scheme 2.5: Synthesis of final imaging agent to be conjugated to magnetic nanoparticles

2.3 Experimental Section

General Experimental Procedures.

All reactions were carried out under nitrogen or argon with anhydrous solvents in oven-dried glassware. Chemicals used were reagent grade as supplied except where noted. Analytical thin-layer chromatography was performed using silica gel 60 F254 glass plate. Compound spots were visualized by UV light (254 nm) and by staining with a yellow solution containing $Ce(NH_4)_2(NO_3)_6$ (0.5 g) and $(NH_4)_6Mo_7O_{24}$ * $4H_2O$ (24.0 g) in 6% H_2SO_4 (500 mL) or a solution of Ninhydrin (1.5g) in n-butanol (100mL) and acetic acid (3mL). Flash column chromatography was performed on silica gel 60 (230–400 Mesh). NMR spectra were referenced using Me_4Si (0 ppm), residual $CHCl_3$ (δ ^{1}H-NMR 7.24 ppm, ^{13}C-NMR 77.0 ppm), H_2O (δ ^{1}H-NMR 4.63 ppm), CH_3OH (δ ^{1}H-NMR 3.30 ppm, ^{13}C-NMR 49.0 ppm), and $(CH_3)_2CO$ (δ ^{1}H-NMR 2.04 ppm, ^{13}C-NMR 29.84 ppm). Peak and coupling constant assignments were based on ^{1}H-NMR, ^{1}H–^{1}H gCOSY and (or) ^{1}H–^{13}C gHMQC and ^{1}H–^{13}C gHMBC experiments. ESI mass spectra were recorded in positive ion mode.

1-(6-Hydroxynaphthalen-2-yl)ethanone (2)

In a 3L three neck round bottom flask, equipped with a reflux condenser, dropping funnel and glass stopper, concentrated HCl (2L) was stirred and heated to boiling. Meanwhile, commercially available 1-(6-methoxynaphthalen-2-yl)ethanone (**1**) (5.92g, 29.57 mmol) was dissolved in the minimal amount of dichloromethane and added to the drop funnel. This solution was added drop-wise to the HCl solution. Once completely added, the reaction was allowed to stir at reflux for 3 hours. The reaction was then allowed to cool to r.t. at which point a solid

precipitated out which was then filtered and then dissolved in EtOAc (130mL). EtOAc was extracted 3x with 100 mL of water and then washed once with 100 mL of brine. The organic phase was dried over anhydrous sodium sulfate, and concentrated under vacuum, and used without further purification. Product was obtained as a white solid in 86-89% yield. Comparison with literature data[3] confirms its identity. ^{1}H NMR (500 MHz, $(CD_3)_2CO$) δ 2.64 (s, 3H), 7.23 (dd, *J* = 2.4, 8.8 Hz, 1H), 7.26 (d, *J* = 2.4 Hz, 1H), 7.74 (d, *J* = 8.7 Hz, 1H), 7.93 (dd, *J* = 1.8, 8.7 Hz, 1H), 7.97 (d, *J* = 8.8 Hz, 1H), 8.52 (d, *J*=1.8 Hz, 1H), 9.01 (broad s, 1H), ^{13}C NMR (150 MHz, $(CD_3)_2CO$) δ 26.5, 109.9, 120.1, 123.3 125.0, 127.3, 128.3, 131.2, 132.4, 133.2, 138.5, 197.5. [HRMS] $[M+H]^+$ m/z: calc. for $C_{12}H_{11}O_2$: 187.0759, found 187.0755.

1-(6-((2-Hydroxyethyl)(methyl)amino)naphthalene-2-yl)ethanone (10)

Compound **2** (2g, 10.74mmol), sodium bisulfite (4.47g, 42.96mmol), and 2-(methylamino) ethanol (4.03g, 53.7 mmol), and water (15mL) were added to a schlenk tube. The atmosphere within the schlenk tube was evacuated under high vacuum and then filled with nitrogen. This process was repeated three times before sealing the schlenk tube filled with nitrogen atmosphere. The reaction vessel was then placed in an oil bath and heated at 140 ^{o}C for 4 days. The reaction was allowed to cool to r.t. and was then extracted with EtOAc and water. The organic phase was then washed once with brine and then dried over anhydrous sodium sulfate, and concentrated under vacuum The desired compound was obtained in a 70% yield after column purification using EtOAc/ Et_2O (1:2). Comparison with literature data[3] confirms its identity. ^{1}H NMR (500 MHz, CD_3OD) δ 2.69 (s, 3H), 3.18 (s, 3H), 3.67 (t, *J* = 5.8 Hz, 2H), 3.83 (dd, *J* = 3.1, 5.8 Hz, 2H), 6.99 (d, *J* = 2.6 Hz, 1H), 7.31 (dd, *J* = 2.6, 9.2 Hz, 1H), 7.66

(d, J = 8.8 Hz, 1H), 7.84 – 7.92 (d, J = 9.2 Hz, 1H), 7.84 – 7.92 (dd, J = 8.8, 1.7 Hz, 1H), 8.42 (d, J = 1.7 Hz, 1H), ^{13}C NMR (125 MHz, CD_3OD) δ 26.4, 39.4, 55.5, 60.4, 105.9, 117.4, 125.1, 126.4, 127.2, 131.4, 131.9, 132.0, 139.5, 151.1, 200.3 [HRMS] $[M+H]^+$ m/z: calc. for $C_{15}H_{18}NO_2$: 244.1338, found 244.1339.

2-((6-Acetylnaphthalen-2-yl)(methyl)amino)ethyl 4-methylbenzenesulfonate (11)

Compound **10** (495 mg, 2 mmol), *p*- toluenesulfonyl chloride (796.2 mg, 4.2 mmol), and dichloromethane (5 mL) were added to a 10 mL round bottom flask. This mixture was allowed to cool to 0 ^{o}C. Once chilled, DMAP (179.6 mg, 0.72 mmol) and pyridine (520 μL, 2.82 mmol) were added to the reaction, which was then allowed to warm to r.t. and stirring continued overnight. Once starting material was consumed as monitored by TLC using EtOAc/Hex (2:3), the reaction was quenched using water. The aqueous phase was extracted using DCM. The combined organic layers were then washed with 1N HCl and then dried over anhydrous sodium sulfate, and concentrated under vacuum. Compound was purified as a yellow solid by column chromatography using EtOAc/Hex (2:3); however, the yield of compound **11** was highly variable due to the formation of byproduct **12**. The ratio of **11** to **12** ranges from 1:1 to 5:1. Once other minor impurities are removed, **11** and **12** can be used together directly in the next step. Reaction was designed based on the following literature precedence[5] for the conversion of compound **10** to **11**. ^{1}H NMR (600 MHz, $CDCl_3$) δ 2.28 (s, 3H), 2.65 (s, 3H) 3.02 (s, 3H), 3.75 (t, J = 5.8 Hz, 2H), 4.23 (t, J = 5.8 Hz, 2H), 6.73 (d, J = 2.6 Hz, 1H), 6.97 – 7.02 (dd, J = 2.6, 9.2 Hz, 1H), 7.09 -7.12 (m, 2H), 7.57 (d, J = 8.7 Hz, 1H), 7.61 – 7.66 (m, 2H), 7.72 (d, J = 9.2 Hz, 1H), 7.91 (dd, J

= 1.8, 8.7 Hz, 1H), 8.28 (d, *J* = 1.8 Hz, 1H), ^{13}C NMR (150 MHz, $CDCl_3$) 21.5, 26.4, 39.3, 51.2, 66.8, 102.4, 105.7, 115.7, 124.7, 125.4, 126.3, 127.7, 129.7, 130.2, 130.9, 131.2, 132.5, 137.5, 144.9, 148.0, 197.6. [HRMS] $[M+H]^+$ m/z: calc. for $C_{22}H_{24}NO_4S$: 398.1426, found 398.1419.

1-(6-((2-Chloroethyl)(methyl)amino)naphthalen-2-yl)ethanone (12)

Compound **10** (495 mg, 2mmol), *p*- toluenesulfonyl chloride (796.2 mg, 4.2 mmol), and dichloromethane (5mL) were added to a 10 mL round bottom flask. This mixture was allowed to cool to 0 ^{o}C. Once chilled, DMAP (179.6mg, 0.72mmol) and pyridine (520 μL, 2.82mmol) were added to the reaction which was then allowed to warm to r.t. and stirring continued overnight. Once starting material was consumed as monitored by TLC using EtOAc/Hex (2:3), reaction was quenched using water. The aqueous phase was extracted using DCM. The combined organic layers were then washed with 1N HCl and then dried over anhydrous sodium sulfate, and concentrated under vacuum. Compound was purified as a brownish yellow solid after column chromatography using EtOAc/Hex (2:3), however, the yield of compound **12** is highly variable due to the formation of byproduct **11**. The ratio of **12**: **11** ranges from 1:1 to 1:5. Once other minor impurities are removed, **11** and **12** can be used together directly in the next step. Reaction was designed based on the following literature precedence[5] for the conversion of compound **10** to **11**. ^{1}H NMR (600 MHz, $CDCl_3$) δ 2.65 (s, 3H), 3.15 (s, 3H), 3.68 (t, *J* = 7.1 Hz, 2H), 3.81 (t, *J* = 7.1 Hz, 2H), 6.91 (d, *J* = 2.6 Hz, 1H), 7.15 (dd, *J* = 2.6, 9.1 Hz, 1H), 7.63 (d, *J* = 8.8 Hz, 1H), 7.81 (d, *J* = 9.1 Hz, 1H), 7.92 (dd, *J* = 1.8, 8.8 Hz, 1H), 8.31 (d, *J*=1.8 Hz, 1H), ^{13}C NMR (150 MHz, $CDCl_3$) δ.26.4, 39.2, 40.4, 54.3, 105.6, 115.7, 124.8, 125.4, 126.3,

130.3, 131.1, 131.3, 137.6, 148.1, 197.7. [HRMS] $[M+H]^+$ m/z: calc. for $C_{15}H_{17}ClNO$: 262.0999, found 262.1003.

1-(6-((2-Azidoethyl)(methyl)amino)naphthalen-2-yl)ethanone (**13**)

To a mixture of compounds **11** and **12** (938 mg, 3.6 mmol, assumes 100% lower molecular weight compound **12)**, sodium azide (3.49 g, 53.7 mmol), and DMF (5 mL) were added. A few drops of water were added to help with the solubility of the sodium azide. The reaction was stirred at r.t. for 1 hour before being heated to 55 ^oC overnight (15-20 hours). Solvent was then removed under reduced pressure. The product was obtained as a bright yellow solid in a 68% yield over two steps after purification by flash column chromatography using either a EtOAc/ Hex (1:3) or an acetone/ toluene (1:9) system. ^1H NMR (500 MHz, $CDCl_3$) δ 2.65 (s, 3H), 3.14 (s, 3H), 3.52 (t, *J* = 6.1 Hz, 2H), 3.68 (t, *J* = 6.1 Hz, 2H), 6.89 (d, *J* = 2.6 Hz, 1H), 7.15 (dd, *J* = 2.6, 9.1 Hz, 1H), 7.63 (d, *J* = 8.8 Hz, 1H), 7.81 (d, *J* = 9.1 Hz, 1H), 7.92 (dd, *J* = 1.8, 8.8 Hz, 1H), 8.28 – 8.33 (d, *J*=1.8 Hz, 1H), ^{13}C-NMR (125 MHz, $CDCl_3$), δ 26.4, 39.0, 49.0, 51.8, 105.6, 115.8, 124.8, 125.4, 126.3, 130.3, 131.0, 131.1, 137.6, 148.4, 197.7 [HRMS] $[M+H]^+$ m/z: calc. for $C_{15}H_{17}N_4O$: 269.1402, found 269.1404.

4-((2-((6-Acetylnaphthalen-2-yl)(methyl)amino)ethyl)amino)-4-oxobutanoic acid (**15**)

Compound 13 (92.6 mg, 0.35 mmol) was dissolved in dry THF (5 mL). To this solution, succinic anhydride (69 mg, 0.69 mmol, 1.97 eq) was added and allowed to dissolve. Once dissolved, 10% Palladium on carbon (10.8 mg, 0.10 mmol, 0.29 eq) was added and allowed to stir at room temperature, under a hydrogen atmosphere for about 5 hours. Upon completion of

the reaction, as monitored by TLC, the reaction mixture was filtered through Celite and concentrated under reduced pressure. The product, **15**, was obtained in an 87 % yield after purification by flash column chromatography using a MeOH/ DCM (1: 19) solvent mixture. ^{1}H NMR (600 MHz, CD_3OD) δ 2.36 (t, *J* = 7.5 Hz, 2H), 2.44 (t, *J* = 7.5 Hz, 2H), 2.63 (s, 3H), 3.10 (s, 3H), 3.34 (broad s, 1H), 3.42 (t, *J* = 6.6 Hz, 2H), 3.61 (t, *J* = 6.6 Hz, 2H), 6.96 (d, *J*=2.5 Hz, 1H), 7.28 (dd, *J* = 2.5, 9.0 Hz, 1H), 7.63 (d, *J* = 8.8 Hz, 1H), 7.82 – 7.85 (m, 2H), 8.37 (d, *J* = 1.8 Hz, 1H), [HRMS] $[M+H]^+$ m/z: calc. for $C_{19}H_{23}N_2O_4$: 343.1658, found 343.1649.

APPENDICES

Appendix 2 – Spectral Data

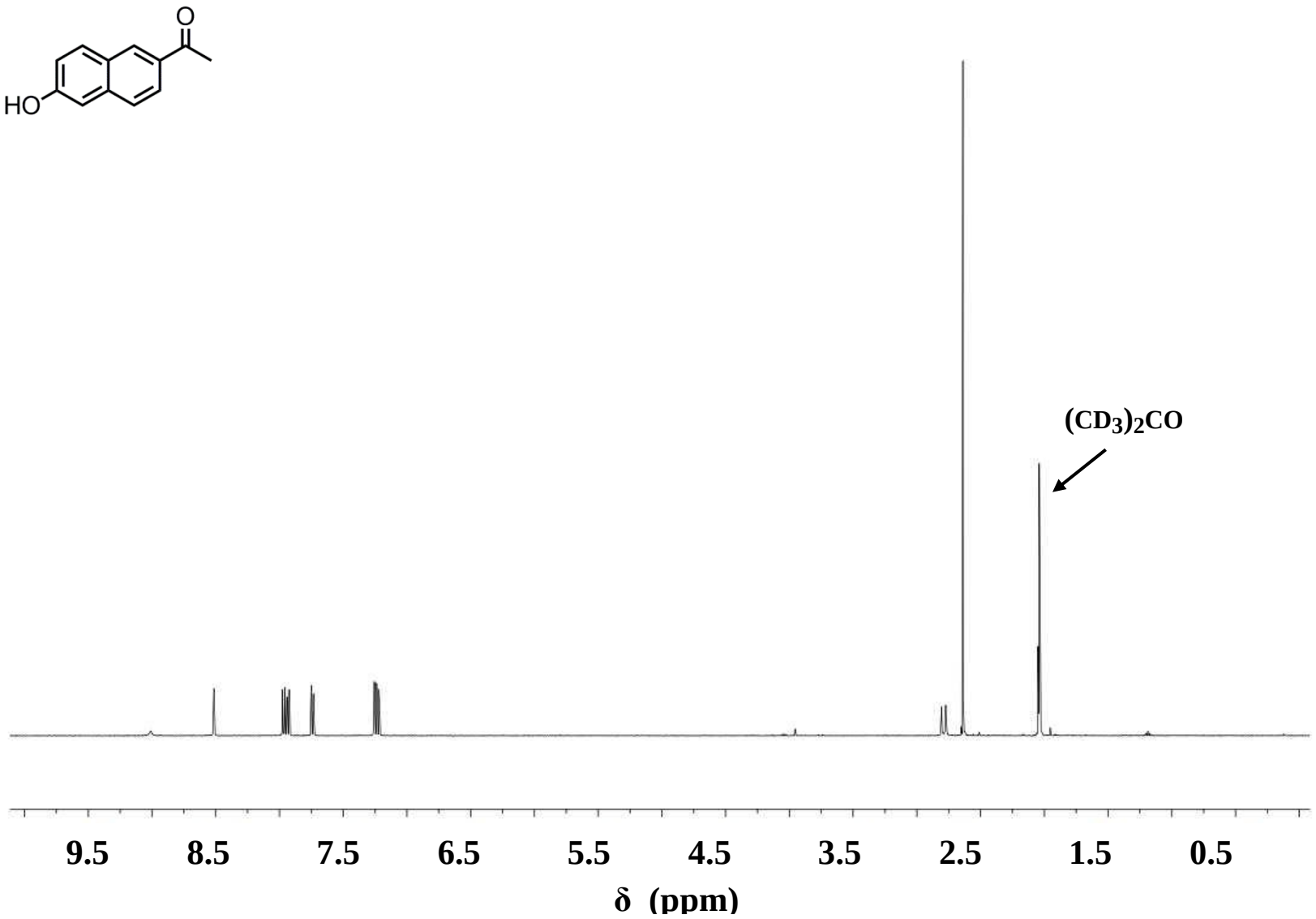

Figure 2.2: 500 MHz, $(CD_3)_2CO$, ^1H NMR of **2**

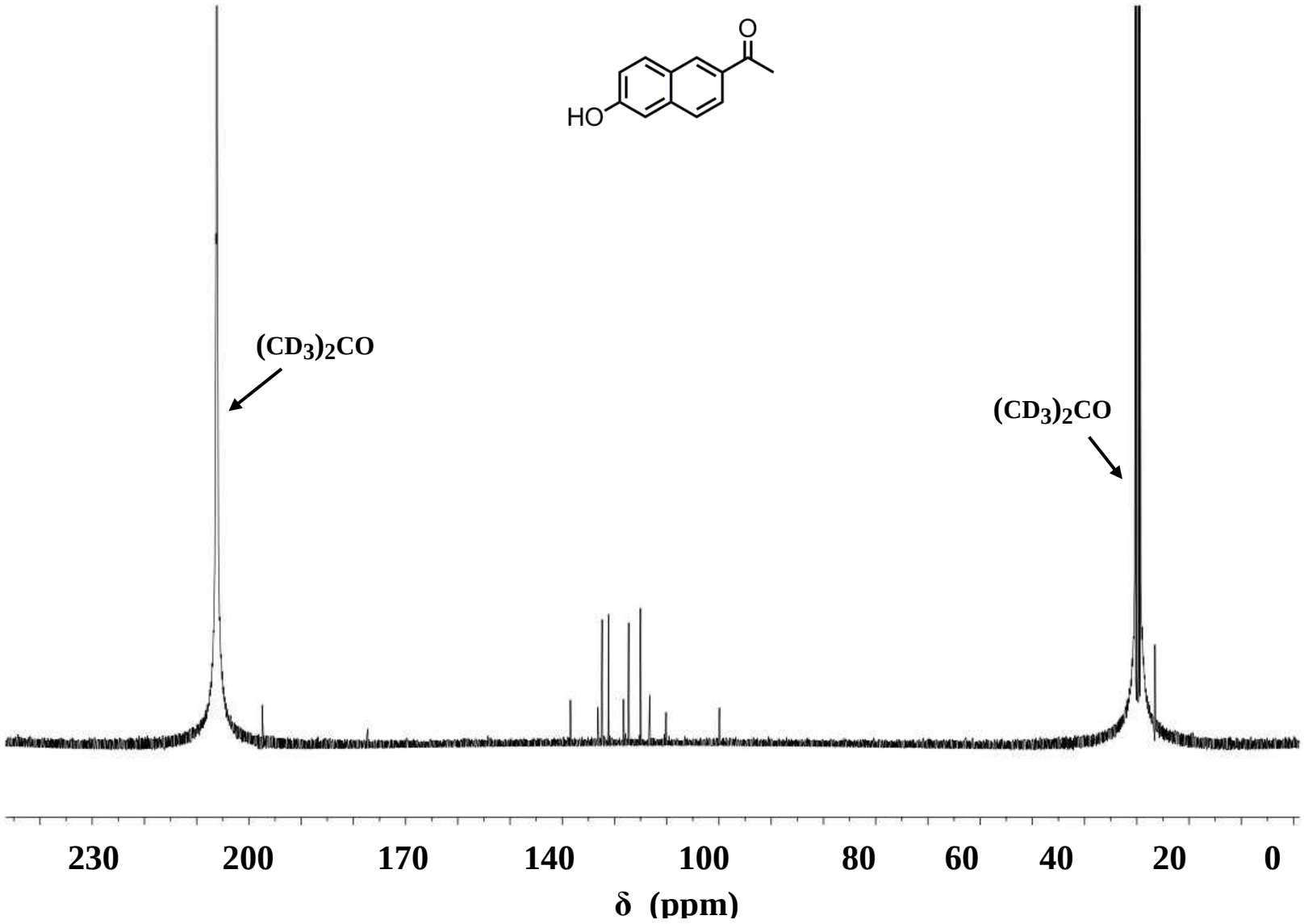

Figure 2.3: 150 MHz, $(CD_3)_2CO$, ^{13}C NMR of **2**

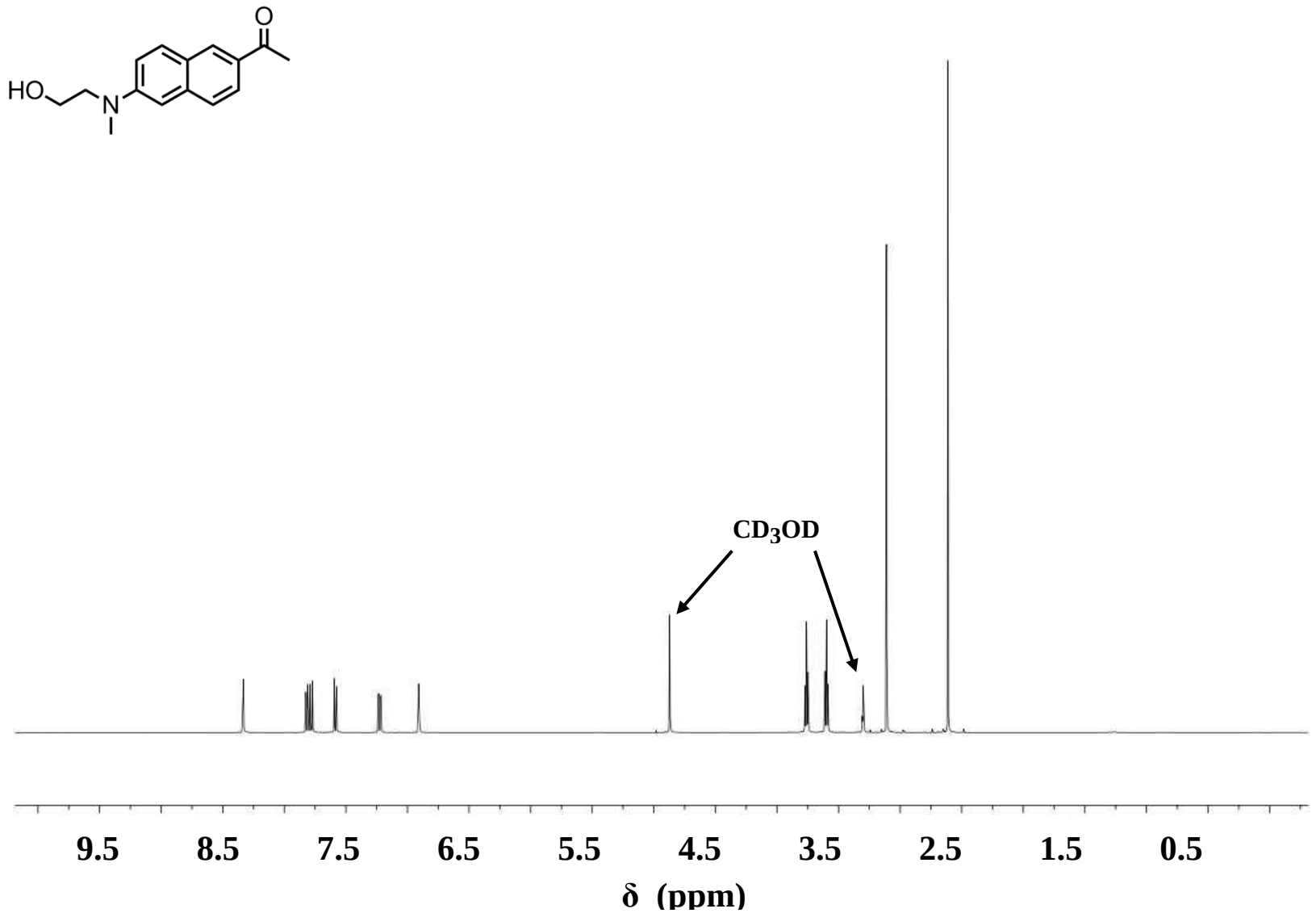

Figure 2.4: 500 MHz, (CD_3CD), ^1H NMR of **10**

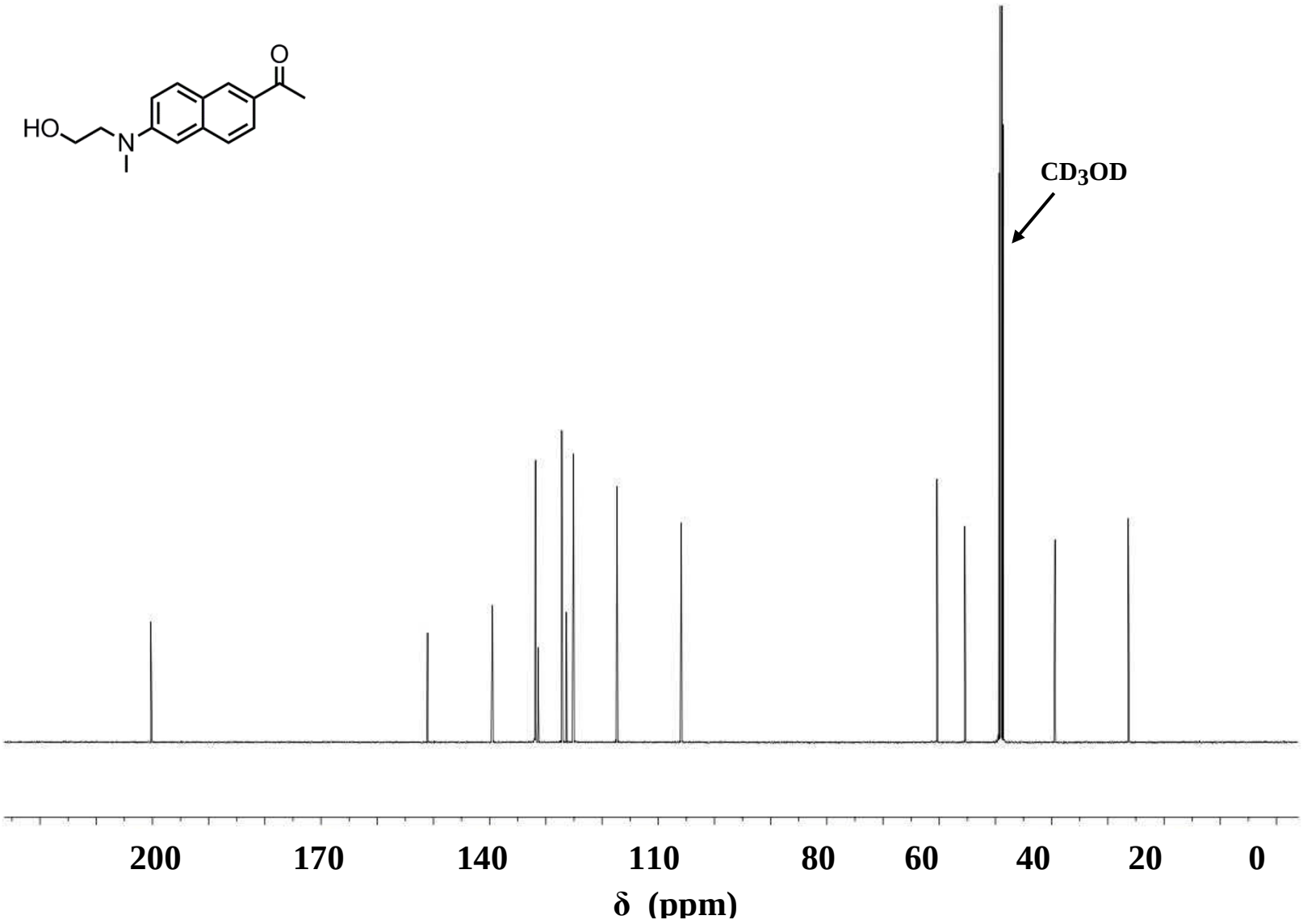

Figure 2.5: 125 MHz, (CD_3CD), ^{13}C NMR of **10**

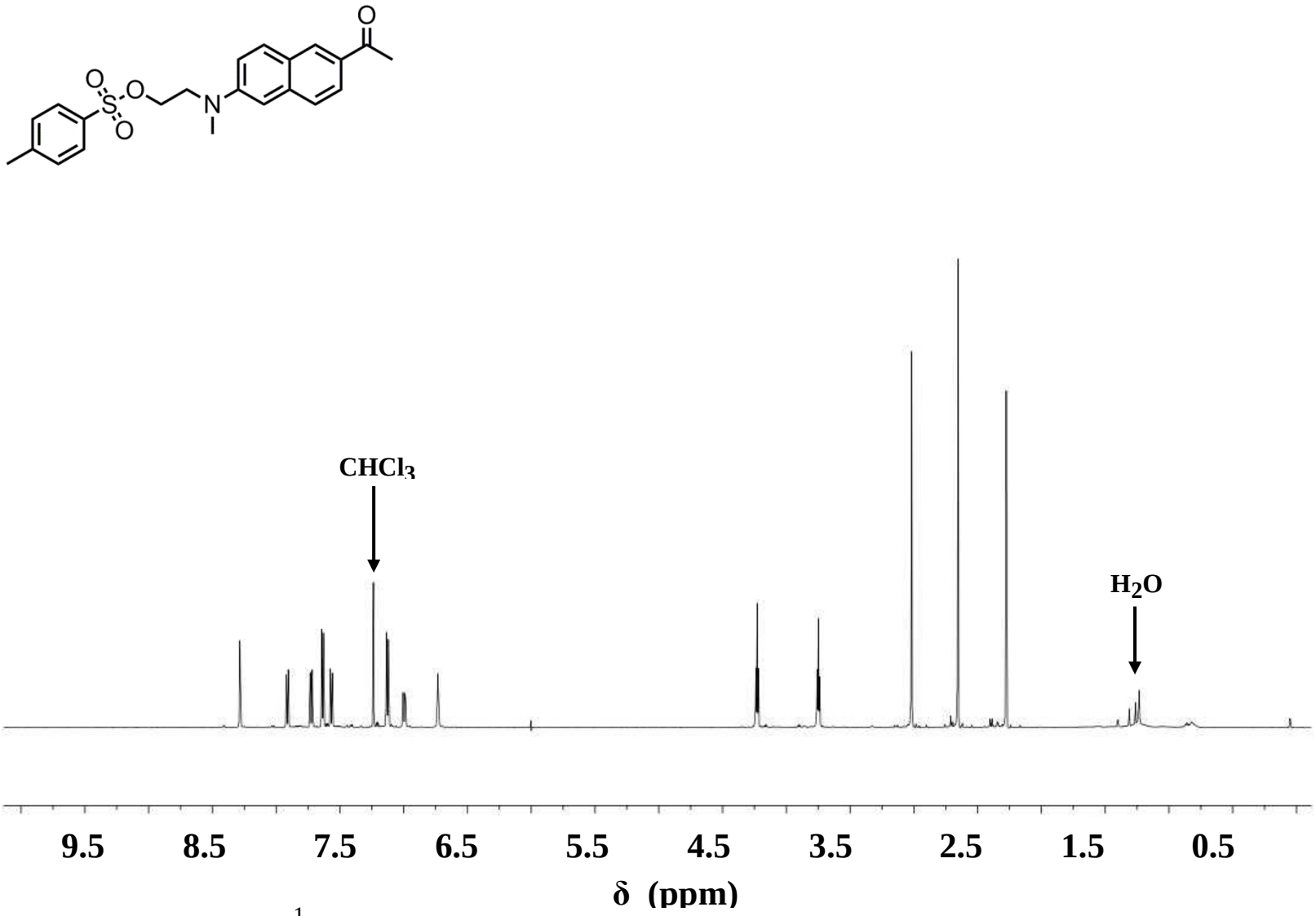

Figure 2.6: 300 MHz, ($CDCl_3$), ^1H NMR of **11**

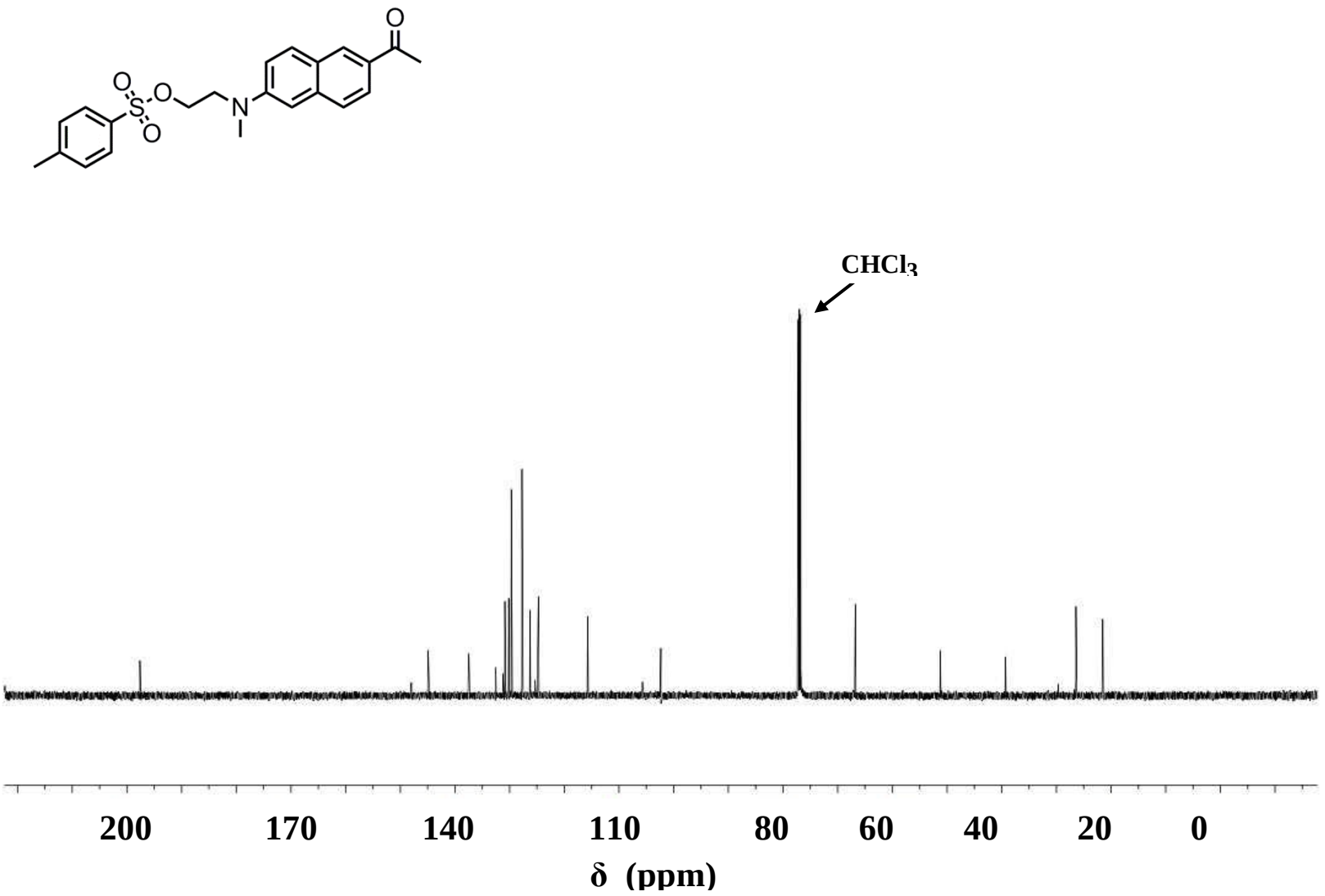

Figure 2.7: 150 MHz, ($CDCl_3$), ^{13}C NMR of **11**

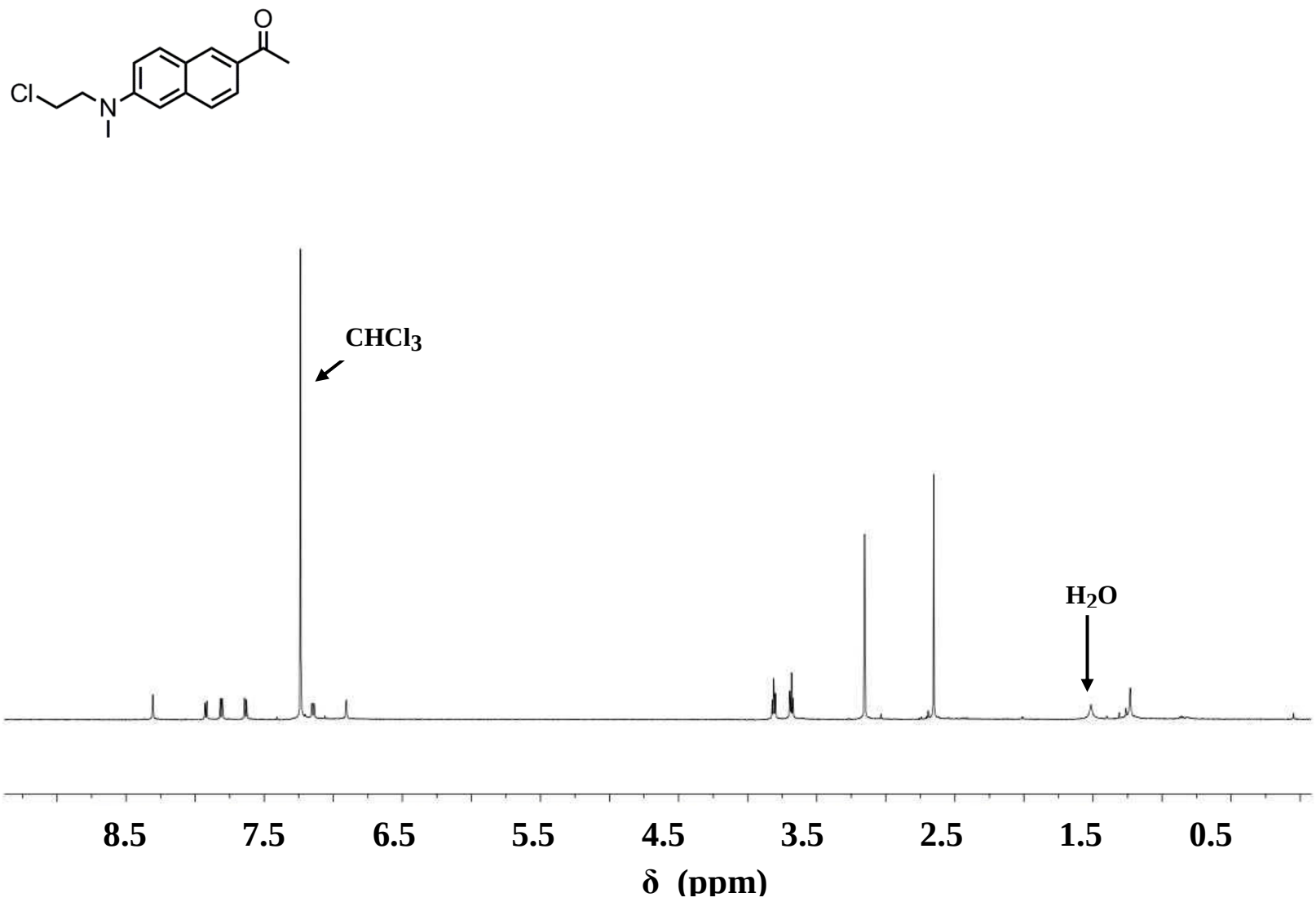

Figure 2.8: 600 MHz, ($CDCl_3$), ^1H NMR of **12**

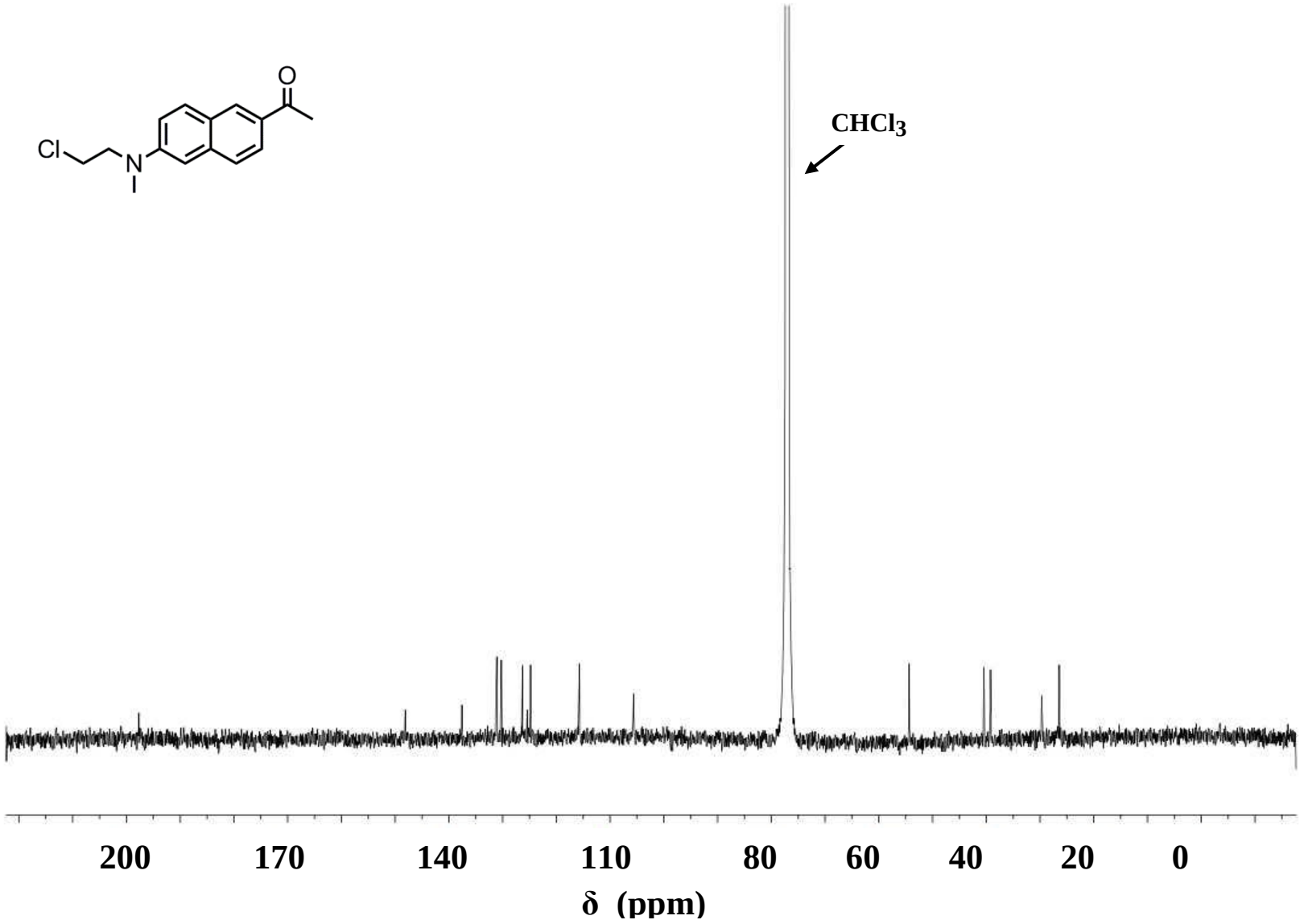

Figure 2.9: 150 MHz, ($CDCl_3$), ^{13}C NMR of **12**

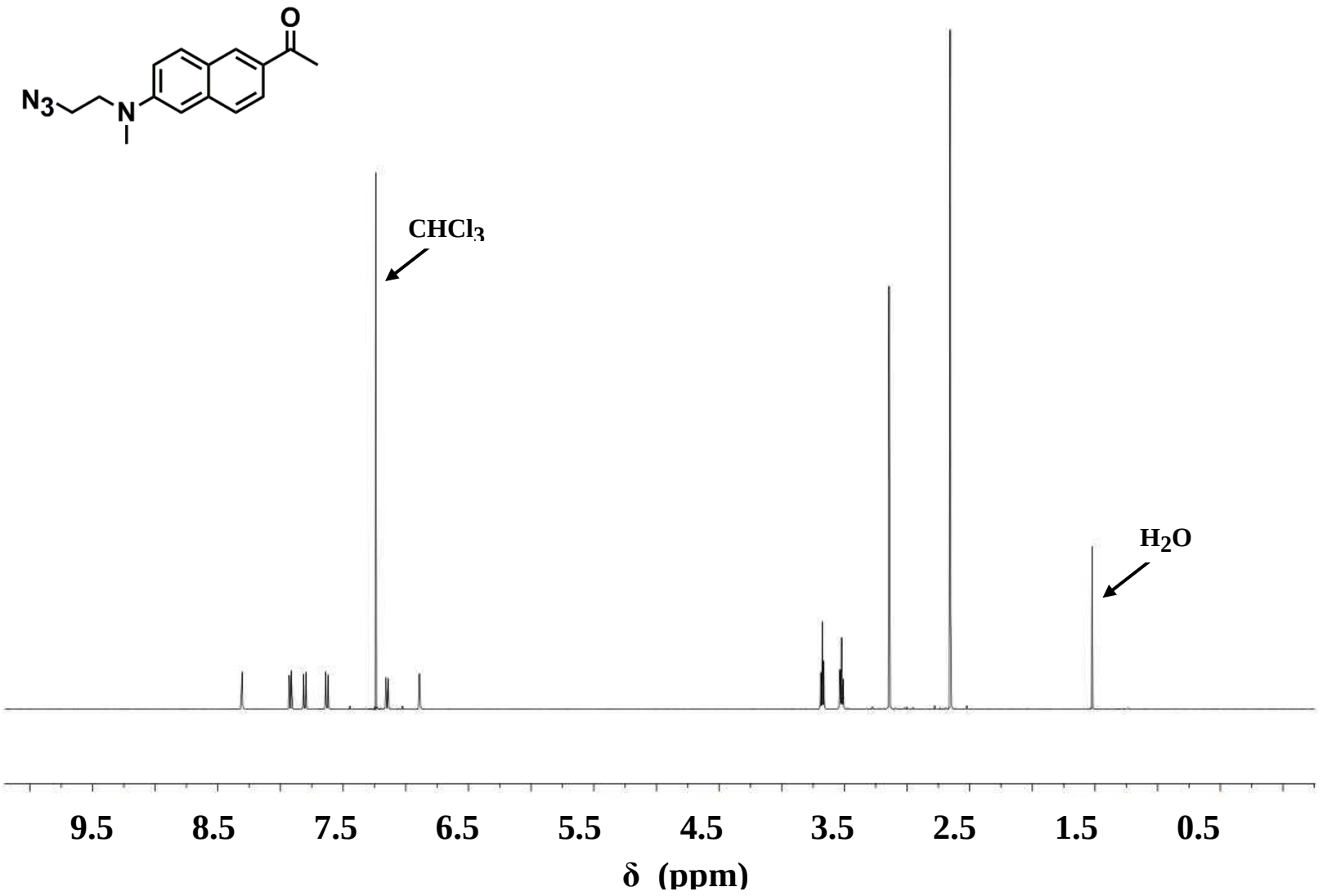

Figure 2.10: 500 MHz, ($CDCl_3$), ^1H NMR of **13**

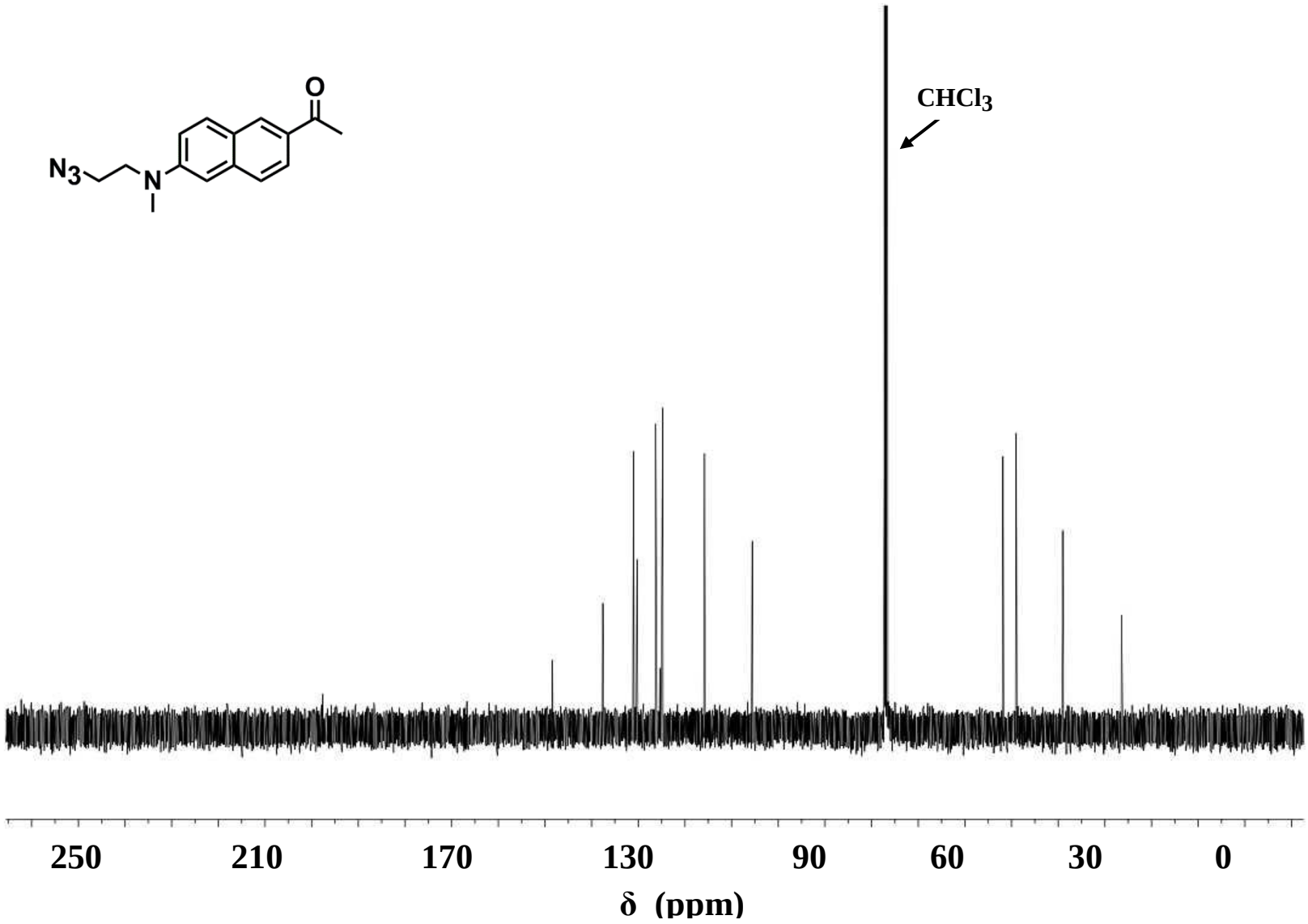

Figure 2.11: 125 MHz, ($CDCl_3$), ^{13}C NMR of **13**

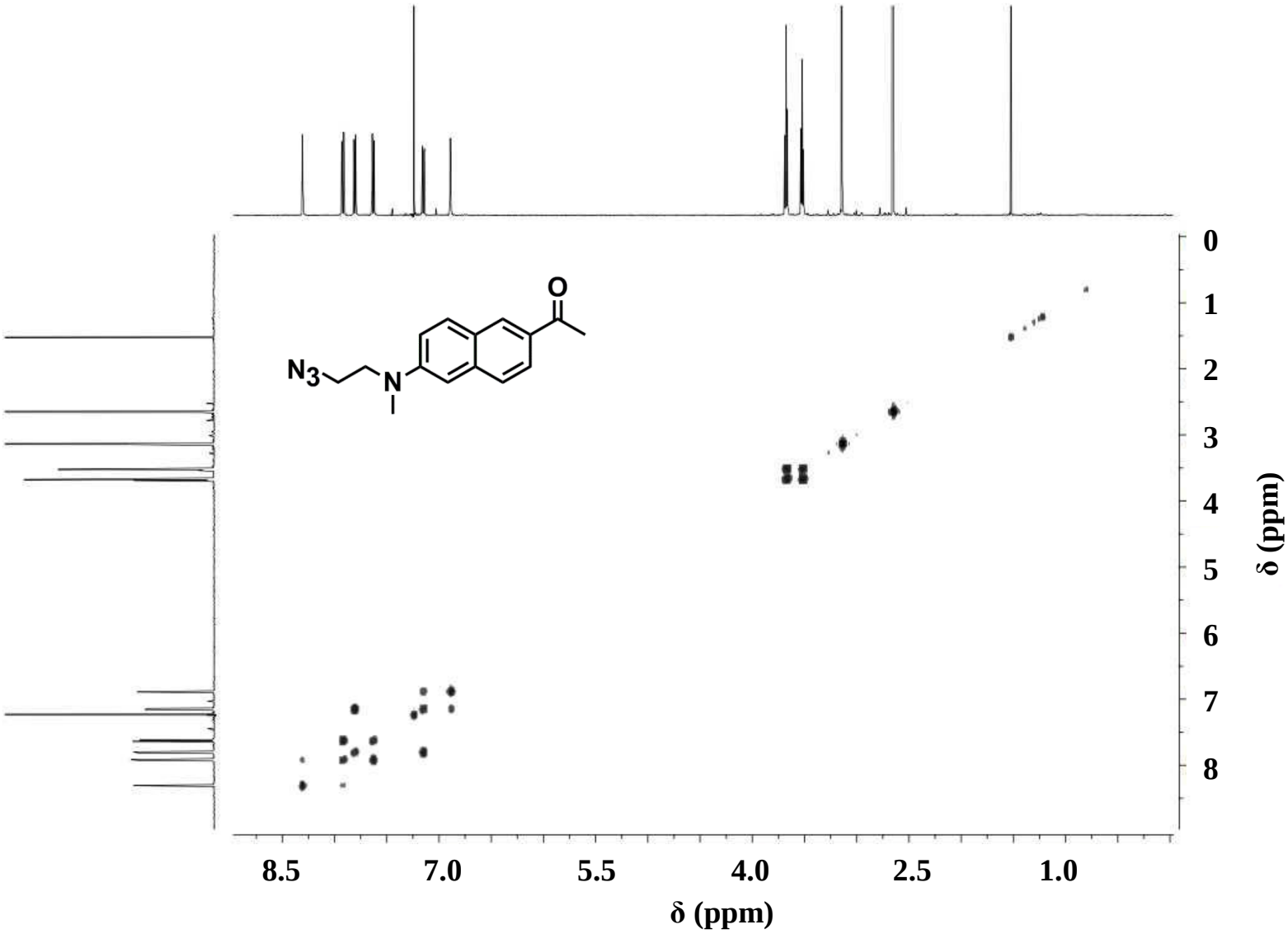

Figure 2.12: 500 MHz, ($CDCl_3$), gCOSY of **13**

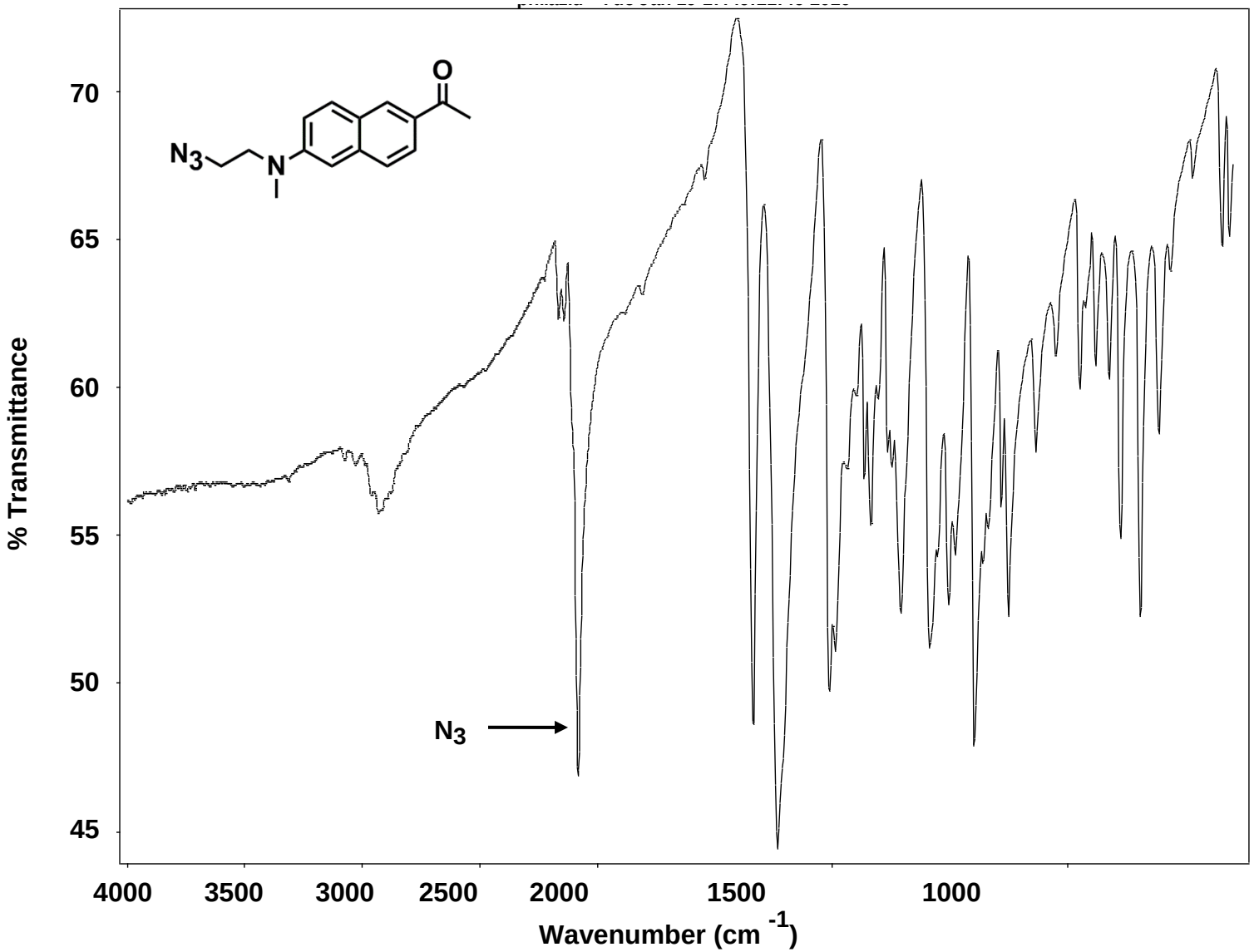

Figure 2.13: Confirmation of azide stretch using IR of **13**

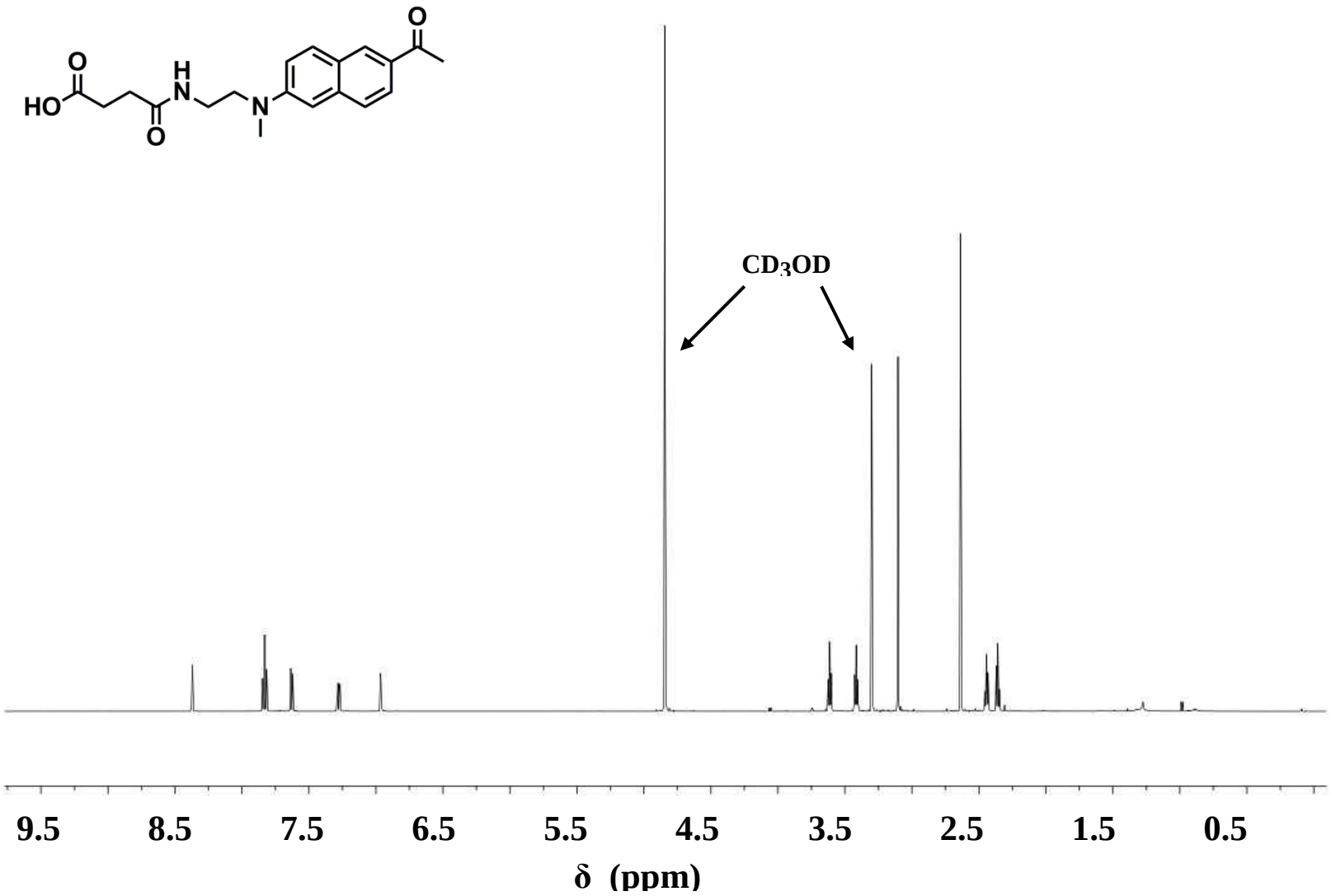

Figure 2.14: 500 MHz, (CD_3OD), ^1H NMR of **15**

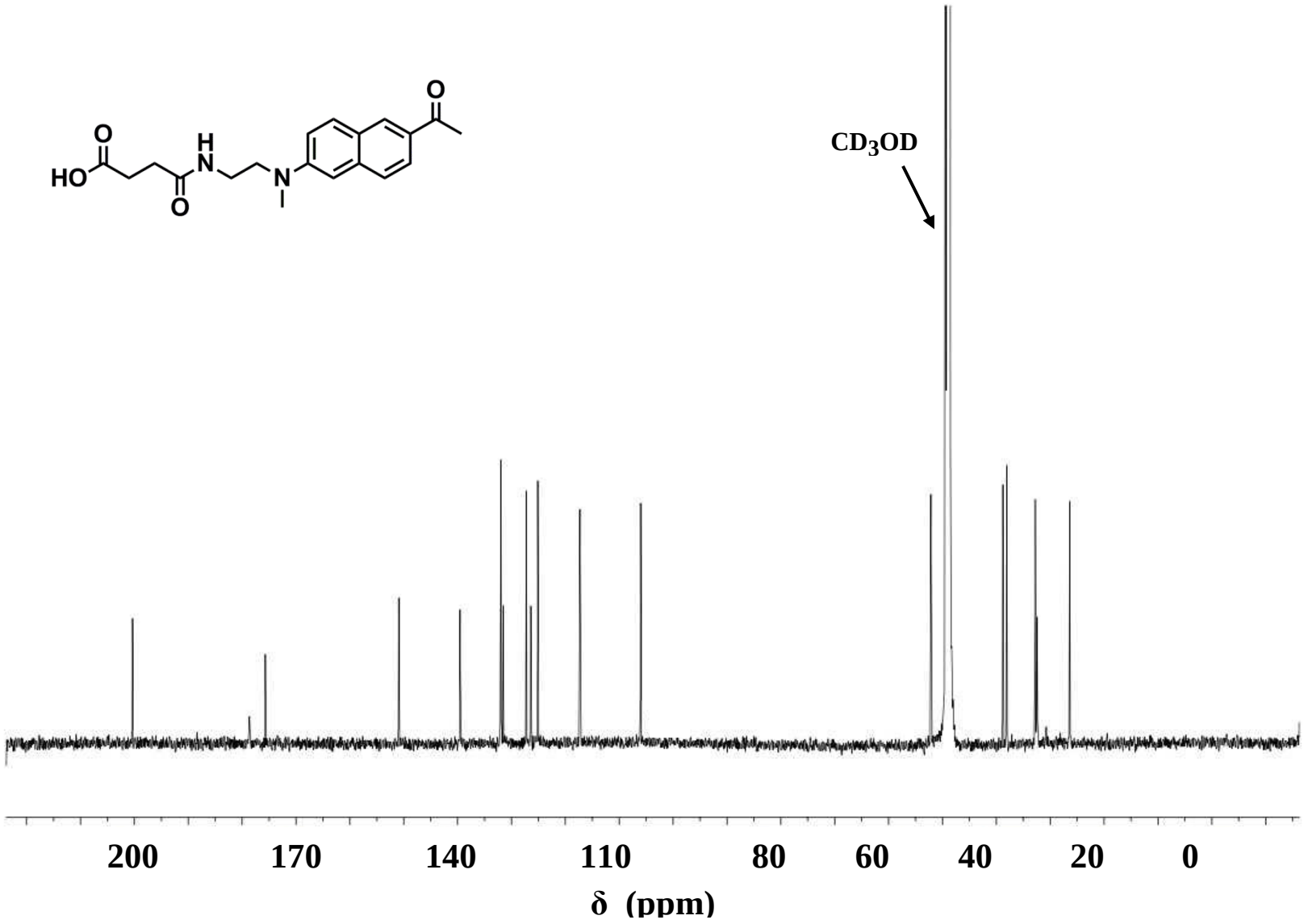

Figure 2.15: 150 MHz, (CD_3OD), ^{13}C NMR of **15**

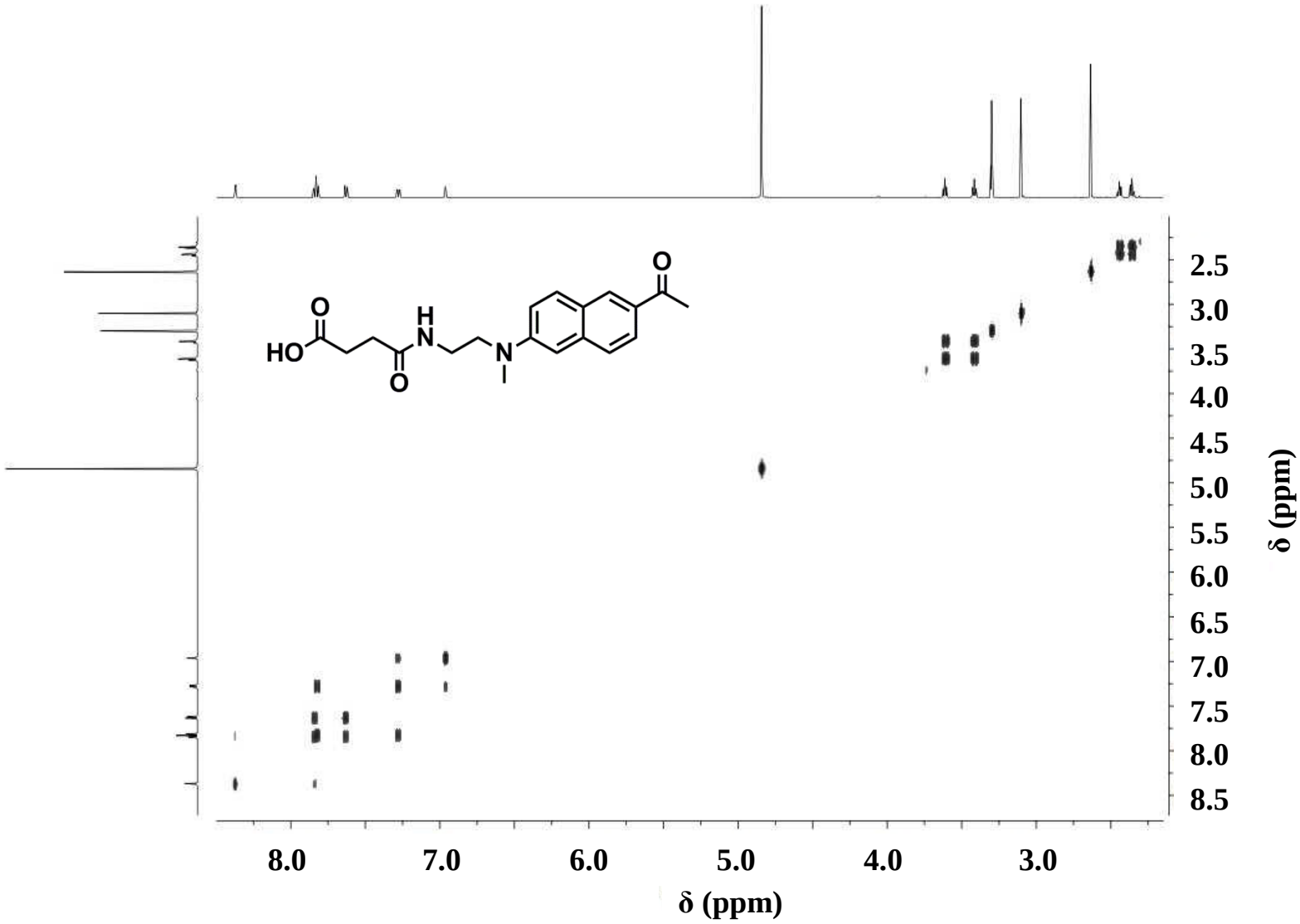

Figure 2.16: 600 MHz, (CD_3OD), gCOSY of **15**

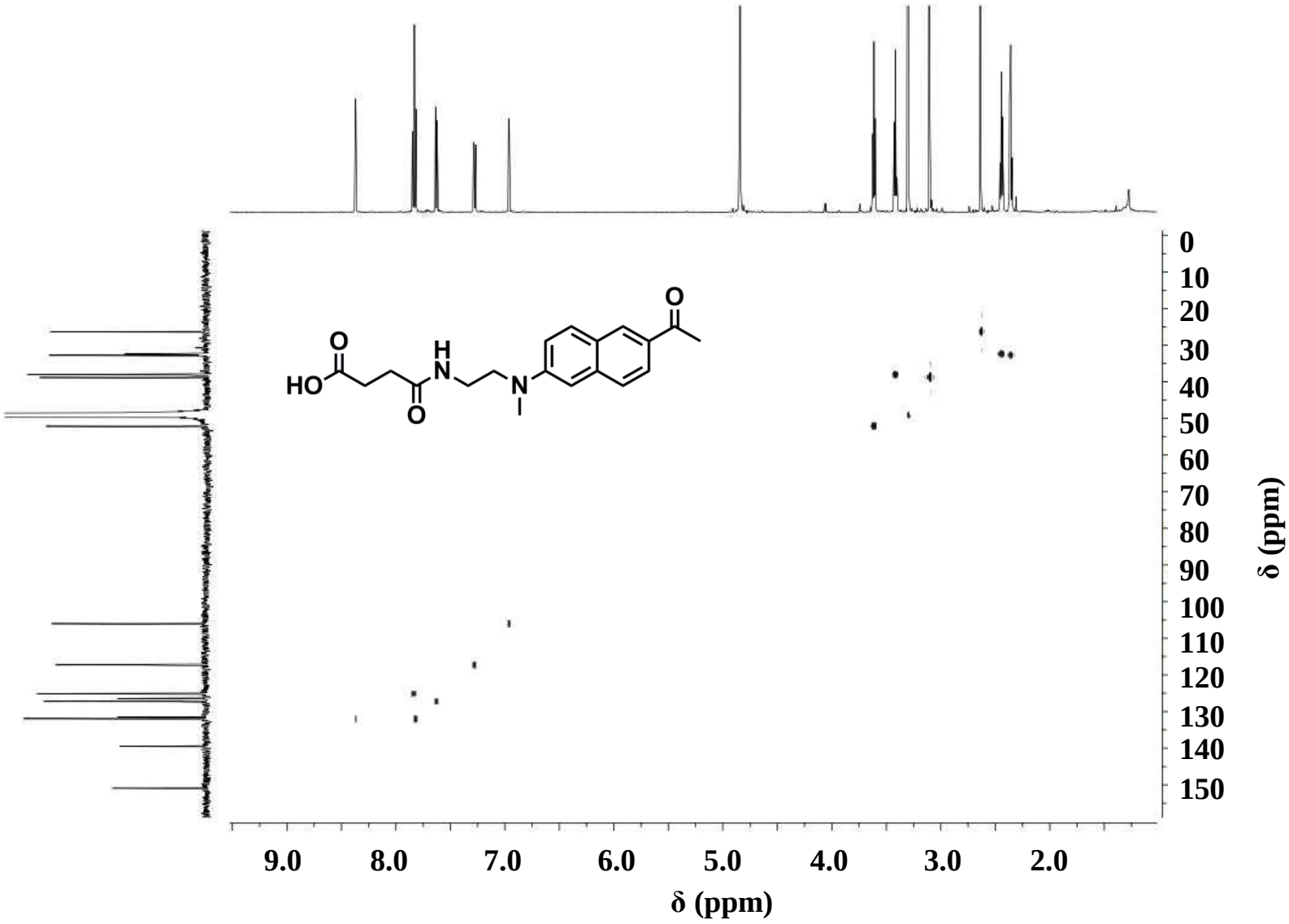

Figure 2.17: 600 MHz, (CD_3OD), HMQC of **15**

REFERENCES

References

1. 2009 Alzheimer's Disease Facts and Figures. *Alzheimer's & dementia: the journal of the Alzheimer's Association* **2009,** 5, 234-270.

2. Barrio JR; Huang SC; Cole G; Satyamurthy N; Petric A; Phelps ME; G, S., PET Imaging of Tangles and Plaques in Alzheimer Disease with a Highly Hydrophobic Probe. *J. Label Compd. Radiopharm* **1999,** 42, S194- S195.

3. Barrio, J. R.; Petric, A.; Satyamurthy, N. Methods for Binding Agents to β- Amyloid Plaques. WO/2005/040337, 2005.

4. Seeboth, H., The Bucherer Reaction and the Preparative Use of its Intermediate Products. *Angew. Chem. Int. Ed.* **1967,** 6, 307-317.

5. Ghosh, A. K.; Leshchenko-Yashchuk, S.; Anderson, D. D.; Baldridge, A.; Noetzel, M.; Miller, H. B.; Tie, Y.; Wang, Y.-F.; Koh, Y.; Weber, I. T.; Mitsuya, H., Design of HIV-1 Protease Inhibitors with Pyrrolidinones and Oxazolidinones as Novel P1'-Ligands To Enhance Backbone-Binding Interactions with Protease: Synthesis, Biological Evaluation, and Protein-Ligand X-ray Studies. *J. Med. Chem.* **2009,** 52, 3902-3914.